5-1-2010

Energy analysis of a Micro-CHP demonstration facility

Paxton Keith Giffin

ENERGY ANALYSIS OF A MICRO-CHP DEMONSTRATION FACILITY

By

Paxton Keith Giffin

A Dissertation
Submitted to the Faculty of
Mississippi State University
in Partial Fulfillment of the Requirements
for the Degree of Doctor of Philosophy
in Mechanical Engineering
in the Department of Mechanical Engineering

Mississippi State, Mississippi

May 2010

ENERGY ANALYSIS OF A MICRO-CHP DEMONSTRATION FACILITY

By

Paxton Keith Giffin

Approved:

Pedro Mago Associate Professor of Mechanical Engineering (Major Professor)	Louay M. Chamra Dean of Engineering Oakland University (Committee Member)
B. K. Hodge Professor of Mechanical Engineering (Committee Member)	Richard Forbes Professor of Mechanical Engineering (Committee Member)
David Marcum Professor of Mechanical Engineering Graduate Coordinator Department of Mechanical Engineering	Sarah A. Rajala Dean of the Bagley College of Engineering

Name: Paxton Keith Giffin

Date of Degree: May 1, 2010

Institution: Mississippi State University

Major Field: Mechanical Engineering

Major Professor: Dr. Pedro Mago

Title of Study: ENERGY ANALYSIS OF A MICRO-CHP DEMONSTRATION FACILITY

Pages in Study: 240

Candidate for Degree of Doctor of Philosophy

Cooling, Heating, and Power (CHP) systems have been around for decades, but systems that utilize 20 kW or less, designated as Micro-CHP, are relatively new. Micro-CHP systems show the most promise for a distributed generation scheme to decentralize the national energy grid. A demonstration site has been constructed at Mississippi State University to show the advantages of these systems.

This study is designed to evaluate the performance of a Micro-CHP system and a conventional high-efficiency system. Performance and cost factors can be evaluated for the demonstration site operating under either the CHP system or the conventional system. These results are computed from an energy analysis on collected data. This dissertation introduces a new comparison factor to examine different CHP systems. This new factor is called the System Energy Transfer Ratio (SETR). Other considerations in this study include an extensive literature survey that reviews CHP systems, their components, modeling, and other topics concerning CHP systems operation. In addition, the demonstration facility will be discussed in detail presenting the various components

and instrumentation. Furthermore, the energy analysis will be presented, examining the equations used to evaluate the raw data from the demonstration site. An uncertainty analysis will be presented for the experimental results.

Raw data was collected for 7 months to present the following results. The combined cycle efficiency from the demonstration site was averaged at 29%. Maximum combined cycle efficiency was evaluated at 58%. The average combined boiler and engine cost, per hour of operation, is shown as $1.8 for heating and $3.9 for cooling. The cooling technology used, an absorption chiller, has been shown to exhibit an average COP of 0.27. The proposed SETR for the demonstration site is 22% and 15%, for heating and cooling, respectively. The conventional high-efficiency system, during cooling mode, was shown to have a COP of 4.7 with a combined cooling and building cost of $0.2/hour of operation. During heating mode, the conventional system had an efficiency of 47% with a fuel and building electrical cost of $0.28/hour of operation.

TABLE OF CONTENTS

LIST OF TABLES

LIST OF FIGURES

NOMENCLATURE

CHP	Cooling, Heating, and Power
MSU	Mississippi State University
IC	Internal Combustion
DOE	Department of Energy
HVAC	Heating, Ventilation, and Air Conditioning
COP	Coefficient of Performance
SETR	System Energy Transfer Ratio
DG	Distributed Generation
FESR	Fuel Energy Savings Ratio
MARR	Minimum Attractive Rate of Return
NPV	Net Present Value
HDR	Heat Dissipation Ratio
MILP	Mixed Integer Linear Programmer
LEED	Leadership in Energy and Environmental Design
BPER	Building Primary Energy Ratio
PEU	Primary Energy Usage
SEC	Site Energy Consumption
PEC	Primary Energy Consumption

FTL	Following the Thermal Load
FEL	Following the Electrical Load
TDM	Thermal Demand Management
EDM	Electrical Demand Management
PGU	Primary Generation Unit
CDE	Carbon Dioxide Emissions
HETS	Hybrid Electric-Thermal Load Operational Strategy
PE-O	Primary Energy Optimization
OC-O	Operational Cost Optimization
ER-O	Emission Reduction Optimization
PFI	Performance Factor Indicator
PURPA	Public Utilities Regulatory Policy Act
EPA	Environmental Protection Agency
CEF	Scenarios for Clean Energy Future
EIA	Energy Information Administration
NEMS	National Energy Modeling System
SEER	Seasonal Energy Efficiency Ratio
RTD	Resistance Temperature Detector
DAQ	Data Acquisition
NI	National Instruments
AI	Analog Input
VI	Virtual Instrument

LHV	Lower Heating Value
UA	Uncertainty Analysis
UPC	Uncertainty Percentage Contribution

Variables

F	Fuel Energy
Q	Thermal Energy
W	Work
R	Resistance
A	Constant for Collendar-Van Dusen Equation
B	Constant for Collendar-Van Dusen Equation
T	Temperature
P	Power
I	Current
V	Voltage
$\dot{V}$	Volumetric Flow Rate
m	Mass
h	Enthalpy
Cp	Specific Heat Capacity
A/F	Air to Fuel Ratio
C	Heat Capacity

Pr	Pressure
RH	Relative Humidity

Greek Letters

η	Efficiency
ρ	Density
ε	Effectiveness
ω	Specific Humidity

Subscripts

SG	Separate Generation
CHP	CHP Generation
a	Absorber
co	Condenser
g	Generator
Comp	Compressor
ev	Evaporator
dc	Driving Cycle
cc	Cooling Cycle
TRI	Trigeneration
CO	Cogeneration
CH	Chiller

EL	Electrical
R	Cooling
f	Fuel
HR	Heat Recovery
conv	Conventional System Operation
T	At Current Temperature
o	At 0℃
R	At Current Resistance
GEN	Generated
NGE	Engine Natural Gas Consumption
e	Exit Conditions
i	Inlet Conditions
c	Combustion
EX	Exhaust
COOL	Engine Coolant
OUT	Outlet
IN	Inlet
RatioHX1	Ratio for Heat Exchanger 1
Max	Maximum
h	Hot Side
c	Cold Side
min	Minimum

HX1	Heat Exchanger 1
RatioHX2	Ratio for Heat Exchanger 2
HX2	Heat Exchanger 2
BW	Boiler Water
NGB	Boiler Natural Gas Consumption
CW	Cold Water
HW	Hot Water
RatioHVAC	Ratio for HVAC System
MA	Moist Air
Conv_Cool	Conventional System Cooling Operation
CHPB	CHP system with Boiler
TriB	Trigeneration with Boiler
B	Boiler
v	Vapor Pressure
SAT	Saturation
ATM	Atmospheric
DA	Dry Air
MA_SI	Moist Air Metric Units
MA_IP	Moist Air Imperial Units

CHAPTER 1

INTRODUCTION

The use of combined heating and power (CHP) systems to produce both electricity and useful heat is increasing rapidly due to their high potential for reducing primary energy consumption, operational cost, and emissions in domestic, commercial, and industrial applications. These reductions are mainly due to the ability of a system to use recovered waste heat to satisfy the thermal demand of a building.

The designation of "micro" for a CHP system is derived from the system's power producing capabilities. Wu and Wang (2006) designate that micro is any system under 20 kW. The CHP system at the Mississippi State University (MSU) demonstration site has a generator with a power producing capability of 15 kW, thus placing it in the micro range. Although large scale industrial CHP systems have been around for 100 years, smaller residential and commercial sized systems have been a recent development.

A CHP system consists of multiple components, the first of which is the prime mover. The prime mover can be an Internal Combustion (IC) engine, gas turbine, or a myriad of other options. The selection criterion for a prime mover typically requires it to have an abundance of recoverable heat to meet the thermal load of the facility. The

electrical load can be met by either a generator or the power grid. For the demonstration site, the thermal load is met by recovering heat from the engine in two locations; a gas-to-liquid heat exchanger, which recovers heat from the engine exhaust, and a liquid-to-liquid heat exchanger, which extracts heat from the engine coolant. The next main component is the cooling technology used to provide for the cooling load of the facility during CHP system operation. At the demonstration facility, a heat powered absorption chiller is used to make use of the recovered thermal energy. In some situations another source of heat may be needed, in these cases a conventional boiler in used to provide additional thermal energy. The final component is the air handling units for space heating and cooling. The demonstration site makes use of a four-pipe fan-coil unit.

1.1 MSU'S CHP Demonstration Site

At MSU a demonstration site has been constructed and instrumented over the past few years, primarily funded by the Department of Energy (DOE). This facility is used to showcase the advantages of using Micro-CHP systems for various applications. The main objectives for the facility include demonstrating existing technologies for small scale applications, developing a test bed for future studies, and providing a location to test bio-fuels that are under development at MSU. The primary goal of the demonstration facility is to bring attention to the performance and reliability of CHP systems and their technologies.

1.2 Energy Analysis Overview

The objective for this study is to compare the energy performance of a CHP system and a conventional system located on site. Special attention is given to performance factors of the system components and the system as a whole. An examination of the operational costs of fuel and electrical power consumption is also provided. The first system discussed is the CHP system, and the second system is a conventional high-efficiency Heating, Ventilation, and Air Conditioning (HVAC) system. For cooling, the conventional system uses a vapor-compression system, and for heating it uses a condensing boiler. These systems are analyzed while operating during both heating and cooling seasons.

The analysis for the CHP system operating in heating and cooling mode includes multiple areas. The first item of interest is the combined cycle efficiency of the engine. Next, the thermodynamic efficiency of the boiler is examined. As this boiler is supplemental, it fires when the recovered waste heat is not sufficient to satisfy the thermal demand. The next component looked at is the four-pipe fan coil unit. To evaluate the performance of this unit it is examined as a heat exchanger, computing the water to air heat transfer ratio. Furthermore, the CHP system requires a cost analysis, given in $/hour of operation. When the system is operating in cooling mode, it has an additional component to be considered, the absorption chiller. To compute the performance for the chiller the Coefficient Of Performance (COP) is calculated. This metric describes how efficiently the chiller utilizes the recovered heat to produce cooling. The final item to be

analyzed for the CHP system is the System Energy Transfer Ratio (SETR). This idea is proposed in this dissertation and presents a new way to relate different CHP systems to each other, without regard to the components utilized within them. This idea considers the entire system as a control volume and, thus, proposes an overall ratio of input energy to output energy. For most situations where the waste heat is only used to satisfy the heating or cooling load of the building, the only input to the system is the fuel consumption of the engine and the boiler and the output is the power generated combined with the space heating or cooling.

The conventional system, as previously explained, must also be analyzed for both heating and cooling seasons. For the heating season analysis, the efficiency of the heat transfer to the office space for the unit's furnace is determined. Next, a cost analysis is performed to examine the natural gas fuel usage in $/hour. The analysis for the cooling season conventional system operation includes, computing the COP for the vapor-compression system and the electrical power consumed by the compressor and fans. These analyses allow determining how well both systems function, and, therefore, identifying areas for possible improvement to the CHP system.

Also included is an examination of particular situations and their impact on the system discussed. The examination begins with the system start-up condition. In the start-up situation the performance of the engine and the boiler are revealed, as well as, how long the system takes to reach steady-state, for both heating and cooling functions. The next item examined is a situation in which the engine coolant flow is completely by-

passing the radiator. By-pass can only be accomplished when the ambient temperature is sufficiently low. During this time the engine can operate while fully by-passing the radiator, increasing efficiency. Following the by-pass situation, the effect of incoming boiler and chiller hot water temperature on their performance is determined. The effect of ambient temperature fluctuation on the performance of individual components will be discussed to reveal the interdependence of the components.

CHAPTER 2

LITERATURE SURVEY

The majority of the world's electrical power is produced from fossil fuels. Soon production of power from fossil fuels will no longer be economic to access these natural resources, and the world will be threatened by an increasingly evident energy crisis. Although many countries are searching for renewable sources of electrical power, large-scale generation from these sources is not yet cost effective. In the meantime, engineers must work to make our society more efficient in power generation and use. One method is to increase the efficiency of existing and new systems. A way to achieve this higher efficiency is to recover otherwise wasted thermal energy. The recovered energy could be used to fulfill the heating or cooling demand of a facility or home. The name for systems that use this excess heat for heating only are called cogeneration or combined heating and power systems. Systems that also produce a cooling effect are named trigeneration or cooling, heating, and power systems. For use in this review, the term CHP, unless otherwise specified, will be used interchangeably for cogeneration or trigeneration systems.

2.1 CHP Systems Introduction

Wu and Wang (2006) describe CHP systems as a reliable technology that has been proven and in use for over 100 years. The main purpose for this technology is to decrease the overall energy consumption in large industrial facilities. CHP systems utilize excess heat from a prime mover, such as an IC engine. Wu and Wang (2006) define CHP systems as "the combined production of electrical or mechanical, and useful thermal energy from the same primary energy source." These systems are designated by their power generating capabilities. Systems which produce less than 1 MW of power are designated as small-scale systems, ones less than 500 kW as mini systems, and systems producing under 25 kW as micro.

Wu and Wang (2006) state that CHP systems typically consist of five components: the first is the prime mover or engine, the second is the electrical generator, third is the heat recovery, fourth are the thermally activated machines, and the management and control systems. Figure 2.1 presents a schematic of a typical CHP system. In this system the only energy input to the system is natural gas, or another fuel, to the engine and the absorption chiller.

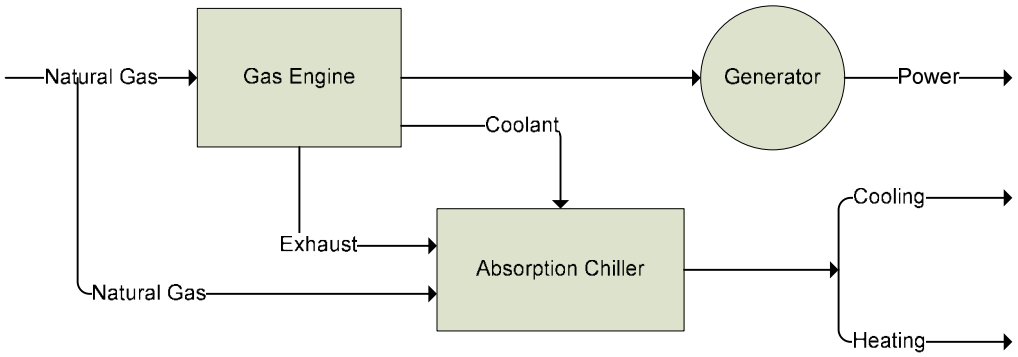

Figure 2.1 Typical Schematic of a CHP System, adapted from Wu and Wang (2005).

Waste heat from the engine is recovered from the exhaust gasses or from the engine coolant system. This thermal energy can be used to heat water or to power a heat-driven chiller to produce cooling. In the event the recovered thermal energy is not sufficient, an auxiliary combustor, such as a boiler, can provide the remaining thermal load. The hot and cold water then provides for the heating and cooling loads of the building. Lastly, a simple generator is needed to convert the mechanical energy to electrical power.

Wu and Wang (2006) describe many benefits of using CHP systems. One benefit is the increased thermal efficiency over conventional separate generation systems. The reliability of on-site power production is an added benefit. A power-generation scheme call Distributed Generation (DG) often uses CHP systems. DG utilizes many smaller power-generation sites to produce power locally rather than a single large power generation facility. Using DG can increase power stability by being a more redundant system than its larger, more centralized counterpart. Another benefit of CHP systems

used in DG power generation scheme is the outlet for recoverable thermal energy in supplying for the thermal loads in buildings in the surrounding area.

2.1.1 Feasibility of CHP Systems

The feasibility of a CHP system depends primarily on the cost-effectiveness of the system. Current analyses of energy savings in CHP systems are based on comparing CHP system performance to conventional separate heat and energy production from coal. Jiang *et al.* (2006) describe how this comparison method is outdated and is a poor judge of how efficiently a CHP system converts the chemical energy in the fuel to usable electrical and thermal energy. The difference in the fuels is a big problem. For example, coal and natural gas have different chemical properties. Thus, using coal plants as a reference is not prudent; one must compare CHP systems to similar systems to observe if the technology is improving. The CHP systems mentioned by Jiang *et al.* (2006) typically use natural gas as fuel for combustion. They indicate that a proper reference condition to base a feasibility decision on is a system, such as a power plant or another CHP system, which uses natural gas as a fuel reducing the number of variables for comparison.

Prime movers in CHP systems that use natural gas are IC engines and gas turbines. Jiang *et al.* (2006) indicate that although IC engines typically produce less electrical power in quantity; they do it more efficiently than gas turbines. Jiang *et al.* (2006) describe a Fuel Energy Saving Ratio (FESR), which is presented in Equation 2.1.

$$FESR = \frac{F_{SG} - F_{CHP}}{F_{SG}} \tag{2.1}$$

This ratio is the total fuel energy used in a separate generation system minus the total fuel energy used in a CHP system divided by the total fuel energy consumed in that same separate generation system. Jiang *et al.* (2006) describe a test situation performed with IC engines and gas turbines to find the FESR for both cooling and heating seasons. The authors indicate that, by using proper reference systems when comparing efficiencies of CHP systems, a system with optimal performance for their particular application could be chosen.

Cardona *et al.* (2006) state that CHP systems typically operate in either of two modes. In the first mode, the system satisfies the thermal demand, and usually produces more electricity than the electrical load requirement. This results in electrical power being sold to the power grid or simply wasted. The second operating mode for a CHP system is on the basis of electrical demand. In this operational mode, the prime mover does not produce adequate thermal energy to satisfy the load and requires an auxiliary heating unit, such as a boiler, to provide the remainder of the load. Cardona *et al.* (2006) present another operating mode for a CHP system. Cardona *et al.* (2006) show that the operator of a given CHP system should compare the costs of the fuel to the costs of the electricity and; depending on which is more economically feasible, operate the system in either the of the two previously explained modes..

2.1.2 Economic Concerns

Many times the primary question to ask when dealing with CHP systems is "how long is the payback period." Biezma and Cristobal (2006) suggest that the proper use and implementation of CHP systems usually result in energy and cost savings to the operator. The optimization of CHP systems requires consideration of two different aspects; the technical aspect and the economic aspect. Analysis of both aspects is the study of thermo-economics. Quoting Biezma and Cristobal (2006), the procedure for economically analyzing a project is:

1. Define a set of investment projects for consideration.
2. Establish the analysis period for economic study. There are three different situations to be considered; the useful life of each alternative equals the analysis period, the alternatives have useful lives which are different from each analysis period, and there is an infinite analysis period.
3. Estimate the cash flow for each project.
4. Specify the Minimum Attractive Rate of Return (MARR).
5. Compare each project proposal for preliminary acceptance or rejection.
6. Accept or reject proposal on the basis of the established criteria.

Biezma and Cristobal (2006) present four basic methods for project evaluation. These methods are the payback method, Net Present Value (NPV) method, rate of return method, and the ratio method. Currently a project is only subjected to one method of

determination to present its worthiness as a project. In the future, proposal determination will be made on several of the above criterion.

2.2 Prime Movers

There are many different types of prime movers available for CHP systems. Wu and Wang (2006) classify prime movers by the type of fuel burned, the power production capacity, and the availability of the technology.

2.2.1 Internal Combustion Engines

The IC engine is the lowest cost and most widely available of the CHP prime movers. These engines operate in two different modes: spark ignition or compression ignition. The spark ignition engine uses an electrical spark to ignite the fuel/air mixture. The compression ignition engine uses "auto ignition" of the fuel by compression of air and, thus, requires no electrical spark. Both of these engines can use a variety of fuels, including renewable, to achieve combustion.

Spark ignition engines have been around for over 100 years and are a relatively mature technology. Onovwiona *et al.* (2007) present that spark ignition IC engines, when used conventionally with an electrical generator, produce nominal thermal efficiencies of 30-35%. They also show that using CHP systems the efficiency can be increased to over 80% by recovering more energy from the fuel. Spark ignition IC engines can use gasoline, natural gas, or fuels created from biomass gasification.

The cost of the fuel used in CHP facilities directly influences their cost effectiveness. Over the past few years, the fuel of choice for a spark ignited IC engines has changed from gasoline to natural gas. Rising natural gas prices are hindering CHP systems that burn natural gas. Honton and Lemar (2004) indicate in 2004 natural gas prices averaged $8.10 per million BTUs for small commercial customers and $5.67 per million BTUs for industrial customers and document an annual increase of 2.4% to 11.2% in natural gas prices. The authors suggest that a 28% decrease in the market potential of CHP is expected if natural gas prices continue to rise. Despite this, they conclude that the electricity produced by distributed generation in this country is expected double by 2025 and that with improving technology the number of CHP systems may triple by 2025.

In the search of non-petroleum based fuels, one arose from a process named biomass gasification. According to A. Demirbas (2005), the future of biomass utilization will stem from the combustion of wastes and residues to create electrical power. A common method that allows biomass to be used in IC engines is by applying heat to the biomass which will chemically convert the solid biomass into liquid pyrolysis oil and a substance referred to as biocrude. Both of these liquid products can be burned in an IC engine in a similar manner to petroleum based fuels.

Concerns associated with IC engines include the emissions generated and the regulations of those emissions. M. Angel *et al.* (2005) uses optimization techniques to minimize operational costs while concentrating on the fuel and emissions produced. M.

Angel *et al.* (2005) discusses that there are numerical methods in which such modeling of emissions can be projected, and constraints may be placed on the model to keep the system under any emission requirement placed upon it.

2.2.2 Turbine Engines

As with IC engines, turbine engines are also considered a mature technology. There are two major types of turbine engines, steam turbines and combustion turbines. Steam turbine engines use a fuel source to produce steam which powers a turbine producing electricity. Combustion turbines, or gas turbines, use fuel and compressed air to achieve combustion, which turns a generator producing electricity. Wu and Wang (2006) describe that combustion turbines are often used as prime movers for two particular reasons; they have a large power range, and they have proven to be very reliable. Changes in turbine technologies as they apply to CHP systems, include new types of fuels and methods to increase power production, reduce emissions, and decrease fuel consumption.

Demirbas (2005) show that biomass generators and power plants are very similar to their coal powered counterparts. In a direct combustion configuration, biomass is burned to produce steam which would drive a turbine to produce electricity. The drawback to this setup is the build-up of ash that can damage system components. One solution is to use very fine biomass as a fuel in a direct combustion system. Another configuration presented by Demirbas (2005) uses biomass as a fuel through gasification.

The gasifiers convert solid biomass to a combustible biogas fuel that can then be used in combined cycle, high-efficiency gas turbine engines.

Savola and Fogelholm (2006) investigated, through simulation, how to increase the power-to-heat ratios of small scale CHP facilities. Heat demand is usually the load basis for CHP facilities, yet the electrical demands must also be considered. The simplest way to increase the economic feasibility of a CHP system is to increase its power-to-heat ratio. Savola and Fogelholm (2006) use a Rankine cycle process in which superheated steam powers a turbine increased power production by reheating the superheated steam with flue gasses to increase the temperature into the heat exchanger. They analyzed the investment costs for the system by considering; the reheater, the high-pressure feed water preheater, and the heat exchanger. The annual electrical production was estimated based on a part load situation; in this case the thermal load is 65% of peak. Another calculation was preformed dealing with the emissions reduction resulting from the changes. After review of the results, Savola and Fogelholm (2006) concluded that only two additions to the system were economically feasible; the heat exchanger, and the reheater to the feed water.

2.2.3 Other Types of Prime Movers

There are other choices when choosing a prime mover for CHP application. These include micro-turbines, Stirling engines, and fuel cells. Wu and Wang (2006) examined micro-turbines as advanced combustion turbine engines that can be used individually or

combined into large multi-unit systems. They also showed that external combustion engines, or Stirling engines, have many benefits. Stirling engines can be fueled by almost any type of fuel making the Stirling engine a versatile prime mover. These authors describe fuel cells as, "quiet, compact power generators without moving parts, which use hydrogen and oxygen to make electricity and; at the same time, can provide heat for a wide range of applications." Fuel cells can be useful when power quality or noise present problems for implementation.

There are my different types of prime movers and fuels to power CHP systems. Depending on the required thermal and electrical loads, the optimal prime mover can be chosen to perform the duty required while remaining within emission and fuel consumption requirements. There are many criteria that one must consider before picking a prime mover and the fuel to power it.

2.3 Cooling Technologies

Trigeneration systems distinguish themselves from cogeneration facilities because they provide cooling in addition to heat and power. There are a few options when choosing equipment that can provide cooling for these systems. The majority of trigeneration systems use either absorption chillers or adsorption chillers. These units are beneficial because they are heat powered and provide a use for the recovered thermal energy.

2.3.1 Absorption Chillers

Wu and Wang (2006) describe absorption chillers as devices that use no moving parts and achieve vapor compression of refrigerants with thermal energy. According to Tozer and James (1998) absorption chillers, driven by hot water or steam, were marketed and widely used until the late 1960's. At that time, many engineers began to rule out absorption chillers for use in industrial application because of their large thermal demands. However, Japan developed the technology further, making Japan a leader in absorption chiller production and technology. A two-stage, direct-fired absorption chiller became the unit of choice in the industry at this time. This unit produces cooling by using two absorption cycles, a high temperature cycle and a low temperature cycle. In the high temperature cycle the condenser rejects heat which is utilized in the generator of the low temperature cycle. Trigeneration CHP facilities use either single or double effect direct-fired absorption chillers.

To analyze different absorption and vapor compression chillers, Tozer and James (1998) use the Heat Dissipation Ratio (HDR), which is defined in Equation 2.2.

$$HDR = \frac{Q_a + Q_{co}}{Q_g} = \frac{Q_{co}}{W_{Comp}} 1 + \frac{1}{COP} \tag{2.2}$$

Equation 2.2 presents an inverse relationship between COP and HDR. Tozer and James (1998) demonstrate that a Carnot driving cycle with a reverse Carnot cooling cycle is a closer match to the ideal absorption cycle described herein. An equation to get the COP of this particular system is presented in Equation 2.3.

$$COP = \frac{Q_{ev}}{Q_a} \tag{2.3}$$

Further analysis indicates that the double-effect absorption cycle COP is equal to the product of the driving cycle efficiency and the cooling cycle COP, shown in Equation 2.4.

$$COP = \eta_{dc} * COP_{cc} \tag{2.4}$$

Equations 2.3 and 2.4 provide a preliminary thermodynamic reason for choosing an absorption chiller. Interest in absorption chillers, according to Tozer and James (1998), is on the rise. They state that, "Cold generation systems are those where a cooling process is generated from a heat source such as a combustion process." Many systems are possible with this approach because they are comprised of absorption cycles with internal mechanical compression refrigeration engines. For CHP applications, chillers need to be flexible in how they work because of the variety of fluid temperatures supplied to them. Double-effect units may offer a higher COP; but in turn require a higher incoming fluid temperature to be effective. This principle promotes many CHP plants to use single stage units where the incoming fluid temperature requirement is lower. Tozer and James (1998) present the theory of cold generation systems by deriving the ideal absorption chiller with use of Carnot cycles.

Yoon *et al.* (2003) presents a system that utilizes a double-effect Lithium Bromide water absorption cycle, which utilizes waste heat from exhaust gases of a high temperature generator. In their system, the exhaust temperature is above 200 degrees Celsius, and the heat is recovered from the exhaust with a gas-to-liquid heat exchanger. The chiller has a high temperature and a low temperature generator. This allows the

system to recover the maximum amount of heat, thus increasing performance. Yoon *et al.* (2003) preformed three different experiments; the first two analyzed the performance when using the waste heat to produce heating and cooling versus a standard single-effect absorption chiller, and the third experiment assesed the efficiency of using a starting-time-shortened method for reducing the delay time when switching from heating or cooling. The data collected showed that the COP for heating was increased by 5.1% and the COP for cooling was increased by 2.8%. This shows that the system using two cycles has an increased COP for all heating or cooling loads. The third experiment showed that the authors' method decreased the time required for changing between cooling and heating mode by 9 minutes, from the total of 30 to 40 minutes. Overall, the new systems proposed by Yoon *et al.* (2003) show improvements in existing setups and would be beneficial for implementation.

2.3.2 Adsorption Chillers

According to Wu and Wang (2006) adsorption chillers have a cycle that is very similar to that of a vapor compression system. Adsorption chillers use incoming thermal energy instead of mechanical energy to produce cooling. These systems also adsorb refrigerant gasses into solids, transferring their heat more efficiently.

Critoph (2004) presents a system that utilizes an adsorption chiller with multiple beds of solids to transfer heat. This setup is similar to a counterflow heat exchanger. Critoph (2004) developed a method to use an adsorption cycle in conjunction with a

regenerative cycle that involves multiple low-cost modular beds. The cycle is broken down into two phases: phase one, shown in Figure 2.1, involves using high temperature fluid to produce the cooling effect by evaporation, and the heat for heating directly. The second half of the cycle, displayed in Figure 2.2, is essential a reverse of the first, and engages when the temperature of the fluid reaches a set value. In this system, the fluid used is oil that has been heated by engine exhaust gasses. Critoph (2004) suggests that this configuration, modules in multirow adsorption beds, is capable of producing very high COP values.

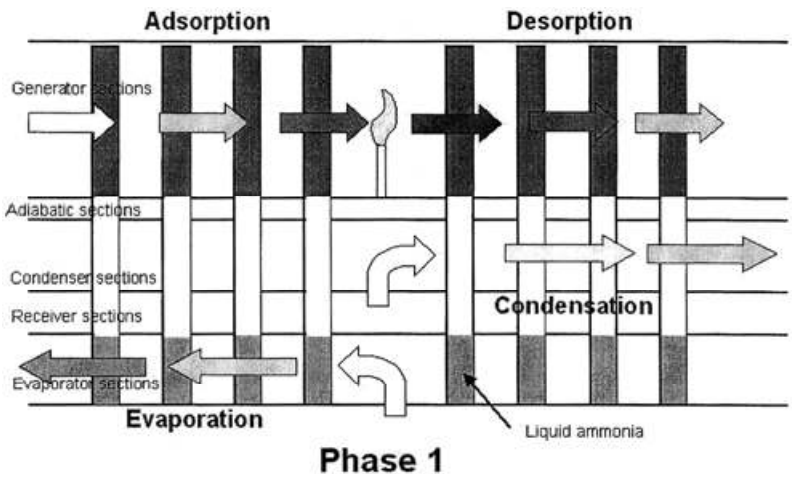

Figure 2.2 Adsorption Cycle Phase 1, Critoph (2004).

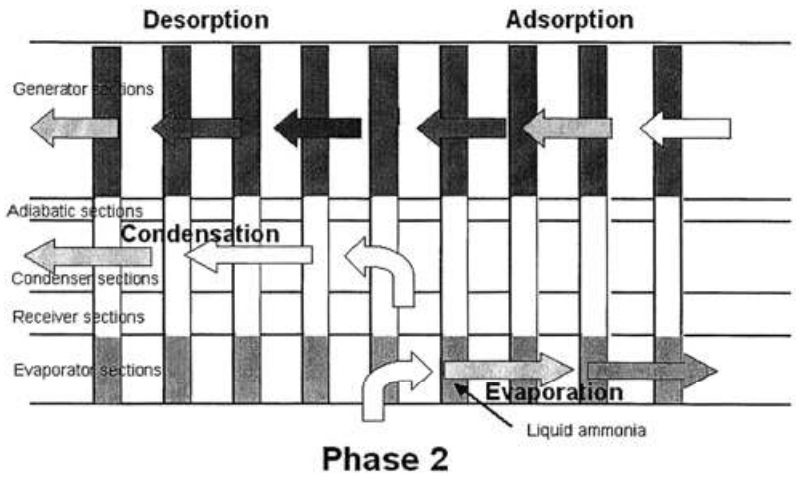

Figure 2.3 Adsorption Cycle Phase 2, Critoph (2004).

2.3.3 Other Types of Cooling Technologies

Other options to produce cooling for CHP exist; some are not widely produced and must be designed on a system-by-system basis. Godefroy *et al.* (2007) present a cooling system when the recovered thermal energy is at low temperature, a common problem with cooling technologies.

The feasibility of CHP systems relies on how well these systems are matched to the electrical and thermal loads of each application. The Mini-CHP systems used by Godefroy et al. (2007) are two SenerTec Dachs Mini-CHP units. Each unit is rated at 5.5 kW electrical output and 12.5 kW thermal output. This Mini-CHP system utilizes an ejector type cooling system that gives better performance in situations where there is a low temperature heat source. Low-temperature heat sources are prevalent in residential systems. Godefroy *et al.* (2007) describe ejector cycles as "a thermo-compressor cycle, in

which the compression effect is achieved using a heat source coupled directly to the ejector to drive the refrigerant out of the evaporator and into the condenser."

The mathematical modeling of the ejector cycle yields a COP, which is then used in the modeling of the entire system. Godefroy *et al.* (2007) used a corrected Keenan model to determine the refrigerant used in the cooling system. HFE7100 was selected as the coolant on the basis that the required pressures were acceptable. With an overall efficiency of 49.8% the system could be cost-effectively used for residential applications.

2.4 Existing CHP Systems

CHP systems are usually customized to fit particular requirements based on the needs of the facility. This customization makes system design difficult without knowing how previous systems are configured. Using knowledge gained from previous CHP systems allows an engineer to choose the best setup for their particular application.

2.4.1 Residential

CHP systems for residential applications can be implemented in single homes, entire neighborhoods, apartment complexes, or hotels. The first system to be examined is a small-scale CHP facility that could be used for either a single home or a small office building. The CHP system described by Kong *et al.* (2005) consists of a double cylinder, four-stroke, water-cooled, natural gas engine which has a power output rated at 12 kW. This prime mover produces electricity at an efficiency of 21.4%, and 28 kW of heat is

recovered from the coolant and the exhaust. Kong *et al.* (2005) uses silica gel-water as the working fluid in the absorption chiller because this fluid improves the chillers performance when the heat source is at a lower temperature. The system was simulated with the electrical loads provided by 60 electric lamps rated at 200 W arranged in a parallel connection. These lamps and connections could be modulated from 600 W to 12 kW to simulate varying electrical loads. Kong *et al.* (2005) made many measurements on the system data gathered by sensors, such as; fuel gas temperature and pressure, air flow rate to the engine, exhaust gas temperature and flow rate, and electrical voltage, frequency and power. This system displayed an efficiency of over 70% and shows that a Micro-CHP system can achieve high efficiencies.

Lin *et al.* (2007) present a household size CHP system. The prime mover of the CHP system investigated by them is a Lister-Petter T diesel engine with a capability to produce 9.5 kW. The generator chosen is a Leroy Somer generator attached to the shaft of the prime mover to produce electrical power equaling 415 Volts and 10 Amps at full load. The last device is the absorption refrigerator used to collect heat and provide for the cooling load. The refrigeration unit is an Electrolux commercially available refrigerator. This system also utilizes emission analyzers that collect data concerning the emissions of the engine. Lin *et al.* (2007) found that the thermal energy recovered from the engine was 5.54 kW during no load and 11.34 kW at full load. The COP from the refrigerator was 0.033 at 50% load and 0.031 at 100% load. Only when the engine was loaded by 50% did the refrigerator have enough heat to operate. Lin *et al.* (2007) proved that trigeneration

systems function at a higher thermal efficiency than separate generation systems, with efficiency increased by 205% to 438%, for 50% load and 100% load respectively.

Paepe *et al.* (2006) describe another residential CHP system in which multiple arrangements of apartment buildings are examined. Three types of residential buildings were presented: detached, terraced, and two story apartments. Paepe *et al.* (2006) used five different types of CHP systems; two with gas engines, two with Sterling engines, and one powered by a fuel cell. Only the two gas engines will be discussed herein. The natural gas engines are a Senertec and an Ecopower, which produce 5.5 kW and 4.7 kW of power, respectively. There are many factors that affect a residential CHP application. The main factor is the load of the building; both electrical and thermal. The situations presented by Paepe *et al.* (2006) describe that for the detached house only about 10 to 15 percent of the energy produced by the generator is used for electricity. The use of a CHP system in a home is only effective if the excess power can be sold back to the power grid. This requirement makes residential CHP systems a less likely choice in the United States, where the housing infrastructure is very different from the European one. For residential CHP systems from an investment standpoint the payback time is not reasonable. Therefore, residential CHP systems must be tailored to operate based on the electrical demand, to avoid having electricity being sold to the grid. Paepe *et al.* (2006) argue that unless the current initial cost of these systems drop by 50%, CHP systems for residential applications are not economically feasible.

Another residential CHP system feasibility assessment, described by Bernotat and Sandberg (2004), utilizes a biomass fired prime mover and pertains to clustered dwellings. As of the late 1940's, Sweden began using district heating to supplement its heating demand, which has expanded to a total of 52 TW by the year 2000. Bernotat and Sandberg (2004) propose conversion and expansion of the district heating systems to CHP systems using biomass as fuel. Bernotat and Sandberg (2004) modeled the local heating demand to locate areas where DG CHP systems would be feasible. The areas shown to have potential were in locations where multiple houses were located in clusters. Clusters, similar to American neighborhoods, have multiple dwellings located in close proximity to each other. Based on this, an area of 36 km by 48 km was chosen as the test area. Bernotat and Sandberg (2004) estimated a theoretical heat demand of this area to be 84 GWh, of which only 7 GWh of heat energy is needed for multi-story buildings. The conclusion was that converting district heating systems to CHP systems is relatively inexpensive and would provide heating and power for local areas. The authors also indicated that the area would have a backup source of power if the nearby power grid fails. Utilizing CHP systems would not only provide benefits, but also reduce the need for fossil fuels consumed at central power producing facilities. Bernotat and Sandberg (2004) summarize the two main concerns with conversion of district heating and CHP systems, "the first factor involves focusing on the total heat demand in an area; the second factor entails defining how long networks can be and still be regarded as efficient or feasible with regard to costs and/or losses."

2.4.2 Hospital

Ziher and Poredos (2006) describe the cooling power costs for a hospital trigeneration system. Cooling can be produced in two ways, from electrical power with vapor-compression chillers or by heat powered absorption chillers. They investigated the possibility of installing a gas engine CHP system in one of Slovenia's biggest hospitals. The upside of a hospital installation is that power, hot water, cold water, and steam are required. This can be an outlet of some of the, possibly excess, thermal energy. Another positive aspect of this system is that it has been allowed to sell its excess electrical power back to the power grid.

Ziher and Poredos (2006) propose that the first law efficiency of a trigeneration CHP system can be described as the cogeneration efficiency multiplied by the coefficient of performance of the chiller, as shown in Equation 2.5.

$$\eta_{TRI} = \eta_{CO} * COP_{CH} = \frac{W_{EL}+Q_{HR}}{Q_f} * \frac{Q_R}{Q_{HR}} \quad (2.5)$$

The costs associated with a chiller can be presented as the sum of the thermal costs, electrical costs, and maintenance costs. Ziher and Poredos (2006) describe that with a relatively simple formula and some information about the electrical and gas costs for different times of the year; then one could easily compute the cooling costs for a particular situation. For the hospital it was found that it averaged at 27.5 Euro's per kWh, or 39.17 Dollars. Another point of interest is the analysis on how the cost-effectiveness, using gas engine and absorption chiller, changes as a function of percent fuel cost change.

At the time this paper was written, 2005, if the gas cost increased by 5% then the gas engine would become less cost effective than using a conventional system. Ziher and Poredos (2006) describe the dependency of natural gas prices on the viability of using natural gas as the fuel of choice in CHP systems.

2.4.3 Agro-Industrial

Designing a CHP system for the agro-food industry has difficulties based on the varied electrical and thermal demands of the facilities. Fantozzi *et al.* (2000) designed a system for an Italian pasta and animal feed factory that displays promise from using an IC engine or gas turbine engine as the prime mover. Fantozzi *et al.* (2000) analyzed the electrical and thermal loads that would be required of the system. The factory is broken down into four sections; the animal food factory, the mill, the pasta factory, and the office complex. The animal food factory has an average energy consumption of 762 MWh/month. The thermal needs for this section come in two parts; the first is saturated steam at 12 bars, and the other is hot water at 80ºC. The mill requires no thermal energy, but requires 416 MWh/month of electrical power. The pasta factory requires an average of 483 MWh/month of electricity, and a thermal requirement of superheated water at 120ºC and 5 bars. The office complex requires hot water at 80ºC and uses 6.3 MWh/month of electrical power. This facility has a variety of demands that must be met. Currently, all the thermal loads are met by natural gas fired boilers which could be improved use waste heat from a CHP system. The most feasible approach concluded

upon by Fantozzi *et al.* (2000) was to use an internal combustion engine that would produce electrical power of 3 MW. Usually when IC engines are used in CHP systems, the heat is recovered in a single pipe and heats water up almost to the boiling point. The factories here require a high temperature line and a low temperature line. Shown in Figure 2.3 is the internal combustion CHP system designed by Fantozzi *et al*. (2000).

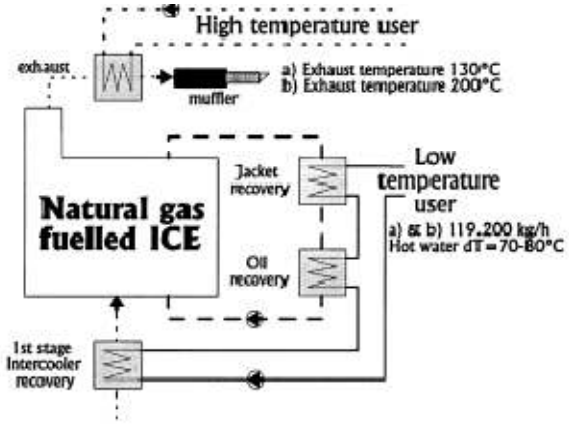

Figure 2.4 Internal Combustion Engine CHP System, Fantozzi *et al.* (2000).

The low temperature line receives heat from the jacket, lubricating oil, and the aftercooler. The high temperature line acquires its heat from the exhaust gas expelled from the engine. An economic analysis of using a single IC engine with thermal recovery reveals a payback period of 3.66 years. Fantozzi *et al.* (2000) shows that by using dual IC engines, the electrical demands of the facility would be met, but the thermal loads would only partially be met. The dual IC engine setup had a payback period of 3.32 years. The payback periods alone present a great improvement in the economic growth for the agro-

food facility, and Fantozzi *et al.* (2000) recommends the CHP system for immediate implementation.

2.4.4 Heavy Industrial

Many problems plague integration of CHP systems into large industrial complexes. Marechal and Kaliventzeff (1998) describe a concept that can help solve this energy integration problem. They use a complex set of graphical data to represent the energy load of the process being examined. The thermal energy flow is represented as a steam network carrying heat to and from locations. This has special advantages when trying to discuss the feasibility of a CHP system because the heat flow is already mapped. In their model, they utilize an mixed integer linear programming (MILP) to map the heat flow from hot and cold streams in which heat is being exchanged. For implementing CHP systems; the authors determine that there are two steps in the process, targeting and synthesis. Targeting involves the preliminary work using the minimum cost of energy requirement, which is done in three steps:

1. Analyze – Assess a list of the utilities and their load requirements.
2. Generate – Use the MILP program to determine the minimum flow rate and heat requirement of the individual components of the system.
3. Evaluate – Use graphical representations of the data to evaluate the results of the optimization.

Synthesis is described as the actual installation of the system. Marechal and Kaliventzeff (1998) describe the most crucial element in the optimization of the system is accurate heat exchange network modeling. This is essentially what has been discussed concerning the steam network, but the heat exchange network deals with the amount of heat transferred to and from steam lines. The authors' methodology enables an engineer to properly model the energy system for CHP system application feasibility analysis.

The system described next was chosen to exhibit large-scale CHP systems prevalent in most industrial applications. Cold storage technologies have been around since 1861 when their primary use was the cold storage of meat. Maidment and Prosser (2000), report that cooling, including the cold storage industry, accounts for 66% of all the energy consumed in the United Kingdom. This energy is used for lighting, vapor compression refrigeration systems, and gas fired boilers for heating. What the authors want to prove is that they could provide electrical and thermal loads more efficiently with a CHP system as opposed to buying power from the existing grid and heating separately with a boiler. They present that by producing the electricity and hot water separately uses 41% more energy than the proposed CHP system. The site Maidment and Prosser (2000) consider a cold storage facility with a storage space of 129,222 cubic meters. The site also has office areas, ambient storage, and chilled storage. The proposed CHP system is presented in Figure 2.4.

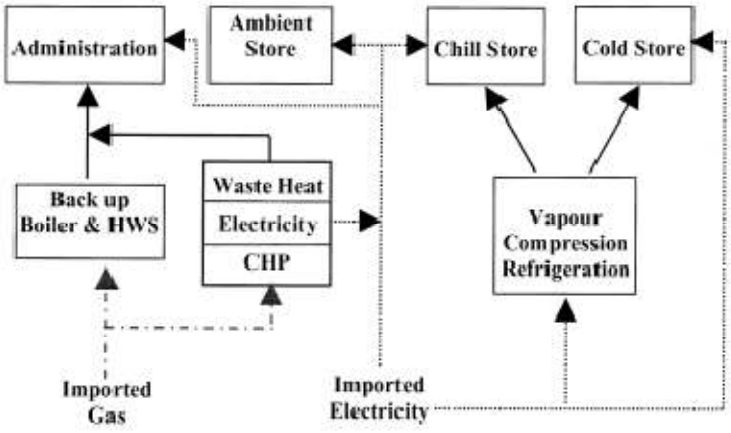

Figure 2.5 Cold Storage CHP System, Maidment and Prosser (2000).

The analysis of the CHP system proposed by Maidment and Prosser (2000) displays a payback period of 10.6 years. The authors show that because the CHP system was not utilized to its full potential. Despite this, after the payback period, a cost savings of 5098 pounds sterling, $8293, was predicted annually. The authors suggest a way to get the payback period down to 4.5 years by using absorption chillers to provide cooling for the chilled storage.

Soares *et al.* (2001) indicate that Brazil's power infrastructure has shifted to natural-gas fired generators. One reason for the power structure shift includes the fact that Brazil has a very unstable energy economy. With an unstable energy grid, using a number of cheap inexpensive power production facilities have the benefits of being more reliable. Soares *et al.* (2001) presents two case studies using cogeneration feasibility. The two applications are a chemical plant and a pulp mill. For these situations to be considered in Brazil, they would have to show an internal rate of return higher than other investments

with no appreciable risks. The chemical plant, which burns fuel oil in boilers to generate electrical power, has an electro-mechanical demand of 29.7 GWh/year. Soares *et al.* (2001) determined that for a CHP system to be feasible, the monetary savings must outweigh the costs of implementation. The authors recommend that another benefit of implementation is the CHP system will provide the facility more electrical power stability. The next site considered is the pulp mill. The electrical load for the mill is .85 MWh per ton of pulp produced. A particular item of consideration for pulp mills is that there is a byproduct that can be used to produce energy; black liquor. This substance is produced at a rate of 1 to 1, unit of pulp to black liquor. The black liquor is then used as fuel in a Rankine cycle to produce electricity. The problem with the Rankine system is the low efficiency associated with the particular cycle used, 18.5%. The feasibility analysis for this system presented by Soares *et al.* (2001) includes a natural gas-fired CHP system to cover the 51.5% of the thermal demand and 19% of the electrical demand for which the black liquor does not provide. These values make this situation very appealing for CHP application. The plan proposed by Soares *et al.* (2001) is to size the CHP system to produce 20% more electrical power than required. This electrical power could be sold back to the grid, allowing it to meet the thermal load of the facility.

2.4.5 Power Production

Pollution and the energy gap has driven the world's engineers to push for more efficient use of energy resources. CHP systems are viable options when there are

demands for power and process heat in a facility or operation. Oztop and Hepbasli (2006) present information describing the cogeneration and trigeneration applications in Turkey. Turkey's electrical demand is growing 7% yearly, increasing the need for new ideas and sources of electrical power. Beginning around 1992, Turkey began using distributed generation as a method for significant power production. In 1994 there were only four cogeneration facilities with a total energy output 30 MW, but by 1999 10% of their total energy requirements were produced in distributed generation cogeneration facilities, amounting to approximately 2000 MW of power. After this point legislation was passed that gave 100% tax exemption to companies who produced their own power through a cogeneration facility. That legislation also required that any excess electrical power produced from these facilities would be purchased by the Turkish electrical distribution company. This led to a boom in cogeneration implementation.

Despite the success of cogeneration in Turkey, primarily from the legislation passed, Oztop and Hepbasli (2006) report only a few trigeneration applications in Turkey based on it being less developed than its cogeneration counterpart. Turkey has made some improvements in the area of trigeneration and presents itself as a leader in the area. The success of CHP systems in Turkey will increase in the years to come.

Energy conservation and efficiency for CHP systems are very important. Exergy analysis can be very important and informative. Balli *et al.* (2008) suggest an exergy analysis that allows the energy losses to be determined in an effective manner. They combined a typical exergy analysis with an economic one to result in an analysis that

yields the cost of inefficiencies in individual components as well as the system as a whole. Their study was of the Bilkent CHP power plant in Turkey. The system consists of a gas turbine generator and heat recovery steam generator. The steam generator utilizes the waste heat from the gas turbine to produce steam which is dispatched to two other turbines, one which utilizes steam at high pressures and one which utilizes steam at low pressures. The two main components of interest in the study conducted by Balli *et al.* (2008) are the exergy destructions, due to irreversibilities in the system, and the exergy losses, due to energy lost to the environment. Adding in the economic aspect, produces multiple equations that allow the present worth, annual fuel cost, and the cost of operation, including maintenance to be computed. Their results display a very promising CHP facility with an exergetic efficiency of 38.3% and the total cost to be$ 3429.85 per hour while it produces 185.31 GW. The total exergy cost of the products was calculated to be $18.51 per GW. The authors compared this value with several results and found that the comparison articles produced value very similar to the value found here. The differences were accounted for by the difference in the power production capabilities and the setup of the individual systems.

2.4.6 Stand-Alone Micro-CHP Systems

Recent improvements in CHP technologies have made possible the production of all-in-one Micro-CHP units. These units are typically used in an apartment or single-family home and provide heating and power, implemented in a similar manner as a

boiler. The difference in these units is that in addition to providing the heat that a boiler does; they also provide electrical power to power the house or to sell back to the power grid. Thomas (2008) presents multiple Micro-CHP units and an analysis of their performance. These units are not trigeneration, as they do not produce cooling, but cogeneration units.

The first unit to be tested by Thomas (2008) is the SenerTec "Dachs." This unit is the market leader with over 17,000 units sold. This unit is able to use a variety of fuels such as natural gas, Diesel, heating oil, and biodiesel. The engine can operate as either an Otto or Diesel cycle engine. The electric power is produced by an asynchronous generator. The primary thermal energy is obtained through the engine coolant, but a separate thermal heat exchanger can be purchased and installed to recover exhaust heat. The model used was the Dachs HKA G 5.5 and utilizes a single-cylinder, 4 stroke, natural gas fuelled engine. It produces 5.5 kW of electric power and 12.5 kW of thermal power. Since this unit can only operate at full load, the ability to sell power to the grid is a must to maintain profitability. The results from this very efficient Micro-CHP unit are an electrical efficiency of 27.7% and an overall efficiency of 91.3% with the exhaust heat exchanger implemented.

The next unit examined by Thomas (2008) is the SOLO Stirling 161 Micro-CHP unit. Currently compatible fuels are natural gas and LPG, yet some have seen success with fuels such as syn-gas, wood pellets, and even solar powered models are available. The unit includes a 2-cylinder Stirling engine with a swept volume of 160 cc's and is in

an alpha configuration. Helium is used as the working gas for the CHP units, whereas the solar models utilize Hydrogen. This unit provides an output of electrical power from 2 to 9 kW and a thermal output of 8 to 26 kW. This unit at full-load displayed an electric efficiency of 26.8% and an overall efficiency of 98.5%. In a partial-load the electrical efficiency was lowered to 24.8%, and the overall efficiency was lowered to 95.1%.

The third unit was manufactured by PowerPlus Technologies and is called the Micro-CHP Ecopower. This unit incorporates a four-stroke engine that is capable of being fuelled by natural gas or LPG. This unit provides 4.7 kW of electrical power and 12.5 kW of thermal energy and is capable of variable output allowing it to vary its speed to provide the needed power without wasting the excess. The electrical efficiency varied from 24.7% to 24% at full load and part load, respectively. The overall efficiency varied from 88.9% to 84.5% at full load and part load. This unit is smaller than the previous units, but is still very efficient.

The final unit surveyed by Thomas (2008) was a SM5A manufactured by Stirling Denmark. The SM5A unit is the status of a pre-production prototype that utilizes biogas and natural gas. As with the previous Stirling engine, the working gas is Helium, and it cannot vary speed, thus, it is locked in to produce 9 kW electrical and 25 kW thermal. The SM5A unit shows electrical and overall efficiencies of 20.8% and 84.5%, respectively. This unit, while having the lowest efficiency of the group, is relatively efficient when compared to the separate generation of power and heat.

2.5 Micro-CHP Modeling Efforts

Multiple studies on modeling a Micro-CHP system have been evaluated to be presented herein. Models for Micro-CHP systems are crucial to maximizing the performance whether for cost, resource efficiency, or emissions. These three factors are the primary focus of modeling efforts to optimize a CHP system.

Mago *et al.* (2007) examined non-economical aspects for CHP system feasibility. Two primary benefits presented are, first, CHP systems are inherently energy efficient, and second, CHP systems exhibit typically lower emissions. When a building is particularly energy efficient, it can qualify for different certifications such as Energy Star or Leadership in Energy and Environmental Design (LEED). The emissions examined are the typical greenhouse gases such as CO_2, NO_x, and SO_2. Typically buildings' receive power from coal fired power plants, which are heavy polluters; whereas CHP system produce their power on-site and can burn a cleaner or renewable fuel. Two particular cases were examined by Mago *et al.* (2007). In case one the building's monthly energy consumption was known and, therefore, yearly totals could be computed. For case two the building's annual energy consumption was known and the monthly energy consumptions were found by using the degree-day method as described by ASHRAE. For both cases there were four locations examined in the United States; northeast, midwest, south, and west. Number of occupants, energy consumption, and hours of operation were examined. CHP systems resulted in a drastic increase in the Energy Star Rating. The largest increase was 56 points, while the least was 41 points. The emission reduction for

CO_2 was found to be as high as 60%. The reduction for NO_x and SO_2 emissions were shown as 82% and 90% respectively. This study presents the other benefit of CHP systems, aside from the possible economical ones.

The model developed by Moran *et al.* (2008) was for a Micro-CHP system using either a spark ignition or compression ignition engine as the prime mover. This model also includes evaluation of the heat exchangers, boiler, and absorption chiller. The performance characteristics to be evaluated are maximum fuel consumption, total monthly fuel consumption, and system energy efficiencies, which are broken into electrical, thermal, and total. To compare the different prime movers, the systems were modeled as if they were operating at a constant maximum power, indicating that the excess power will be either sold to the power grid or stored in some way. For the model, several assumptions were made, such as, the combustion process will be approximated as a heat addition from an external source. Moran *et al*. (2008) ran the simulation based on their model using a 10 kW prime mover, and a 10 ton absorption chiller with a COP of 0.8. The assumed heat exchanger effectiveness and boiler efficiency are 0.8 and 0.9 respectively. The model was based on a 4300ft^2 building in Meridian, MS which operates from 7:00 a.m. to 7:00 p.m., Monday through Friday. The results from the simulation displayed that the compression ignition engine consumed less fuel than the spark ignition engine due to the greater efficiency from a higher compression ratio. The total efficiency ranged from 75-80% in the summer to 70-73% in the winter.

Fumo *et al.* (2008) propose an operational strategy through modeling that suggests CHP systems operate based on maximum fuel energy savings. For this model a new comparison parameter, the Building Primary Energy Ratio (BPER), is proposed. BPER is a ratio of actual building energy usage to CHP system building energy usage, thus returning a value greater than one when CHP system energy usage is less than actual building energy usage. When a value greater than one is found, the building should use the CHP system. Fumo *et al.* (2008) utilizes this value to determine CHP system feasibility based only on Primary Energy Usage (PEU). The results from this model suggest that cooling operation increased PEU, thus a BPER less than one was found. For heating operation, the PEU decreased.

Fumo *et al.* (2009) describes the impact on Site Energy Consumption (SEC) for buildings. They proved that the SEC increases with use of CHP systems. Three operational modes were analyzed: cooling, heating, and power; heating and power; cooling and power. The SEC increase considering cooling was more significant than for heating alone. One common misconception is the difference in Primary Energy Consumption (PEC) and SEC; the PEC and PEU are can be used interchangeably. SEC is the consumption of energy at the point of entrance to the building. PEC is SEC plus losses that occur in the generation and delivery of energy.

Mago *et al.* (2009) indicate that the operation of a CHP system is highly dependent on seasonal electrical and thermal loads. This operation can be controlled in several ways. The two simplest operation modes are to operate the prime mover

Following the Thermal Load (FTL) or Following the Electrical Load (FEL). Factors such as the ability to sell power back to the grid if excess is produced and the price of natural gas versus the price of electricity must be considered before adopting an operational strategy. FTL or Thermal Demand Management (TDM) uses the prime mover to satisfy for the thermal demand, which typically produces excess electricity. FEL or Electrical Demand Management (EDM) requires that the prime move only produce the required electrical power, while usually the recovered thermal energy is insufficient to meet the demand. Mago *et al.* (2009) utilized these operational modes in a model to presents the effect of FTL and FEL on PEC, operational cost, and CO_2 emissions. The model examines four cities in different regions and utilizes site-to-primary energy conversion factor to adjust for comparison to large scale power production facilities. The results of the simulation proved that FTL was a better strategy for PEC, operational cost, and reduction of emissions.

The study by Fumo *et al.* (2009b) demonstrated that an economic analysis of a CHP system without consideration of primary energy savings could yield misleading results. Also the authors present that by using a primary energy operational strategy, the facility will increase primary energy savings and reduce operational costs. The primary energy operational strategy utilizes the BPER. Operation is dictated by this ratio indicating when the Primary Generation Unit (PGU) should be operated. The model was modified to implement the primary energy operational strategy utilizing BPER. The analysis considered eight cities with varying nominal PGU efficiencies, ranging from .25

to .35. The primary energy use was reduced as much as 16% using the CHP systems. The authors note that primary energy savings do not necessarily result in cost savings. The primary energy savings operational strategy sees an additional 5.4% cost savings in some of the cities examined. Fumo *et al.* (2009, 2) concludes that BPER operational strategy should always be used if maximum energy savings is the target. In some instances the costs were increased, indicating an economic analysis is required to determine the viability of implementation of CHP systems.

The model presented by Fumo *et al.* (2009c) compares conventional cooling system vapor compression with that of a hybrid system using both absorption chillers and a vapor compression system. This model assumed that the generating efficiency and performance of the components to be a constant. The results of the model were presented for two cities, one northern city and one southern city. The differences in these locations were the heating degree days, and cooling degree days. The results demonstrate that for the location with more heating degree days the CHP system efficiency was greater than that for the location with less due to the relative inefficiency of the absorption chiller. This study examined the PEC reduction in using a hybrid system based on which unit would offer the greatest PEC. For the PGU at 25% efficiency both cities used much more vapor compression than absorption chiller. At 30% energy efficiency the southern city used more vapor compression than absorption chiller, while the northern city used only slightly more vapor compression than absorption chiller. This information confirms the

viability of using a CHP system with a hybrid cooling system to achieve greater PEC reduction.

The model examined PEC, Carbon Dioxide Emissions (CDE), and operational costs in the optimization for multiple climates to investigate the effect of location on the performance of the system. Cho *et al.* (2009) used a model previously created, which uses an optimal energy dispatch algorithm, which identifies the optimal operating mode. A network flow diagram assists in the linear programming involved in the model. The network flow diagram breaks the system up into nodes showing the energy flow, either as fuel, electrical energy, or heat. The nodes are presented as demands or component in the system. The optimization strategy was evaluated for five cities: Columbus, MS; Minneapolis, MN; San Francisco, Ca; Boston, MA; and Miami, FL. The results of the simulation revealed that there were no common trends between the three optimizations; thus, only one city, Columbus, MS, will be discussed herein due to its relevance to the Micro-CHP demonstration site at Mississippi State University. For Columbus, MS all optimization modes, PEC, cost, and CDE, resulted in a trend. PEC and CDE decreased for all three optimization modes, while the costs increased for all modes. Despite no common trend between cities, the model presented by Cho *et al.* (2009) could be applied to any city and any building to determine CHP system feasibility.

Mago *et al.* (2009b) presents the final model to be discussed. This model focuses on analyzing and optimizing different operational strategies for energy savings, operational cost, and environmental impact. The authors present an optimized Hybrid

Electric-Thermal load operational Strategy (HETS). Mago *et al.* (2009b) discuss the previously mentioned FEL and FTL operational strategies. Three optimization criterions are input into the model: Primary Energy Optimization (PE-O), Operational Cost Optimization (OC-O), and Emission Reduction Optimization (ER-O). The HETS operational strategy is used because trigeneration CHP systems operate at peak efficiency when the thermal and electrical loads are matched. Another important item discussed by Mago *et al.* (2009b) is the Performance Factor Indicator (PFI). This is used because PFI allows for examination of PEC, cost, and CDE. The defination for PFI is presented below.

$$PFI = \frac{PEC_{CHP}}{PEC_{Conv}} + \frac{Cost_{CHP}}{Cost_{Conv}} + \frac{CDE_{CHP}}{CDE_{Conv}} \quad (2.6)$$

Although one can optimize systems to maximize any particular attribute; PEC, cost, or CDE; the effect on the other parameters must always be considered.

2.6 CHP Legislation

Legislation passed promotes the implementation and use of CHP technologies. According to Cardona *et al.* (2005), in 1978 Congress presented the Public Utilities Regulatory Policy Act (PURPA). This legislation was the first to promote high efficiency technologies and assist the CHP system market. Recently, the DOE and the Environmental Protection Agency (EPA) presented a goal of doubling the power generation from CHP systems in the country from 48 GW to 92 GW by 2010. Many different incentives are provided to business and building owners to use CHP systems in

their respective applications. The EPA and DOE have various awards that are given to business that adopt CHP systems. The best known of these awards is the Energy Star Award and the CHP system Certificate of Recognition. In California, the energy market has shifted to using a program called the Self-Generation Incentive Program that offers incentives of $1.00 per watt of clean distributed generation plants up to 1 MW. California is the first state that has interconnected power generation and utilization grids and is the most CHP system promoting state. Most CHP system facilities utilize natural gas as a fuel, and the fluctuating prices of natural gas may deter CHP systems as a whole. The United States has only a few states that promote CHP system use. This has created a poor market equilibrium, which as of now does not satisfy the minimum standards for energy services.

In 1997 the DOE conducted a five lab study to examine the potential for programs and policies to create clean and efficient energy to avert the threat of a global climate change from pollution. Lemar (2001) speaks on the follow-up to this study dubbed *Scenarios for a Clean Energy Future* (CEF). He explained that the CEF study used various methods to analyze the impacts of such policies to achieve their goals. Changing existing policies was determined to be the quickest method of making discernable changes in emissions. Lemar (2001) describes that the CEF's primary goal was to examine new clean energy technologies addressing emissions, and energy changes in the near future. There were three different models used: business as usual, moderate, and advanced. The business as usual model would signify that no new policies would be

enacted and only present goals would be attained. Moderate and advanced models would indicate enhanced tax benefits for states with CHP systems and distributed generation systems as well as other incentives and regulations. The data attained by the CEF come from the Energy Information Administration (EIA) National Energy Modeling System (NEMS). Lemar (2001) interpreted the data in the following ways: moderate models would attain a 50 percent increase in CHP system and DG research and development budget from the government and increased tax credits for states using these systems. Another advantage of the moderate model would be the removal of some utility barriers by enactment of the national interconnection standard allowing CHP and DG systems to be able to sell excess electricity back to the grid. Advanced models show a doubling in research and development budget for CHP systems and DG technologies expediting some of the certification and permit requirements for CHP systems and DG technologies;,thus easily increasing their growth and implementation. Lemar (2001) presents data pertaining to this setup in Figure 2.5.

	Moderate		Advanced	
	2010	2020	2010	2020
Fuel used by CHP (TBtu)	627	1,991	1,579	4,434
Fuel displaced by CHP (TBtu)	277	873	743	2,097
Electricity generated by CHP (TWh)	71	179	227	501
Net heat rate (Btu/kWh)	4,944	6,246	3,683	4,665
Heat rate of combined cycle (Btu/kWh)	6,389	6,389	6,389	6,389
Improvement of CHP over combined cycle (%)	22.6	2.2	42.4	27.0

Figure 2.6 Moderate and Advanced Modeling Data, Lemar (2001).

Figure 2.5 presents the advantages of pursuing a moderate or advanced policy. There are many improvements that must be made to CHP system policies to achieve implementation on a large scale; this method could present real results if action is taken.

CHAPTER 3

EXPERIMENTAL APPARATUS

The demonstration site began construction in 2005. The work for this study began with finalizing the instrumentation to the system. This consisted of ordering, calibrating, and installing various sensors. In addition, LabView programs were created to analyze the data and to provide results in real time as the raw data are collected. The data collection began on December 18, 2008 and was completed on the end of the next cooling season. During this time the data collection proceeded with as little down time as possible. Using the knowledge gained from the instrumentation of the natural gas engine, a diesel engine was also instrumented, although that engine is not part of this study. In this chapter the systems components, instrumentation, and the data acquisition system will be presented.

3.1 System Components

The demonstration site is made up of multiple components. The building can be operated under CHP system power or under grip power. The CHP system components will be discussed first.

The prime mover is a 15 kW Olympian IC engine fueled by natural gas. The model number for this engine is G15U3S. The prime mover is presented in Figures 3.1 and 3.2.

Figure 3.1 Generator Outside View

Figure 3.2 Generator Inside View

The heat recovery is performed by two heat exchangers. The first heat exchanger transfers heat from the engine exhaust to the engine coolant. This heat exchanger is a VaporPhase Model ECXWD-640-0.875 manufactured by Kickham Boiler Inc. A picture of this heat exchanger can be seen in Figure 3.3.

Figure 3.3 Exhaust-Coolant Heat Exchanger

The second heat exchanger, displayed in Figure 3.4, is a Flat Plate FP 5X12L-12 which transfers heat from the engine coolant to the heat recovery line. A schematic of the heat recovery piping network is shown in Figure 3.5.

Figure 3.4 Coolant-Heat Recovery Heat Exchanger

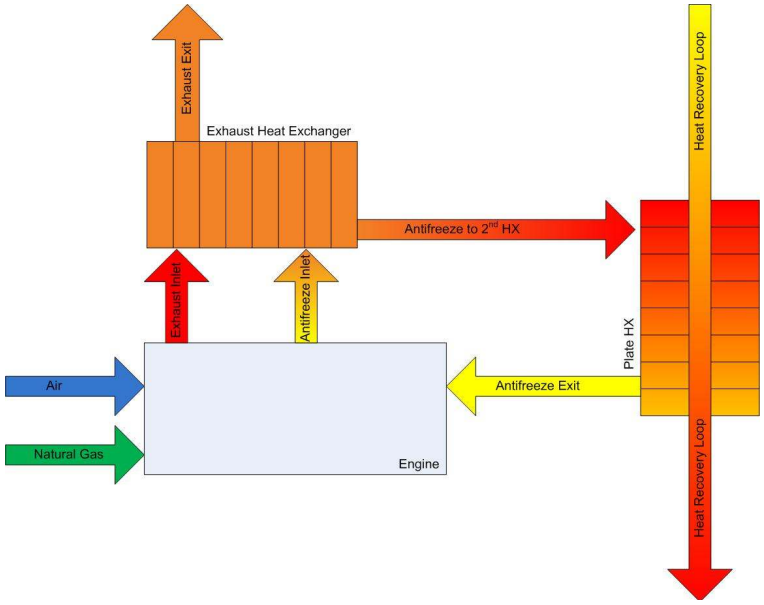

Figure 3.5 Heat Recovery Schematic

The CHP systems operates FEL, thus the electrical power produced is equal to the electrical power requirements of the building. This operation meets the electrical demand, but does not always meet the thermal demand. When the waste heat is not enough to

satisfy the thermal demand, an auxiliary boiler is used to supplement the heat. The boiler used is a Laars Mighty manufactured by Teledyne. This two-stage boiler has an input of 200,000 BTU/hr and is fueled by natural gas. A picture of the boiler is displayed in Figure 3.6.

Figure 3.6 Auxiliary Boiler

A Yazaki WFC-SC10 10-Ton water fired absorption chiller is used to meet the building cooling load, presented in Figure 3.7

Figure 3.7 Water Fired Absorption Chiller, Yazaki Energy Systems

The absorption chiller makes use of a 25-Ton Marley Model 492A cooling tower, presented in Figure 3.8.

Figure 3.8 Cooling Tower

The CHP system's HVAC uses a Trane FCAB 080 four-pipe air handling unit. This unit uses four water pipes, two hot and two cold, to heat or cool the air space by using the appropriate heat exchanger coils. The unit's capacity is 20,000 BTU/hr for heating, and 2 Tons for cooling. This unit is displayed in Figure 3.9.

Figure 3.9 Four-Pipe Fan Coil Unit

During conventional operation, the building cooling load is met by a Trane high efficiency unit with a SEER of 15.25. This is a split unit which produces heating and cooling by separate systems. The cooling is provided by a high efficiency vapor-compression system with a capacity of two Tons of cooling. This unit is pictured in the Figure 3.10. The heating requirement is fulfilled under conventional operation by a condensing furnace that preheats the combustion air to improve efficiency. The furnace has a input capacity of 60,000 BTU/hr.

Figure 3.10 Conventional Vapor-Compression System Condensing Unit

3.2 Instrumentation

The system has been fully instrumented and collects data from multiple sources. This system includes temperature sensors, flowmeters, pressure sensors, and relative humidity sensors. The first sensors to discuss are the temperature sensors.

3.2.1 Temperature Sensors

There are four types of temperature sensors implemented into the system. The first temperature sensor type to be discussed is used to measure pipe fluid temperature. These sensors have been installed so that there are two sensors measuring temperature in each location. These sensors have been upgraded to a more accurate sensor to decrease the uncertainty in the measurements, which will be discussed in more detail in Chapter 5. The initial temperature sensors were Minco model number S884PE2Z108. These sensors

are Resistance Temperature Detectors (RTD) that use resistance to measure temperature. They are Class C RTD with an uncertainty calibrated to 0.5°C, and they have a range of -50°C to 260°C. The new temperature sensors used in the water pipes from Minco model number is S554PM28Z108. They are Class A RTD's with an uncertainty of (0.15 + 0.002*Temperature) °C, meaning their uncertainty is dependent upon the nominal temperature. At 100°C, these sensors have an uncertainty of only 0.35°C. These sensors are tip-sensitive and only require the tip of the sensor to be in contact with the fluid to get a correct temperature reading. The new temperature sensors gave resistances that had to be converted to temperature. The old sensors were very inaccurate and required in-house calibration. The curve-fits resulting from the calibration were used to compute temperature from resistance. The new sensors use a modified Callendar-Van Dusen equation to present resistance as a function of temperature. For temperatures above 0℃:

$$R_T = R_0(1 + A * T + B * T^2) \tag{3.1}$$

Where, A and B are constants equal to 0.0039083 and -5.775E-07, respectively. For this investigation, the temperature as a function of resistance can be solved as a quadratic equation presented in Equation 3.2.

$$T_R = \frac{-A+\sqrt{A^2-4*B(1-\frac{R_T}{R_0})}}{2*B} \tag{3.2}$$

This equation is used as a sub-program to the Data Acquisition (DAQ) system called a SubVI. The flowchart for the RTD SubVI is presented in the next chapter, and the program is displayed in Appendix H.

These sensors are mounted in copper wells that are brazed into the water pipes and filled with OT-201 Omegatherm thermally conductive silicon paste from Omega to ensure maximum thermal conduction from the fluid to the tip of the sensor. A picture of this type of temperature sensor is shown in Figure 3.11.

Figure 3.11 Fluid Pipe Temperature Sensors

The next temperature sensor to be discussed is the exhaust RTDs. Because these RTDs had to be capable of withstanding very high temperatures, they were selected with a temperature range of -200°C to 850°C. These sensors are manufactured by Minco with a model number of S99306G60Z845, and have an uncertainty rated as a class B sensor. This uncertainty is (0.3 + 0.005*Temperature) °C. A picture of these sensors is presented in Figure 3.12.

Figure 3.12 Exhaust RTD Sensors

The temperature sensor used to measure ambient and ground temperature is manufactured by Omega with a model number of 1PT100FR828. These are Class B sensors. As with the Class A sensors the uncertainty varies with the nominal temperature. The ambient temperature sensors were placed outdoors in a location that would not be in direct sunlight. The ground sensors were placed three feet into the earth to assure an accurate ground temperature measurement. This type of sensor is displayed in Figure 3.13.

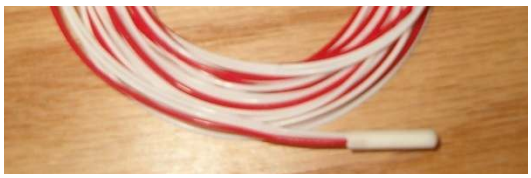

Figure 3.13 Ambient and Ground Temperature Sensors

The final temperature sensor is the air flow temperature sensor used to measure the air temperature in the HVAC intake and exit duct. This is needed to accurately compute the heat transfer to the air space. These are TE200DC sensors manufactured by

Graystone. These sensors have two components: the sensor and the transmitter. The sensor element has a range of 0°C to 70°C and an uncertainty of 0.06% of the reading. The transmitter has a range of -40°C to 85°C with an uncertainty of 0.1% of the full scale, which is evaluated at 0.125°C.

3.2.2 Flowmeter Sensors

There are three types of flowmeters used in the system. The first type is a turbine flowmeter that is used to measure liquid flowrate. This flowmeter operates by taking a pulse reading from the turbine and converts that into 4 - 20 mA output that is read by the DAQ system, which is then converted to its corresponding flowrate. This type of flowmeter is configured depending on the range of flows in the pipe and upon the size of the pipe. These flowmeters are manufactured by Omega with the model number FTB-90X, where the X represents the different configurations. These flowmeters convert signal pulses to the output. The signal conditioner used is also from Omega, model number FLSC-62A. The uncertainty for these meters is .5% of the reading. This flowmeter is displayed in Figure 3.14.

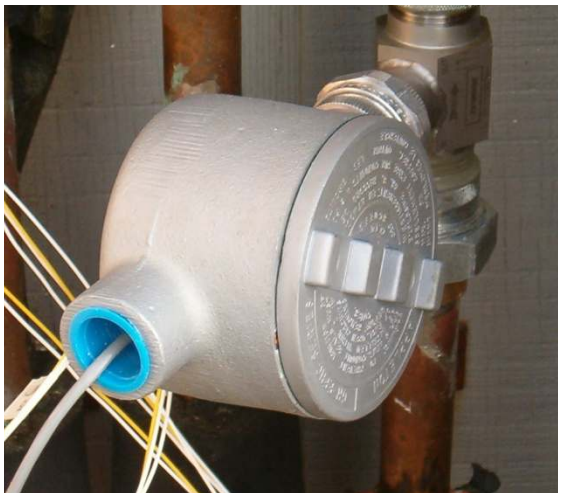

Figure 3.14 Turbine Flowmeter

The flowmeters used to measure natural gas flowrates are placed on the engine, boiler, and the conventional non-condensing furnace. The manufacturer for these flowmeters is FloCAT, and they have the model number LA10. These flowmeters must be sized according to the maximum flowrate for the natural gas through them. The engine and the boiler have a maximum flowrate of 250 L/min, and the conventional condensing furnace has a maximum flowrate of 100 L/min. The uncertainty for these units is 1% of the full-scale of the flowmeter. A photo of this type of flowmeter is depicted in Figure 3.15.

Figure 3.15 Natural Gas Flowmeter

The flowmeter used to measure air flowrate in the ductwork work by measuring the differential pressure in the duct. These flowmeters have two components, pressure sensors and differential pressure transducers. Two sensors spaced evenly apart are used in each duct to get an accurate reading. The pressure sensors are made by Omega, model number PX655-0.5DI. The differential pressure transducer is manufactured by Paragon Controls Incorporated. The FE-1000 has an uncertainty rated at 2% of the reading. This flowmeter can be seen in Figure 3.16.

Figure 3.16 Differential Pressure Transducer for Air Flowrate

3.2.3 Relative Humidity Sensors

The first sensor is used to find the relative humidity of the air at the inlet and outlet to the HVAC system. The sensor presented in Figure 3.17 was manufactured by Omega with the model number HX94C. The uncertainty of these sensors is evaluated at 2% of the reading.

Figure 3.17 Relative Humidity Sensor

The other type of relative humidity sensor acquires the relative humidity for ambient outdoor conditioning. This HX/HR 91X sensor is manufactured by Ohmic Instruments.

Figure 3.18 Ambient Relative Humidity Sensor

The ambient humidity is very important in calculating ambient enthalpy. This sensor has an uncertainty rated at 2% of the reading, and can be seen in Figure 3.18.

3.2.4 Pressure Sensors

These sensors are located at almost every location that temperature is measured and can be used to determine the thermodynamic state of a fluid. The pressure sensors are manufactured by Cole Palmer, model number EW-68073-10. This instrument has a range of 0 to 50 Psi and uncertainty of 0.065 Psi. This instrument is displayed in Figure 3.19.

Figure 3.19 Pressure Sensor

3.2.5 Power Sensors

The final piece of instrumentation is used to determine the power generated or used by different components of the system. All of these components are manufactured by Ohio Semitronics. The first device, model number PTB412EI, is used to compute the

power generated by the engine. This is done by calculating the current and voltage separately and finding the power by Equation 3.3.

$$P = I * V \tag{3.3}$$

This instrument has a maximum range of 150 V and 100 A. The uncertainty of the PTB412EI is 0.5% of the full scale of the instrument. The remaining instruments detect current and are model ACT. They measure current through a wire or bundle of wires. They vary in the maximum current they can detect from 20 A to 50 A. These current transducers have an uncertainty rated at 0.25% of the full scale.

3.3 Data Acquisition System

The DAQ system refers to the manner in which the signals from the instruments are manipulated and recorded into a database. Most signals from the instruments have the output of 4-20 mA. Following the instrumentation, the cables are routed to quick disconnect terminal boxes to make maintenance and debugging simpler. Next, the cables are routed to National Instruments (NI) FieldPoint Modules. There are two primary types of these modules: RTD modules and Analog Input (AI) Modules. The AI modules are used to process any 4-20 mA signal. The AI modules has an uncertainty rated at .04% of the reading. The RTD modules have an uncertainty of 0.25°C. An AI module can be observed in Figure 3.20. Each of these modules can process up to eight signals and can be placed in an array as displayed in Figure 3.21.

Figure 3.20 Analog Input Module

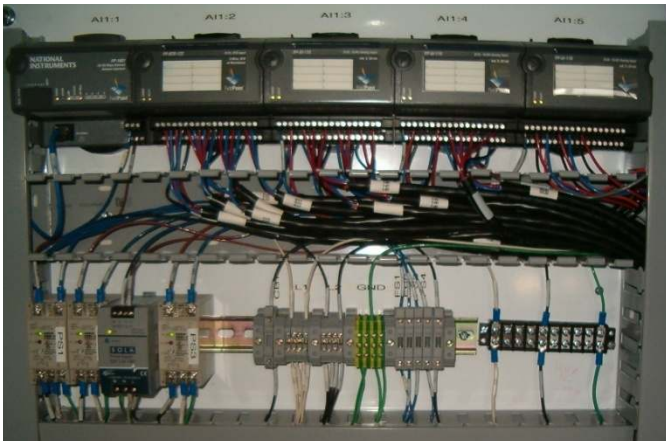

Figure 3.21 DAQ Panel

The DAQ arrays transmit the collected information to a computer through ethernet cables. The computer makes use of NI LabView Virtual Instruments (VI) to process the collected information. There are two primary VI's used, the diagnostic program and the database program. This first program is used to present real-time raw information pertaining to the system. Also displayed in the diagnostic program are various performance calculations; including cost, heat transfer, etc. Another useful thing about this program is that there are balance checks on the system to detect error in the

instrumentation, which will be further discussed in Chapter 5. A screenshot of this program is shown in Figure 3.22.

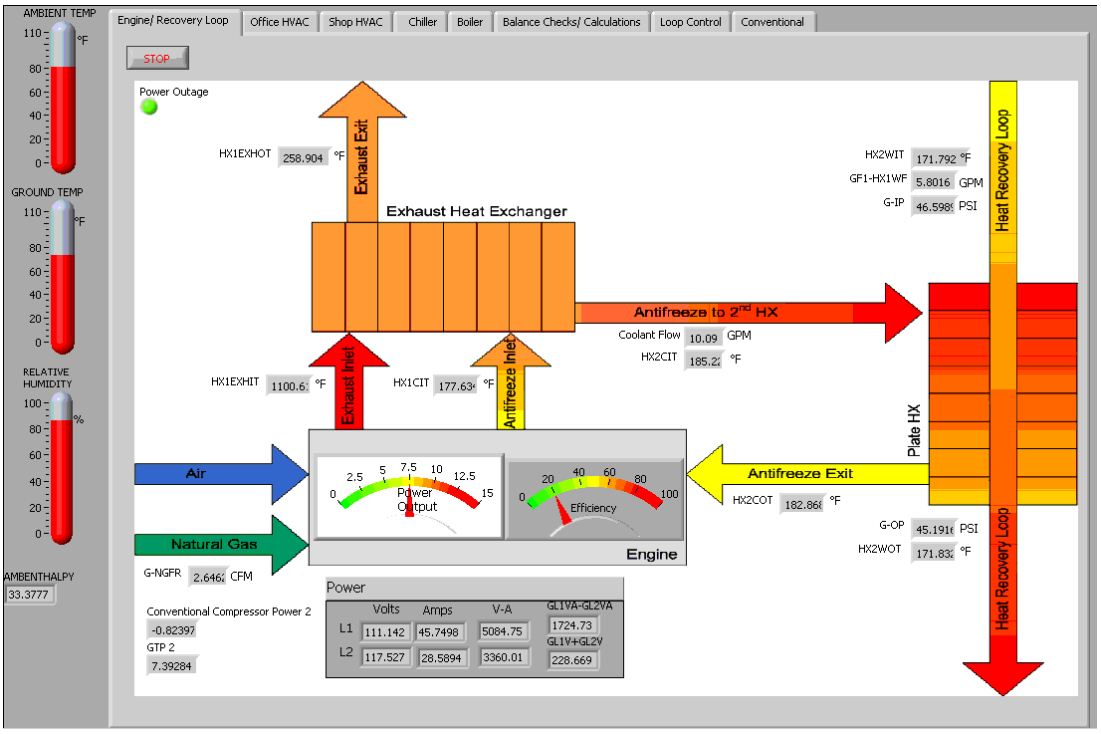

Figure 3.22 CHP Diagnostic LabView Program

The second program is the database program. This program is used to take the data, process it, and input it into a MySQL database program. The analysis programs, discussed in the next chapter, are implemented into this program to record real-time performance and cost calculations in addition to the raw data. The program collects the data by averaging a set number of samples. With this program, a delay can be set for the time between taking samples, and the pause after the samples are taken. A screenshot of this program is presented in Figure 3.23.

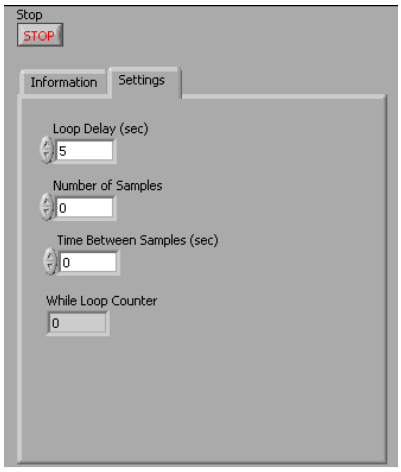

Figure 3.23 LabView Database Program

The MySQL database has the capability to export to Microsoft Excel. This post processing has been used to compile daily averages for the information. These daily averages make presentation of the data simplier and easier. The post processing has also been useful in correcting data that were incorrect when initially taken. This completes the review of the components, instrumentation and DAQ system at the demonstration site.

CHAPTER 4

ENERGY ANALYSIS

The goal of the research is to perform an energy analysis on both the CHP system and the conventional system. Components of the CHP system to be analyzed include the engine-generator set, heat exchangers, boiler, absorption chiller, and the four-pipe fan coil unit. In addition, the CHP system is analyzed by computing the SETR value. The parameters of interest for the conventional system are cost per hour of operation, the COP for cooling, and the efficiency during heating. Seven different programs have been written in LabView VIs to analyze the system: the engine analysis, heat exchanger analysis, boiler analysis, absorption chiller analysis, CHP system's HVAC analysis, and the conventional system's HVAC analysis. The purpose of these programs is to accommodate the vast quantities of data that needs to be analyzed. The VIs has been developed to calculate the results in real time as the data sets are recorded. The equations used in the computations have been grouped according to the program in which they appear. In addition, flowcharts are presented to illustrate the data flow in the VIs.

4.1 Analysis Equations

This section presents the equations used for modeling the different CHP system components.

4.1.1 Engine Analysis

The first goal for the engine analysis is to compute the combined cycle efficiency. The micro- Cooling, Heating, and Power (m- CHP) Instructional Module by the Mechanical Engineering Department at Mississippi State University presents the combined cycle efficiency in Equation 4.1.

$$\eta_{CHP} = \frac{Useful\ Thermal+Electrical\ Output}{Fuel\ Input} = \frac{\dot{Q}_{HR}+P_{GEN}}{\dot{Q}_{NGE}} \quad (4.1)$$

The fuel input for Equation 4.1 can be described as the energy addition from the combustion of natural gas, presented in Equation 4.2.

$$\dot{Q}_{NGE} = \dot{V}_{NGE} * LHV_{NGE} \quad (4.2)$$

where $\dot{V}_{NGE}$ is the natural gas fuel volumetric flowrate and LHV_{NGE} is the Lower Heating Value (LHV). The thermal energy recovered from the second heat exchanger can be determined as,

$$\dot{Q}_{HR} = \dot{V}_{HR} * (\rho_e * Cp_e * T_e - \rho_i * Cp_i * T_i) \quad (4.3)$$

where $\dot{V}_{HR}$, ρ , and Cp are the volumetric flow rate, density, and specific heat of water, respectively. The subscripts e and i refer to the exit and inlet conditions, respectively. All terms in Equation 4.3 are measured except for density and specific heat which are calculated in the water properties sub-analyses.

The fuel costs incurred from engine operation can be expressed as,

$$Cost_{Engine} = Price_{NGE} * \dot{V}_{NGE} \quad (4.4)$$

where $Price_{NGE}$, is the price of natural gas. In this investigation the price of natural gas used is \$12.83/1000ft^3. This value is obtained by the EIA's average fuel prices for residential and commercial customers in 2008.

4.1.2 Heat Exchanger Analysis

To evaluate the performance of the heat exchangers, the heat exchanger heat transfer ratio and the heat exchanger effectiveness are computed. The heat transfer ratio indicates losses in the heat exchanger to the surroundings. There are two heat exchangers in the heat recovery system so calculations are performed for both. The first heat exchanger examined is the exhaust heat exchanger. This heat exchanger recovers heat from the exhaust gasses and transfers that thermal energy to the engine coolant line. To compute the heat transfer ratio the heat transfer from the exhaust side and the heat transfer to the engine coolant side must be found. Modifying Equations 4.3, the heat transfer for the exhaust side of heat exchanger 1, exhaust heat exchanger, can be found as,

$$\dot{Q}_{EX} = \dot{V}_{EX} * \rho_{EX} * Cp_{EX} * (T_i - T_e) \quad (4.5)$$

where $\dot{V}_{EX}, \rho_{EX}, Cp_{EX}$ are the volumetric flow rate, density, and specific heat of the exhaust gasses, and *Ti* and *Te* are the inlet and exit temperature of the exhaust. In Equation 4.5, the gas temperature is measured by the instrumentation. The exhaust density and specific heat are calculated by taking air properties at a mean temperature of approximately 600°F. This temperature is the average of the inlet temperature of 1000°F

and the outlet temperature of 200°F. The exhaust flow rate is calculated by using stoichiometric fuel combustion and applying conservation of mass to the fuel combustion.

$$\dot{m}_{EX} = \dot{m}_{AIR} + \dot{m}_{NG} \tag{4.6}$$

The mass flowrate of the exhaust gas is computed as the mass flowrate of the incoming air plus the mass flowrate of the fuel. Equation 4.7 can be used to determine the volumetric flowrate of the exhaust gas as follows;

$$\dot{V}_{EX} = \frac{(\dot{V}_{NG} * \rho_{NG} * A/F_{NG}) + (\dot{V}_{NG} * \rho_{NG})}{\rho_{EX}} \tag{4.7}$$

The stoichiometric Air to Fuel ratio for natural gas, A/F_{NG} , is referenced from Ferguson and Kirkpatrick (2001) as 17.12. The coolant side heat transfer is computed similarly and results in Equation 4.8.

$$\dot{Q}_{COOL} = \dot{V}_{COOL} * \rho_{COOL} * Cp_{COOL} * (T_e - T_i) \tag{4.8}$$

where $\dot{V}_{COOL}, \rho_{COOL,} Cp_{COOL}$ are the volumetric flow rate, density, and specific heat of the coolant, and *Ti* and *Te* are the inlet and exit temperature of the coolant. The density and specific heat of the engine coolant are approximated at a temperature of 180°F with a 50% mix of ethylene-glycol and water. This information was obtained from the *ASHRAE Handbook - Fundamentals* (2005). The heat transfer ratio can be computed as,

$$Q_{RatioHX1} = \frac{\dot{Q}_{OUT}}{\dot{Q}_{IN}} = \frac{\dot{Q}_{COOL}}{\dot{Q}_{EX}} \tag{4.9}$$

The second item in examining heat exchanger performance is the heat exchanger effectiveness. The heat exchanger effectiveness is defined by Incropera *et al.* (2007) as,

$$\varepsilon = \frac{Q_{Actual}}{Q_{Max}} \tag{4.10}$$

Equation 4.10 presents the heat exchanger effectiveness is a ratio of the actual heat transfer to the total possible heat transfer, which is calculated in Equation 4.11 and 4.12, respectively.

$$Q_{Actual} = C_h(T_{h,i} - T_{h,o}) = C_c(T_{c,o} - T_{c,i}) \tag{4.11}$$

$$Q_{Max} = C_{min}(T_{h,i} - T_{c,i}) \tag{4.12}$$

In the above equations, $T_{h,i}$, represents the hot side inlet temperature, and , $T_{h,o}$, the hot side outlet temperature. The same nomenclature applies for the cold side temperatures as well. The variable, C_h, is the heat capacity for the hot side of the heat exchanger, and , C_c, is the heat capacity for the cold side of the heat exchanger. The next variable to examine is C_{min}, this variable is set equal to the lesser of the two heat capacities. Note that the actual heat transfer should be the heat transfer associated with the cold side to account for the non-ideal behavior of the heat exchangers. The heat capacity of a fluid can be determined as,

$$C = Cp * \dot{V} * \rho \tag{4.13}$$

For the first heat exchanger, the exhaust heat exchanger, the hot side of the heat exchanger is the exhaust side and the cold side for the heat exchanger is the engine coolant, which for this case C_{min} is the exhaust side heat capacity. The heat exchanger effectiveness for the first heat exchanger can be found as;

$$\varepsilon_{HX1} = \frac{C_{COOL}(T_{c,o} - T_{c,i})}{C_{EX}(T_{h,i} - T_{c,i})} \tag{4.14}$$

A similar procedure can be utilized to compute the heat transfer ratio for the second heat exchanger, the heat recovery heat exchanger. The second heat exchanger transfers heat from the engine coolant to the heat recovery line. To find the heat transfer from the coolant side Equation 4.9 is used. The heat transfer for the heat recovery side can be found modifying Equation 4.3. For the second heat exchanger, the heat transfer ratio appears as,

$$Q_{RatioHX2} = \frac{\dot{Q}_{OUT}}{\dot{Q}_{IN}} = \frac{\dot{Q}_{HR}}{\dot{Q}_{COOL}} \tag{4.15}$$

The output is the heat transfer to the heat recovery line and the input is the heat transfer from the engine coolant. Note that this coolant heat transfer is for the second heat exchanger and is not equal to the coolant heat transfer for the first heat exchanger. To determine the heat exchanger effectiveness for the second heat exchanger the hot side is the engine coolant, and the cold side is the heat-recovery line. The C_{min} for the second heat exchanger is found to be the heat recovery side heat capacity. The heat exchanger effectiveness for the second heat exchanger can be found as:

$$\varepsilon_{HX2} = \frac{C_{HR}(T_{c,o} - T_{c,i})}{C_{HR}(T_{h,i} - T_{c,i})} = \frac{T_{c,o} - T_{c,i}}{T_{h,i} - T_{c,i}} \tag{4.16}$$

Since the minimum heat capacity is also the cold side heat capacity, those terms in the heat exchanger effectiveness cancel, leaving only a temperature ratio.

4.1.3 Boiler Analysis

The goals of the boiler analysis are to determine the thermal efficiency and cost per hour of usage. The thermal efficiency for the boiler can be found from Equation 4.17.

$$\eta_{Boiler} = \frac{Q_{BW}}{Q_{NGB}} \tag{4.17}$$

where Q_{BW} and Q_{NGB} are the boiler water heat transfer and natural gas fuel input, respectively. The fuel energy input can be calculated using Equation 4.2. The only difference is the natural gas flow is the boiler fuel consumption. The other item required is the heat transfer to the boiler water. Equation 4.3 is modified determine the boiler water heat transfer.

$$Q_{BW} = \dot{V}_{BW} * (\rho_e * Cp_e * T_e - \rho_i * Cp_i * T_i) \tag{4.18}$$

The water properties are found by the water properties sub-analysis. Operation costs for the boiler are computed using Equation 4.5.

4.1.4 Absorption Chiller Analysis

The primary goal of the absorption chiller analysis is to determine the COP of the cooling device. Tozer and James (1998) describe how to compute the COP using the heat transfer from the evaporator and generator. For the absorption chiller used in this investigation, they are represented as the hot water heat transfer and the cold water heat transfer, shown in Equation 4.19.

$$COP = \frac{Q_{Evaporator}}{Q_{Generator}} = \frac{Q_{CW}}{Q_{HW}} \tag{4.19}$$

In Equation 4.19 the subscripts 'CW' and 'HW' refer to cold and hot water, respectively. The heat transfers are computed by using an energy balance.

4.1.5 CHP System HVAC Analysis

This section discusses the CHP system HVAC computations. The same set of equations can be used in both the heating and the cooling seasons. The goal of the CHP system HVAC analysis is to determine the heat transfer ratio of the four-pipe fan coil unit. The heat transfer ratio is computed as in Equation 4.20.

$$Q_{RatioHVAC} = \frac{\dot{Q}_{OUT}}{\dot{Q}_{IN}} = \frac{\dot{Q}_{AIR}}{\dot{Q}_{WATER}} \tag{4.20}$$

The air side heat transfer is required. The instrumentation records the relative humidity, temperature, and the volumetric air flow rate. The moist air enthalpy and the moist air density are required to compute the air side heat transfer. These values are found in the moist air properties sub-analysis, discussed later in this chapter. The air side heat transfer can be calculated as,

$$Q_{AIR} = \dot{V_{MA}} * \left(\left[\rho_{MA,e} * h_{MA,e}\right] - \left[\rho_{MA,i} * h_{MA,i}\right]\right) \tag{4.21}$$

where $V_{MA}, \rho_{MA,}\ h_{MA,e}$ are the volumetric flow rate, density, and the enthalpy of the moist air. The water side heat transfer is determined. The volumetric flow rate and temperature are acquired by the instrumentation. The remaining items are the density and specific heat found in the water properties sub-analysis. The water side heat transfer is again found by an energy balance. The heat transfer ratio is found by Equation 4.21

4.1.6 Conventional HVAC Cooling Analysis

The conventional HVAC system is used during the heating and the cooling seasons. The COP for cooling and the operational costs due to electrical power

consumption are considered. As the air heat transfer calculations are the same as the CHP system, the only item required is the electrical power consumption of the compressor and fans. The instrumentation provides the current used by these devices. The voltage for the compressor and fans are 240 V and 115 V, respectively. The power is computed as,

$$P = I * V \tag{4.22}$$

The COP is found using Equation 4.23.

$$COP_{Conv\_Cool} = \frac{\dot{Q}_{MA}}{P_{Compressor}+P_{Fans}} \tag{4.23}$$

To determine the utility costs, the 2008 average power costs for residential and commercial properties are used. The EIA gives this price at 0.108 $/kWh. The cost is found by Equation 4.24

$$Cost_{Conv\_Cool} = Price_{Electrial} * (P_{Compressor} + P_{Fans}) \tag{4.24}$$

4.1.7 Conventional HVAC Heating Analysis

In this system, the heating is provided by a condensing furnace. The heating efficiency and operational cost are found. The equations for the furnace are similar to those used in the boiler analysis. Using Equation 4.2, the chemical fuel energy input to the furnace is found. The furnace efficiency is computed as,

$$\eta_{Furnace} = \frac{\dot{Q}_{AIR}}{\dot{Q}_{NG}} \tag{4.25}$$

The cost of natural gas for the conventional heating system is found using Equation 4.3.

The remaining items are the cost of electricity for building operation and the computation of the ambient enthalpy. The cost for the building is found using Equation

4.25, replaces the compressor and fan power with the building power consumption. The ambient enthalpy is computed using the moist air properties sub-analysis.

4.1.8 SETR Analysis

As Micro-CHP is a developing technology it is important to be able to properly evaluate the performance, and compare different systems. In performing a proper comparison of different CHP systems the technology can progress and improve. SETR aims at providing a single metric to provide system comparison. Conceptually SETR is an efficiency, which keeps all of the CHP components inside the control volume. This allows for an 'overall' examination of the system. The control volume is presented in Figure 4.1.

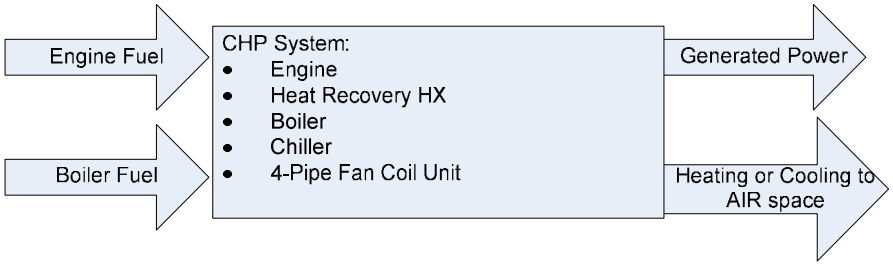

Figure 4.1 Schematic of the SETR Control Volume

As displayed in Figure 4.1, the inputs are the engine fuel and the boiler fuel, and the outputs are the generated power and HVAC heating or cooling. There are two items that need to be addressed: the generated power and the inclusion of the boiler performance in the CHP system efficiency. In most CHP systems the majority of the electrical power produced is consumed by the various components of the system. It has been chosen to

include the total power produced, as this is a judge of the performance of the system based on its components, of which, the engine is a critical part.

The second item to consider is the inclusion of the boiler in the system performance. Many CHP systems require some form of additional thermal energy, yet those components are typically not included into the cogeneration or trigeneration efficiencies. It would seem prudent to include these components, so that the effect on overall performance can be evaluated. To include the boiler, Equation 4.1 as follows;

$$\eta_{CHPB} = \frac{\dot{P}_{GEN}+\dot{Q}_{HR}+\dot{Q}_{BW}}{\dot{Q}_{NGE}+\dot{Q}_{NGB}} \tag{4.26}$$

This can be combined with Equation 2.5 to show Equation 4.27.

$$\eta_{TriB} = \frac{\dot{P}_{GEN}+\dot{Q}_{HR}+\dot{Q}_{BW}}{\dot{Q}_{NGE}+\dot{Q}_{NGB}} * \frac{\dot{Q}_{CW}}{\dot{Q}_{HW}} \tag{4.27}$$

Equations 4.26 and 4.27 indicates how the boiler can be included in efficiency calculations to examine its effect on the system performance.

In most heat transfer textbooks, including Incropera *et al.* (2007), heat exchangers are assumed to have a heat transfer ratio of one, meaning that the same amount of heat leaves the hot side as enters the cold side. In actual situations there are often losses to the ambient so that the heat transfer ratio is less than one. By selecting the control volume as the entire CHP system, SETR takes into account losses such as this and/or other thermal losses in the system. Based on the control volume, the SETR relation is presented in Equations 4.28 and 4.29.

$$SETR = \frac{\dot{P}_{GEN}+\dot{Q}_{AIR}}{\dot{Q}_{NGE}} \tag{4.28}$$

$$SETR_B = \frac{\dot{P}_{GEN} + \dot{Q}_{AIR}}{\dot{Q}_{NGE} + \dot{Q}_{NGB}} \quad (4.29)$$

Equation 4.28 is used when the boiler is not firing, while Equation 4.29 can be used when the boiler is firing.

4.1.9 Sub-Analyses

As the major analyses are programmed as VIs, the sub-analyses are described as SubVIs. The first sub-analysis to discuss computes water properties based on the fluid temperature. This sub-analysis uses relations presented by Popiel and Wojtkowiak (1998). This SubVI is a simple mathematical relation that does not require a flowchart.

A sub-analysis calculates the moist air properties. This analysis computes moist air enthalpy, saturation pressure, and moist air density. The inputs for this analysis are the air dry bulb temperature and relative humidity. From these, the water vapor saturation pressure can be found using a relation from the *ASHRAE Handbook – Fundamentals* (2005) devised by Hyland and Wexler. This relation computes saturation pressure as a function of temperature. Next, the partial pressure of the vapor is found using Equation 4.30

$$Pr_v = RH * Pr_{SAT} \quad (4.30)$$

Where, RH is the relative humidity and Pr_{SAT} is the saturation pressure. The specific humidity can be found in Equation 4.31.

$$\omega = .622 * \frac{Pr_v}{Pr_{ATM} - Pr_v} \quad (4.31)$$

Equation 4.31 uses the partial pressures of the air with the known atmospheric pressure to compute the specific humidity. The moist air density becomes,

$$\rho_{MA} = \frac{1+\omega}{1+1.608*\omega} * \rho_{DA} \tag{4.32}$$

The moist air enthalpy can be computed using Equation 4.33 from *ASHRAE Handbook – Fundamentals* (2005).

$$h_{MA\_SI} = 1.006T + \omega * (2501 + 1.86T) \tag{4.33}$$

Equation 4.33 is presented in SI units where temperature has units of ℃ and enthalpy is computed in $^{kJ}/_{kg}$. Equation 4.34 represents this relation in imperial units.

$$h_{MA\_IP} = .24T + \omega * (1061 + .444T) \tag{4.34}$$

with the temperature given in °F and enthalpy is computed in $^{BTU}/_{lbm}$.

4.2 LabView Analysis Program Flowcharts

In this section, flowcharts that describe the manner in which calculations are performed to compute results based on the energy analysis equations described above are presented. The engine analysis flowchart is displayed in Figure 4.2.This figure describes the inputs, known values, and outputs. It also presents the equation number used for some calculations. The LabView VI for the engine analysis is shown in Appendix A.

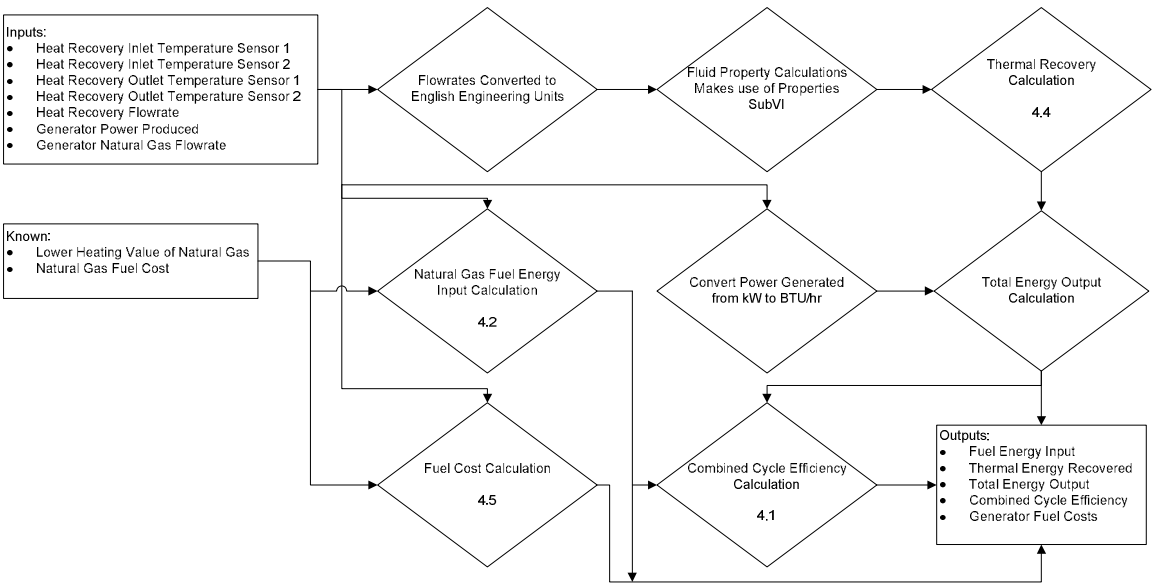

Figure 4.2 Engine Analysis Program Flowchart

The flowchart for the heat exchanger analysis program is presented in Figure 4.3. This analysis program is displayed in Appendix B. The flow chart for the boiler analysis program is presented in Figure 4.4, while the boiler analysis program is presented in Appendix C. The absorption chiller flow chart appears in Figure 4.5 while the absorption chiller LabView VI is shown in Appendix D.

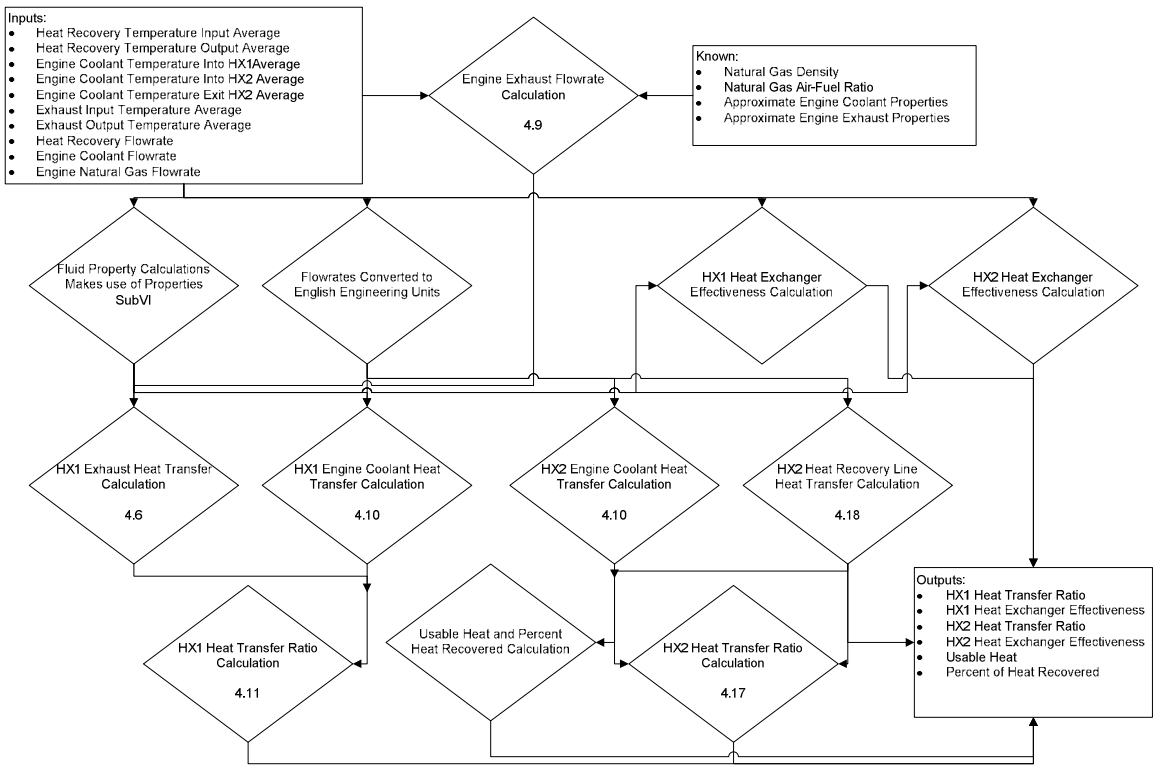

Figure 4.3 Heat Exchanger Analysis Program Flowchart

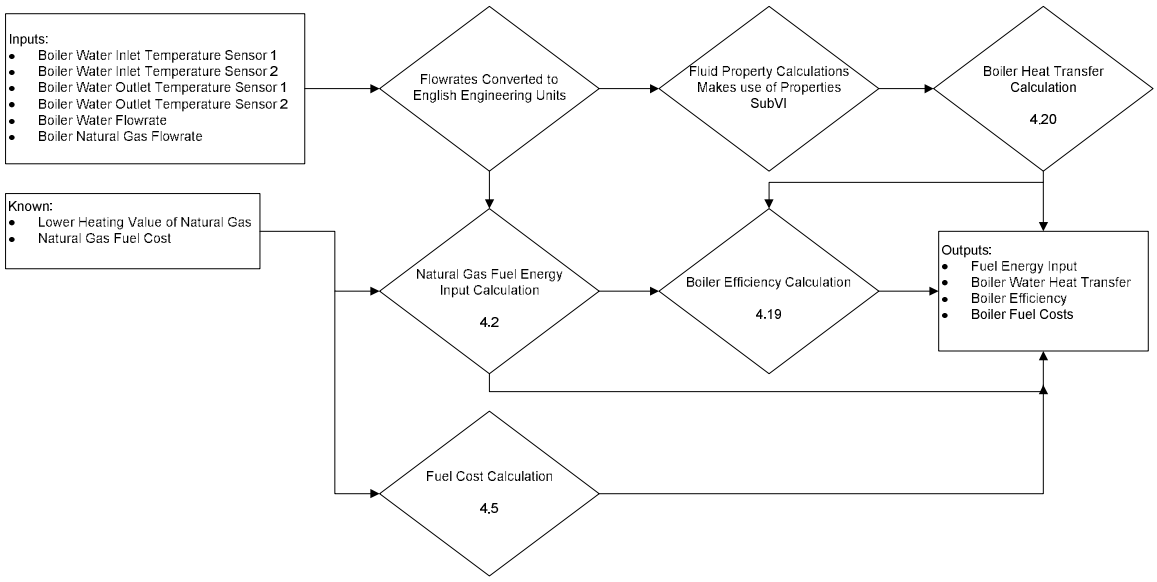

Figure 4.4 Boiler Analysis Program Flowchart

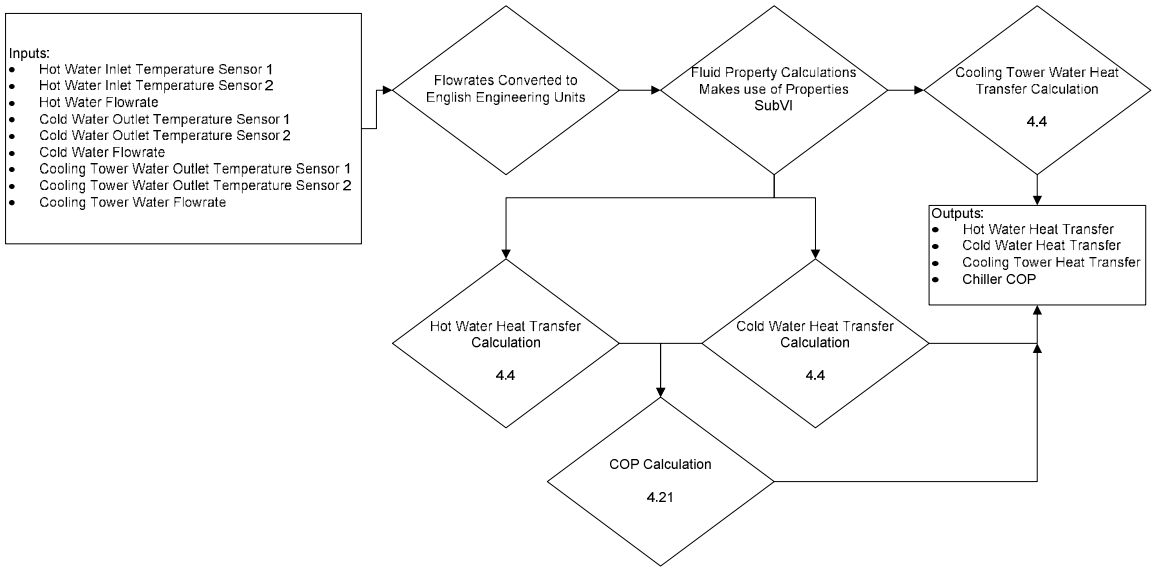

Figure 4.5 Absorption Chiller Analysis Program Flowchart.

The next flowchart presented is the last flowchart related to the CHP system. The flowchart for the CHP system HVAC analysis is presented in Figure 4.6.

The CHP system HVAC analysis appears in Appendix E. The system under conventional operation is examined. The first conventional analysis flowchart presents the dataflow during cooling operation, displayed in Figure 4.7.

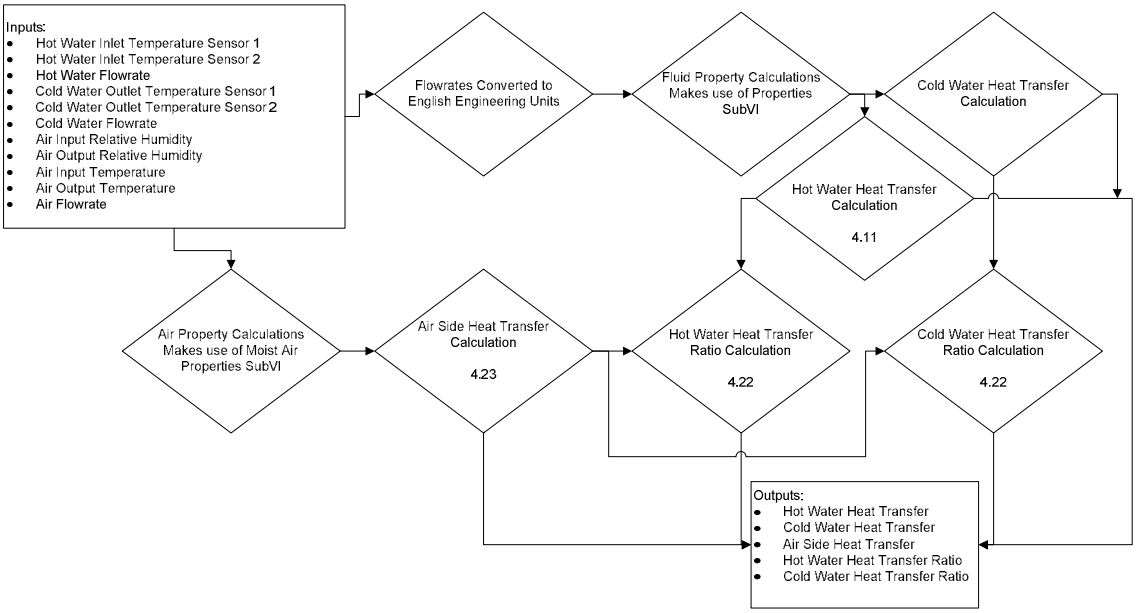

Figure 4.6 CHP HVAC Analysis Program Flowchart

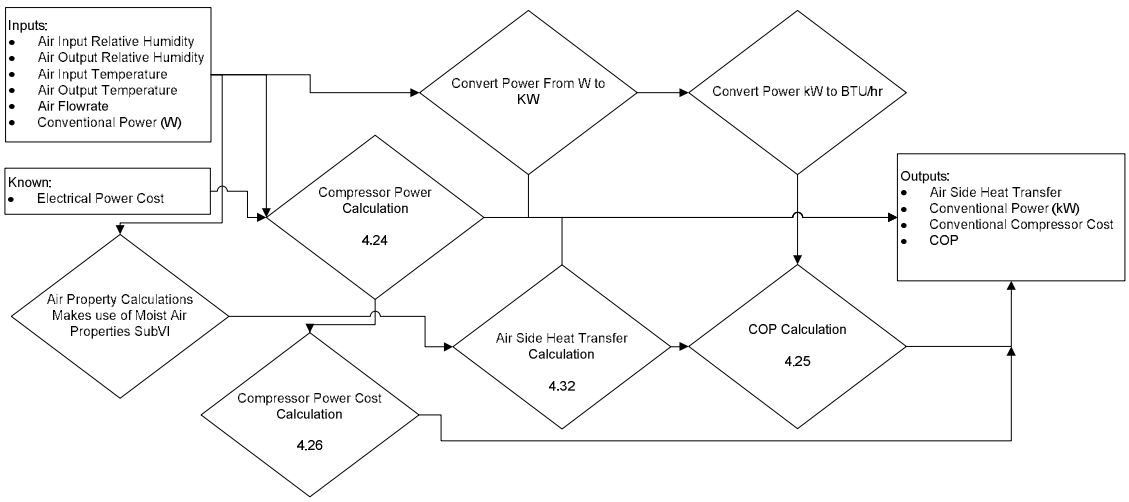

Figure 4.7 Conventional Cooling Analysis Flowchart

The conventional HVAC cooling analysis is shown in Appendix F. Next, the flowchart for the heating system under conventional operation is presented. Again, this analysis also calculates the ambient air enthalpy and the building electrical costs. Figure 4.8 displays these computations.

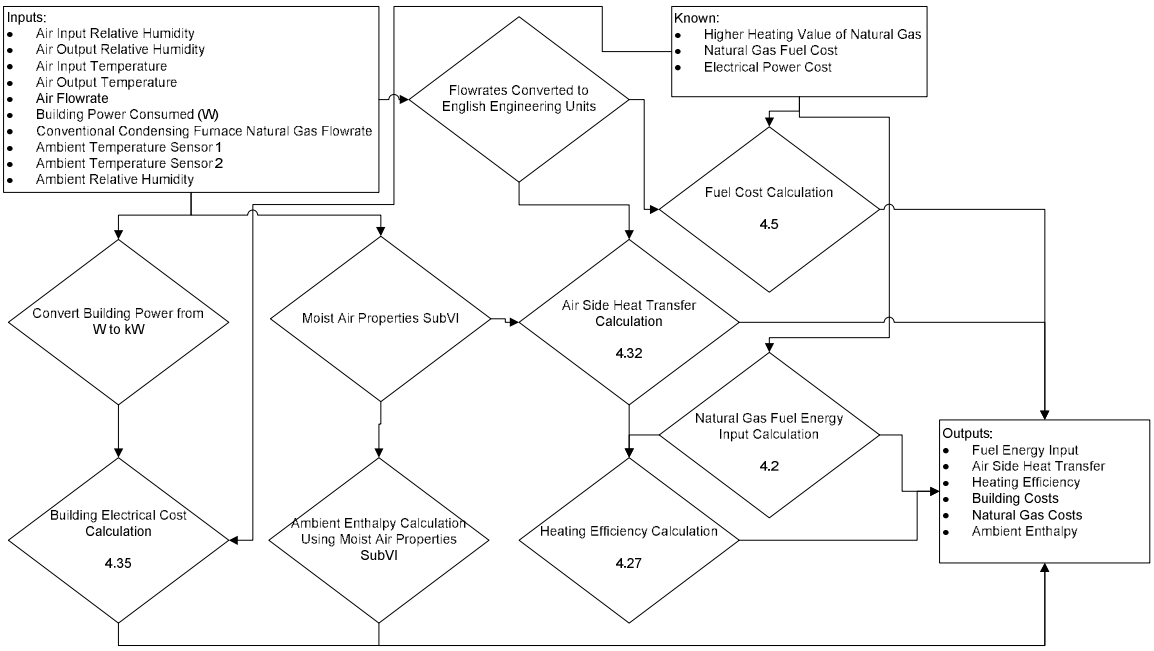

Figure 4.8 Conventional Heating Analysis Flowchart

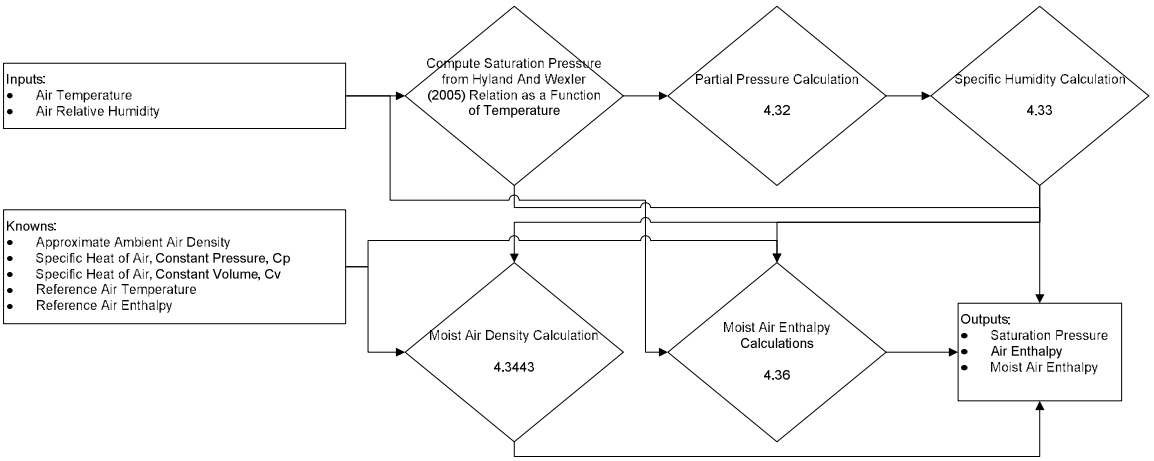

Figure 4.9 Moist Air Properties SubVI Flowchart

The conventional heating analysis LabView program appears in Appendix G. The moist air heat transfer SubVI is presented in Figure 4.9.

The moist air properties SubVI is displayed in Appendix J. The final flowchart to be presented describes the calculations in the new RTD sensor SubVI.

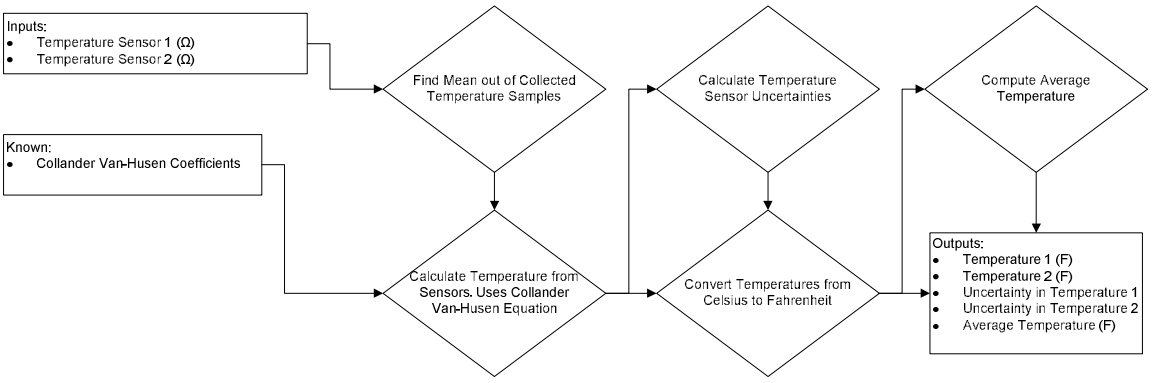

Figure 4.10 RTD SubVI Flowchart

This sub-program describes the method in which the resistance is converted temperature. This sub-program also calculates the uncertainty in each of the sensors.

CHAPTER 5

UNCERTAINTY ANALYSIS

An Uncertainty Analysis (UA) is a vital component for any experiment. To evaluate the validity of results some type of uncertainty analysis and error balance checks should be performed. The uncertainty analysis performed herein examines the systematic biases associated with the instrumentation. The random errors were not examined because the quantities of data collected were averaged daily, and thus it can be assumed that the random errors were effectively averaged out. When looking at uncertainty there are effectively two errors, systematic 'bias' errors and random errors Coleman and Steele [1999]. This dissertation focuses on the systematic bias errors. The distribution of the data readings is the random errors and by averaging them and computing the mean, a accurate estimate of the overall uncertainty by considering only the bias uncertainty can be obtained. A propagation approach was used to determine the uncertainty in the results. To find the errors in the results, this propagation method was used on each result individually and computed as a percent of a nominal value.

5.1 General Uncertainty Analysis

Each sensor has bias uncertainty associated with it as well as the uncertainty associated with the NI DAQ System. To assist with the quantities of data collected and to require less post processing, the uncertainty is computed as a percent of the nominal value. Midway through the year-long data collection, the temperature sensors were upgraded to a more accurate hardware. This upgrade is the reason that in the following table, there are designations of new and old on some of the items, which correlate to the new and old temperature sensors. One difference in the new and old temperature sensors is that the uncertainties of the new sensors are a function of their nominal temperatures. The uncertainties of these sensors are computed at a typical nominal value for each application which explains why different systems have a different uncertainty in the new temperature sensors. The results of the uncertainty analysis are broken up into five sections: engine and heat exchanger UA, boiler UA, absorption chiller UA, CHP system HVAC UA, and conventional system UA. The following tables represent the individual uncertainties of the instruments already compounded with the DAQ panel and those of the results. Table 5.1 presents the engine and heat exchanger uncertainty results.

Table 5.1

Engine and Heat Exchanger Uncertainty Analysis Results

Item	Nominal Value	Uncertainty	Percent
Engine			
Heat Recovery Temperature - old (°F)	N/A	1.006	N/A
Heat Recovery Temperature - new (°F)	N/A	0.717	N/A
Heat Recovery Flowrate (GPM)	5.8	0.029	N/A
Water Density (lbm/ft^3)	61	0.025	N/A
Water Specific Heat (BTU/(lbm * °F))	1	0.00047	N/A
Engine Power (W)	7300	0.075	N/A
Natural Gas Flowrate (ft^3/min)	2.44	0.088	N/A
Combined Cycle Efficiency (old)	0.387	0.02545	**6.58%**
Combined Cycle Efficiency (new)	0.387	0.0207	**5.36%**
Engine Cost ($/hour)	1.881	0.068	**3.60%**
Heat Exchanger			
Engine Coolant Temperature (°F)	N/A	1.006	N/A
Engine Coolant Flowrate (GPM)	10.1	0.051	N/A
Exhaust Temperature (°F)	N/A	1.943	N/A
Exhaust Flowrate (ft^3/min)	52.872	1.905	N/A
Heat Exchanger 1 Heat Transfer Ratio (old)	0.999	0.159	**15.94%**
Heat Exchanger 1 Heat Transfer Ratio (new)	0.999	0.116	**11.64%**
Heat Exchanger 1 Effectiveness (old)	0.929	0.148	**15.88%**
Heat Exchanger 1 Effectiveness (new)	0.929	0.178	**11.60%**
Heat Exchanger 2 Heat Transfer Ratio (old)	0.93	0.168	**18.11%**
Heat Exchanger 2 Heat Transfer Ratio (new)	0.93	0.12	**12.95%**
Heat Exchanger 2 Effectiveness (old)	0.253	0.026	**10.20%**
Heat Exchanger 2 Effectiveness (new)	0.253	0.018	**7.26%**

The percentage uncertainties that are used in the results to determine the acceptable error are given on the far right. The boldface print designates results that will be discussed in the results section. The engine and heat exchanger UA are shown in Appendix H. Table

5.2 displays the results of the boiler UA. The boiler UA can be found in Appendix I.

Table 5.3 presents the results of the UA on the absorption chiller.

Table 5.2

Boiler Uncertainty Analysis Results

Item	Nominal Value	Uncertainty	Percent
Boiler			
Boiler Water Temperature - old (°F)	N/A	1.006	N/A
Boiler Water Temperature - new (°F)	N/A	0.717	N/A
Boiler Water Flowrate (GPM)	19.39	0.063	N/A
Water Density (lbm/ft^3)	61	0.025	N/A
Water Specific Heat (BTU/(lbm * °F))	1	0.00047	N/A
Natural Gas Flowrate (ft^3/min)	2.31	0.088	N/A
Boiler Efficiency (old)	0.35	0.076	**21.75%**
Boiler Efficiency (new)	0.35	0.056	**15.87%**
Boiler Cost ($/hour)	1.778	0.068	**3.81%**

Table 5.3

Absorption Chiller Uncertainty Analysis Results

Item	Nominal Value	Uncertainty	Percent
Absorption Chiller			
Cold Water Temperature - old (°F)	N/A	1.006	N/A
Cold Water Temperature - new (°F)	N/A	0.55	N/A
Hot Water Temperature - old (°F)	N/A	1.006	N/A
Hot Water Temperature - new (°F)	N/A	0.717	N/A
Cold Water Flowrate (GPM)	26.9	0.14	N/A
Hot Water Flowrate (GPM)	37.7	0.19	N/A
Water Density (lbm/ft^3)	61	0.025	N/A
Water Specific Heat (BTU/(lbm * °F))	1	0.00047	N/A
Chiller COP (old)	0.356	0.102	**28.71%**
Chiller COP (new)	0.356	0.064	**17.93%**

The absorption chiller UA can be found in Appendix J. The next table presents the HVAC UA during CHP system operation.

Table 5.4

CHP System HVAC Uncertainty Analysis Results

Item	Nominal Value	Uncertainty	Percent
CHP System HVAC Heating			
Hot Water Temperature - old (°F)	N/A	1.006	N/A
Hot Water Temperature - new (°F)	N/A	0.717	N/A
Hot Water Flowrate (GPM)	2.6	0.014	N/A
Air Flow Rate (ft^3/min)	1964.46	39.6	N/A
Air Temperature (°F)	N/A	0.505	N/A
Relative Humidity	N/A	0.004	N/A
Water Density (lbm/ft^3)	61	0.025	N/A
Water Specific Heat (BTU/(lbm * °F))	1	0.00047	N/A
Generator Natural Gas Flowrate (ft^3/min)	1.86	0.088	N/A
Boiler Natural Gas Flowrate (ft^3/min)	0.386	0.088	N/A
Generator Power Produced (W)	4387.9	75.021	N/A
HVAC Heat Transfer Ratio (old)	0.946	0.276	**29.18%**
HVAC Heat Transfer Ratio Heating (new)	0.946	0.251	**26.57%**
System Heat Transfer Ratio	0.176	0.017	**9.41%**
CHP System HVAC Cooling			
Cold Water Temperature - old (°F)	N/A	1.006	N/A
Cold Water Temperature - new (°F)	N/A	0.55	N/A
Cold Water Flowrate (GPM)	3.57	0.018	N/A
Air Flow Rate (ft^3/min)	1145.6	23.1	N/A
Air Temperature (°F)	N/A	0.505	N/A
Relative Humidity	N/A	0.02	N/A
Water Density (lbm/ft^3)	61	0.025	N/A
Water Specific Heat (BTU/(lbm * °F))	1	0.00047	N/A
Generator Natural Gas Flowrate (ft^3/min)	2.63	0.088	N/A
Boiler Natural Gas Flowrate (ft^3/min)	2.31	0.088	N/A
Generator Power Produced (W)	7132	75.05	N/A
HVAC Heat Transfer Ratio (old)	1.094	0.265	**24.25%**
HVAC Heat Transfer Ratio Cooling (new)	1.094	0.22	**20.31%**
System Heat Transfer Ratio	0.132	0.009	**6.65%**

For the HVAC UA, the heating and cooling had to be considered individually. As one can see the heat transfer ratio for heating and cooling using the old temperature sensor was the same because that sensor was calibrated on a curve independent of the nominal temperature. The CHP system HVAC uncertainty analysis can be found in Appendix K. This analysis presents only the cooling operation and not the heating operation as they are mathematically identical. Furthermore, SETR is in this analysis. The final UA is the HVAC system under conventional operation using the vapor compression system. Included in this analysis is the uncertainty in the ambient enthalpy calculation. The MathCAD worksheet for this analysis was used twice, once for heating season and once for cooling season. Also, the UA was done the same way as in the CHP system HVAC uncertainty analysis to save space. The importance of knowing this is to see that depending on what air flow data is inputted in to the worksheet it will present the proper solution in the proper area. For cooling, the worksheet outputs COP, and for heating the heating efficiency is attained.

Table 5.5

Conventional HVAC and Misc. Uncertainty Analysis Result

Item	Nominal Value	Uncertainty	Percent
Conventional HVAC Heating			
Natural Gas Flowrate (ft^3/min)	0.237	0.035	N/A
Air Flow Rate (ft^3/min)	341	6.874	N/A
Air Temperature (°F)	N/A	0.505	N/A
Relative Humidity	N/A	0.005	N/A
Conventional Heating Efficiency	0.98	0.149	**15.15%**
Conventional Heating Cost ($/hr)	0.182	0.027	**14.77%**
Conventional HVAC Cooling			
Compressor Power (W)	1240	15	N/A
Air Flow Rate (ft^3/min)	588	11.854	N/A
Air Temperature (°F)	N/A	0.505	N/A
Relative Humidity	N/A	0.02	N/A
Conventional Cooling COP	3.483	0.619	**22.44%**
Conventional Cooling Cost ($/hr)	0.134	0.002	**1.21%**
Conventional Building Power Cost			
Power Usage (W)	5000	75	N/A
Building Power Cost ($/hr)	0.54	0.0081	**1.50%**
Ambient Enthalpy			
Ambient Temperature (°F)	88	0.636	N/A
Ambient Relative Humidity	0.6	0.007	N/A
Ambient Enthalpy (BTU/lbm)	24.335	0.268	**1.10%**

The above results can be found in Appendix L. All the above UAs have been computed with details given to the Uncertainty Percentage Contribution (UPC) in the MathCAD worksheets. Examining the UPC can give further insight into the individual contribution by the different sensors and how they affect the uncertainty in the results.

5.2 Error Balance Checks

Balance checks have many uses in an experiment. Coleman and Steele [1999] describe the balance check as, "an application of the basic physical conservation laws to an experiment." For example by applying conservation of energy, it can be checked if the error falls within the uncertainties found in the previous tables. The balance checks can assist in the diagnosis and debugging of equipment or instrumentation errors. Some items are not applicable towards balance checks such as performance factors like efficiencies. Conservation of energy can be applied to the heat exchangers and the absorption chiller. In the heat exchangers, the heat transfer ratios will result in a value of one if they are operating perfectly. The balance checks here can determine that if the heat transfer ratio deviates more than the acceptable uncertainty away from one then an error is present. The absorption chiller uses conservation of energy to examine the heat flows into and out of the system to provide error checking. The DAQ system has been implemented with these balance checks in such a way to flag instrument errors outside of their corresponding uncertainties. Balance checks can offer further insight into the error of a system and are a crucial part of any uncertainty analysis. A SubVI was developed and implemented into the system to notify the user if any values were not within the rated uncertainty. This program does not require a flowchart due to the nature of its calculations. The heat transfer balance check SubVI appears in Appendix K.

CHAPTER 6

RESULTS

This chapter presents the results obtained for this investigation. To obtain useful results data sets were collected for an extended period of time. Information for the heating season was accumulated from January through March, and for the cooling season data was collected from June through September. The information recorded required much more post-processing than previously anticipated, but the LabView analysis programs proved to be very helpful in alleviating some of this post-processing. The first item of interest for this study is the nominal results. These results are tabulated values that present the performance of the system for each month. Next, a cost analysis of the system is examined to determine the difference in operational cost between the CHP system and conventional system. Following this, the SETR values are examined for heating and cooling seasons. To close, particular items of interest pertaining to the system are also discussed and explained.

6.1 Nominal Results

To discuss the nominal results, the information is divided between mode and season. The mode of operation indicates if the building were operating with CHP system

running or utilizing city power and the conventional HVAC system. The season indicates if the system were operating in heating or cooling mode for winter and summer, respectively. This information has been computed using daily averages. The results presented in this section display a worst, best, and average bar on the plots. Worst represents the daily average of the worst performance, best presenting the daily average of the best performance, and average indicating the average performance for the entire month.

6.1.1 CHP System Heating Results

For CHP system operation during a heating season, the CHP, boiler, and combined CHP boiler efficiencies, the heat recovery heat exchanger heat transfer ratios and effectiveness, and the HVAC heat transfer ratio are examined. Figure 6.1 illustrates the CHP system efficiency for the heating months of January through March.

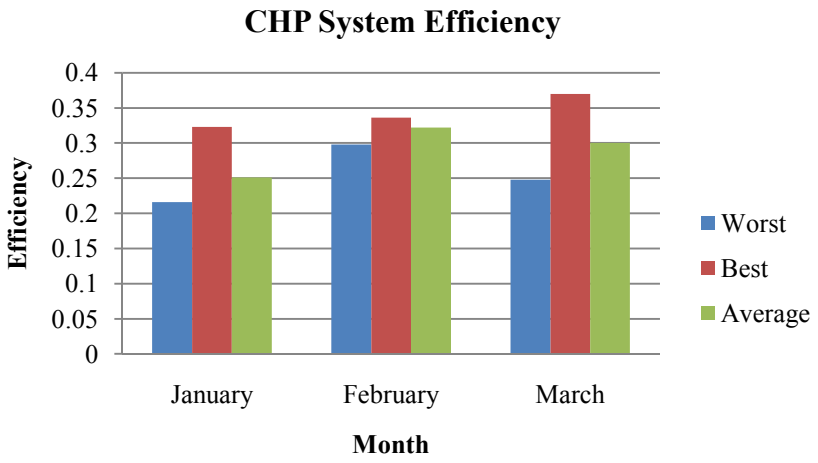

Figure 6.1 CHP System Efficiency - Heating

The best average efficiency for this period was in February at 32%, while the worst month was January at 25%. Next, the boiler efficiency for the heating months is examined. These results are depicted in Figure 6.2.

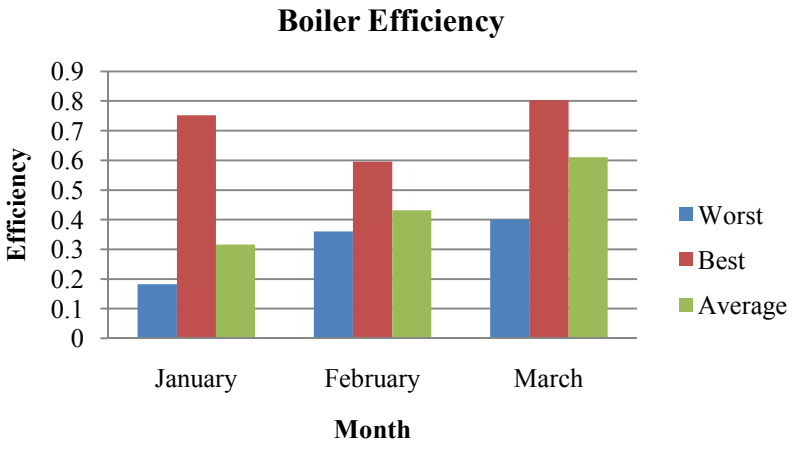

Figure 6.2 Boiler Efficiency - Heating

The boiler performance varies significantly from the best and the worst for each month. This variation is due to ambient temperature effects and boiler operational conditions, such as the incoming hot water temperature and ambient temperature. The peak average efficiency appeared in March at approximately 60%, while the worst was in January at around 36%. The item to be presented next is the CHP system boiler efficiency which is displayed in Figure 6.3. This efficiency, as discussed in Chapter 4, shows the combined efficiency of the CHP system and the boiler.

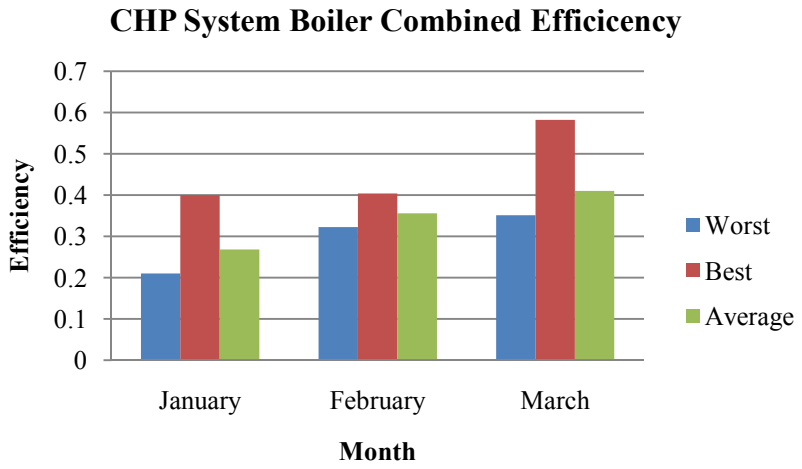

Figure 6.3 CHP System Boiler Combined Efficiency - Heating

The information presented in Figure 6.3 confirms that when the boiler is operating, usually the case for the demonstration facility, it affects the CHP efficiency and, therefore, must be considered in the performance evaluation.

The next group of items to be discussed is the two heat exchangers. The first heat exchanger transfers heat from the engine exhaust to the engine coolant, and the second heat exchanger transfers heat from the engine coolant to the heat recovery water line. The two performance metrics to be discussed for the two heat exchangers are the heat exchanger heat transfer ratio and the heat exchanger effectiveness. The heat transfer ratio is a ratio of the heat gained on the cold side of the heat exchanger divided by the heat lost on the hot side. The heat exchanger effectiveness is the ratio of the actual heat transfer to the total possible heat transfer based on the hot and cold side incoming temperatures. The results for heat exchanger 1 are presented in Figure 6.4.

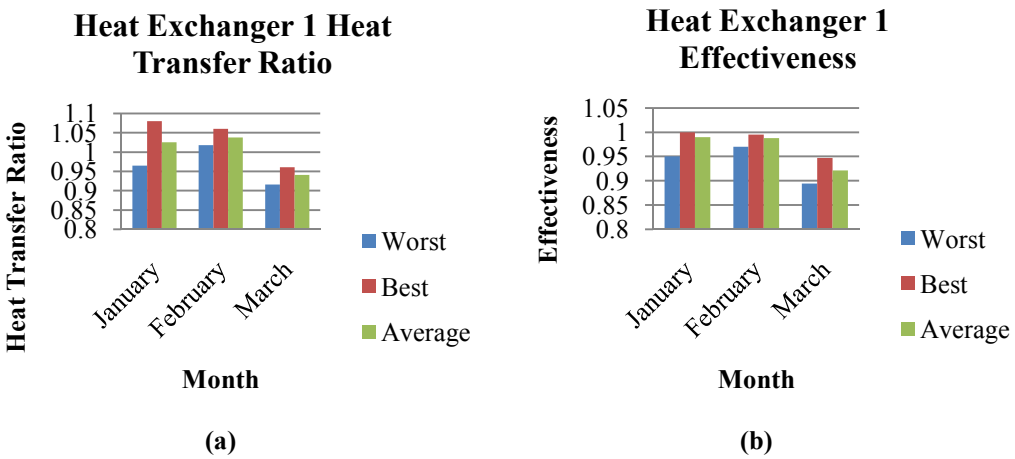

Figure 6.4 Heat Exchanger 1 (a) Heat Transfer Ratio and (b) Effectiveness - Heating

The heat transfer ratio and heat exchanger effectiveness for heat exchanger 1, the exhaust heat exchanger, is above 0.9. This indicates that the heat exchanger is operating at peak performance. Despite this, properties for exhaust gasses are difficult to approximate and are a source of error in the exhaust heat transfer calculations. Next, the same items for heat exchanger number 2, the heat recovery heat exchanger are examined and presented in Figure 6.5.

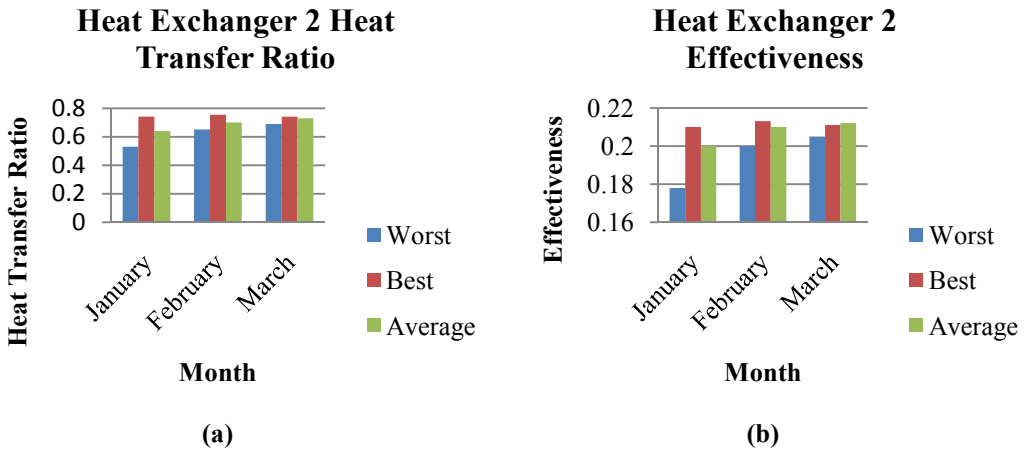

Figure 6.5 Heat Exchanger 2 (a) Heat Transfer Ratio and (b) Effectiveness - Heating

The heat transfer ratio presents a nominal value between 0.65 to 0.75. This means that that approximately 70% of the heat leaving the hot side of the heat exchanger is transferred to the cold side. This heat transfer ratio can be viewed as an efficiency indicator of the energy loss. The effectiveness displays a nominal value of 0.21 which is a low value for this type of heat exchanger.

The final item to examine is the four-pipe fan coil unit heat transfer ratio, the ratio of the heat that leaves the water coils to the heat gained from the air flow past those coils. The results are presented in Figure 6.6.

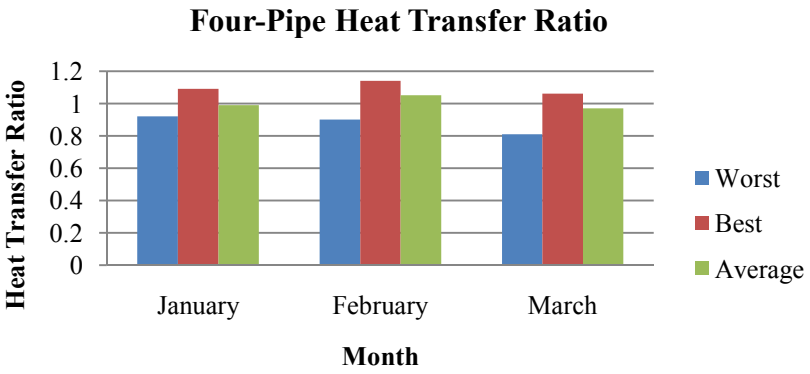

Figure 6.6 Four-Pipe Heat Transfer Ratio - Heating

The ratio shown in Figure 6.6 depicts a nominal value around one. This value indicates that there are little to no losses in this component. A value above one is displayed, which is explained by the nature that these values having a nominal value around one. Another consideration why the true value could be greater than one is the transient nature of the air and water flow rate.

6.2.2 CHP System Cooling Results

The cooling results include the same topics discussed for the heating season with the addition of the absorption chiller COP. The CHP system efficiency is examined and presented in Figure 6.7.

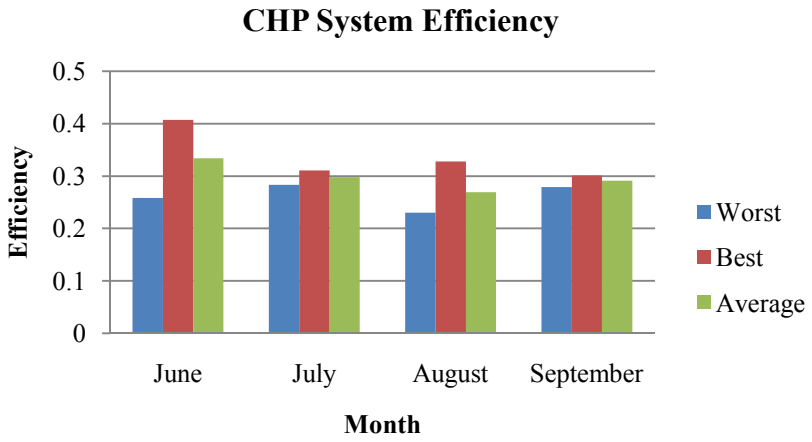

Figure 6.7 CHP System Efficiency - Cooling

The combined cycle efficiency averages 30%. The month with the best average is June, and the month with the worst average is August. This discrepancy pertains to the average ambient temperature, at topic to be discussed later in this chapter, and the effect of the absorption chiller operation.

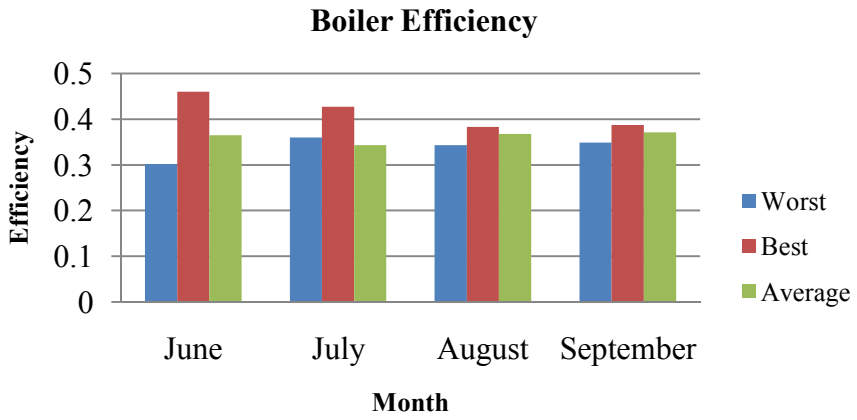

Figure 6.8 Boiler Efficiency - Cooling

The boiler, during cooling operation, presented efficiencies of approximately 35%. The worst and best boiler efficiencies did not fluctuate as much as with the heating season because the boiler during cooling operation runs almost continuously to provide adequate heat for the absorption chiller. In the heating season, the boiler does not need to run continuously. The CHP system and boiler efficiency must be examined together, as displayed in Figure 6.9.

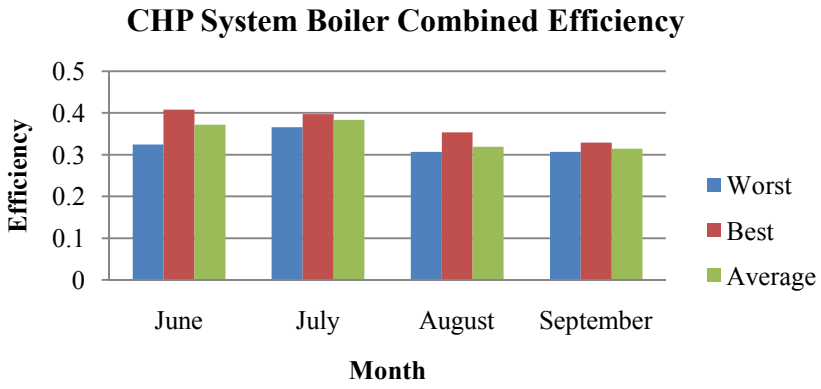

Figure 6.9 CHP System and Boiler Combined Efficiency - Cooling

The CHP system and boiler combined efficiency varies from approximately 31% to 38%. The CHP boiler combined efficiency can give a better estimate of CHP system operational performance for instances when the boiler is utilized a large percent of the time. Including the boiler usually increases the performance metric describing a system that operates more efficiently but does not necessarily assist in the conservation of resources.

Heat exchanger 1 and 2 are next to be evaluated for cooling operation. The heat exchanger ratio and effectiveness of heat exchanger 1 and 2 are presented in Figure 6.10 and 6.11, respectively.

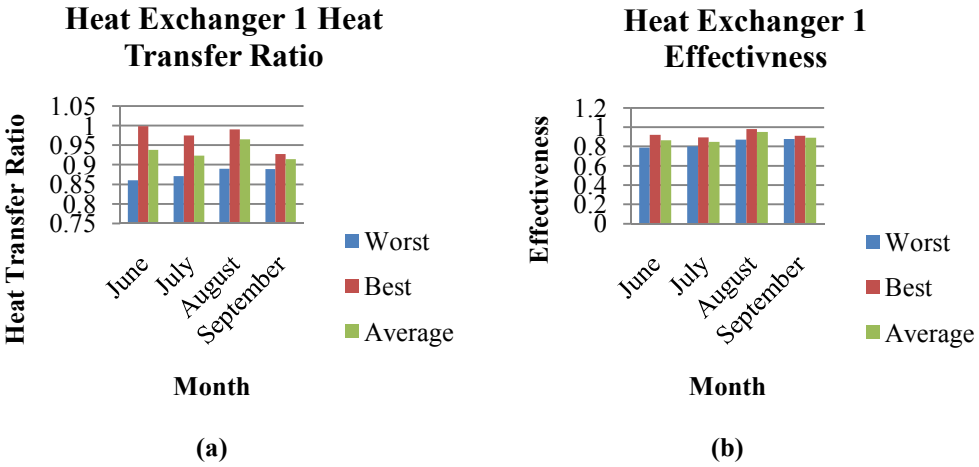

Figure 6.10 Heat Exchanger 1 (a) Heat Transfer Ratio and (b) Effectiveness - Cooling

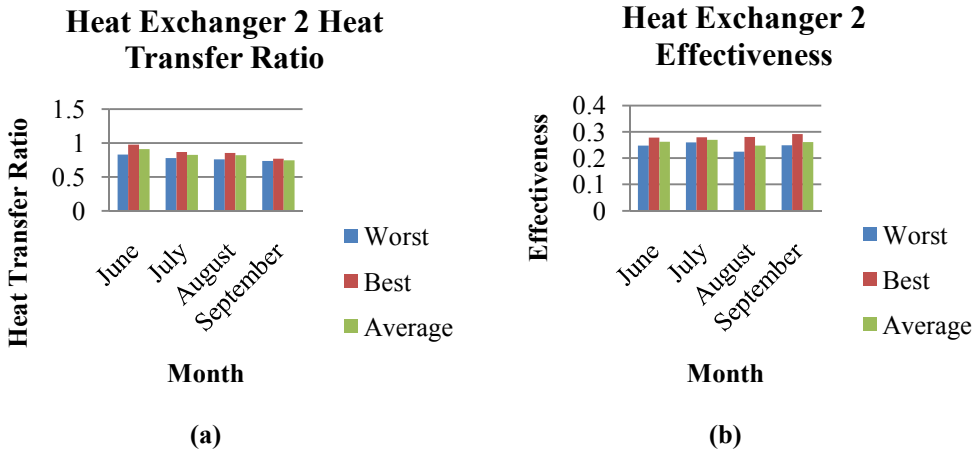

Figure 6.11 Heat Exchanger 2 (a) Heat Transfer Ratio and (b) Effectivness - Cooling

Figure 6.10 presents the nominal heat transfer ratio values are averaged at 0.9 and higher, similar to the results from the heating season. The values for the second heat exchanger, the heat recovery heat exchanger, presented in Figure 6.11, are similar as before, yet a slight increse in the heat transfer ratio and effectiveness can be observed. The increase in these metrics can be attributed to less losses in the heat transfer from the

hot side to the cold side due to the ambient temperature being higher for the cooling season than the heating season. The lower temperature difference reduces the heat transfer to the surroundings, increasing the heat transfer across the heat exchanger.

Finally, the HVAC system is evaluated which is comprised of the absorption chiller and the four-pipe fan coil unit. First, the absorption chiller COP is examined. Figure 6.12 displays the absorption chiller COP value averages at approximately 0.26. This value is much lower than the rated value, approximately 0.8, because the absorption chiller is oversized. The COP is different for different months of the cooling season. This issue will be discussed later.

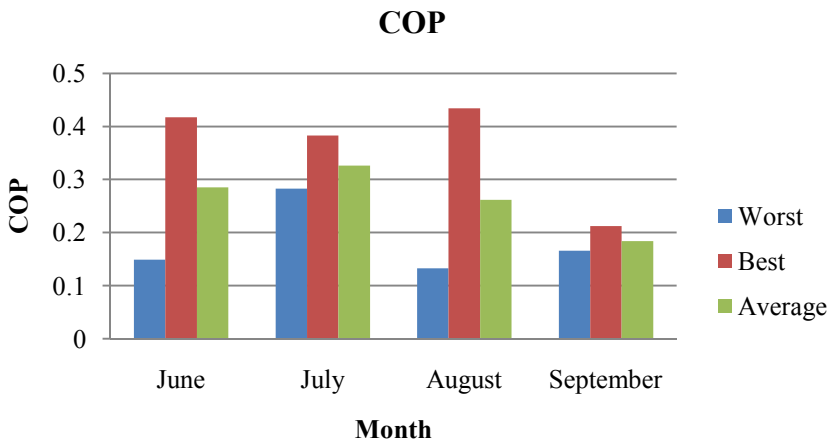

Figure 6.12 Absorption Chiller COP

Lastly, the four-pipe unit is examined. The four-pipe heat transfer ratio is presented in Figure 6.13. This value hovers around one, which confirms that there are not substancial losses in this component.

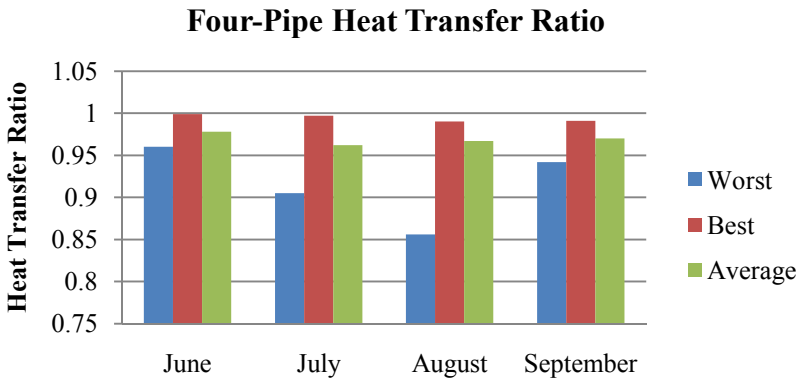

Figure 6.13 Four-Pipe Heat Transfer Ratio

6.1.3 Conventional Heating Results

The conventional heating results only pertain to the furnace. This furnace is fueled by natural gas to produce space heating.

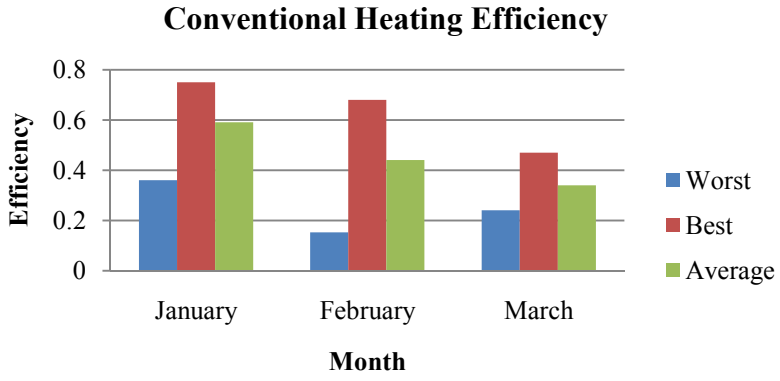

Figure 6.14 Conventional Heating Efficiency

Figure 6.14 indicates that the furnace efficiency averages around 45%. This may seem like a low value, but the efficiency can vary depending on the load, thus explaining why the efficiency is higher for the colder months of January and February.

6.1.4 Conventional Cooling Results

The cooling results for the conventional system pertain to the COP of the vapor-compressions unit. Figure 6.15 examines the COP of the chiller for the months of January through March. From this figure the COP stays around 4.7. The unit is a high efficiency unit with a SEER of 15.25, which when converted to COP is approximately 4.5. This verifies the data collected during the investigation.

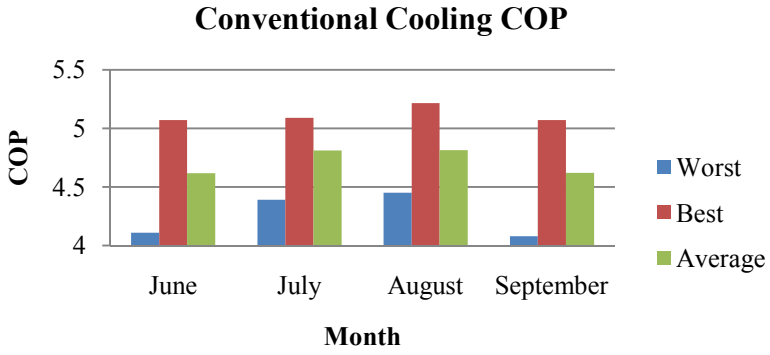

Figure 6.15 Conventional Cooling COP

6.2 Cost Comparison

To examine the operational cost of the CHP system, the cost of electricity and natural gas were obtained from the EIA. The values chosen were the 2008 average for residential and commercial buildings. These values are presented as worst, best, and average for each month. For this situation, worst indicates the highest cost day and best indicates the lowest cost day. Average indicates the average for the month. For the CHP

system the items of interest are the engine natural gas cost, boiler natural gas cost, and the CHP system total operating cost. This cost is computed for the heating and cooling seasons. Next, the conventional system is examined. The conventional heating system includes the natural gas cost for the furnace and the building electrical power consumption. The conventional cooling system examines the vapor-compression electrical power consumption, and the building electrical power consumption. Lastly, the difference between the CHP system and conventional system for heating and cooling is examined. The CHP system heating costs are presented next. Figure 6.16 observes the natural gas cost for the engine, presented in $/hour of operation, while Figure 6.17 displays the natural gas cost for the boiler in $/hour of operation. Figure 6.17 presents the large discrepancy between worst and best because the boiler is only operated when needed and the fuel cost may vary greatly if the boiler is not firing for extended periods of time.

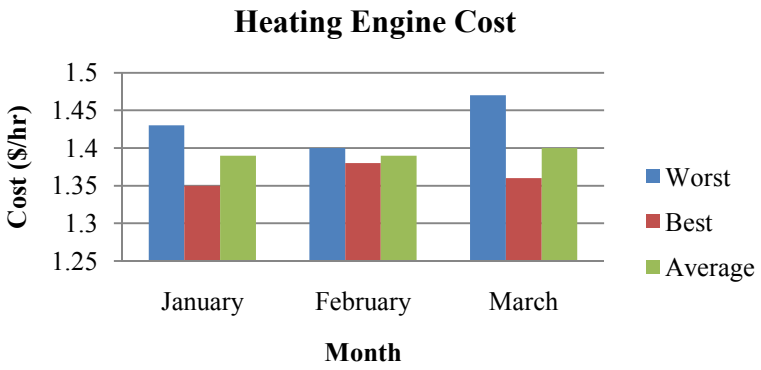

Figure 6.16 Heating Engine Cost

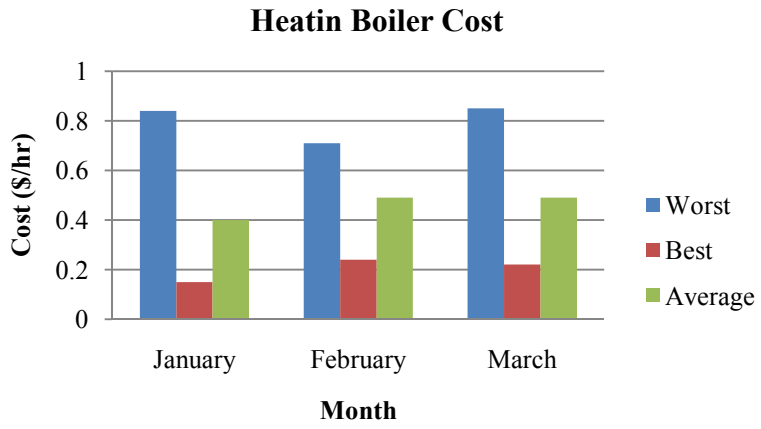

Figure 6.17 Heating Boiler Cost

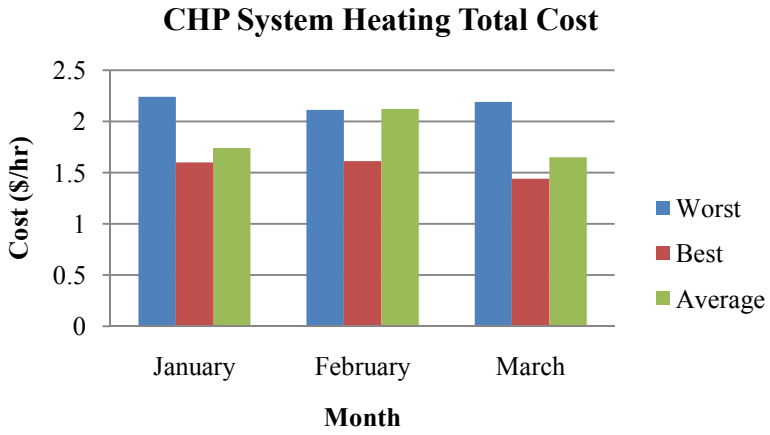

Figure 6.18 CHP System Heating Total Cost

Figure 6.18 examines the combined natural gas fuel cost, given in $/hour of operation. Also this figure presents the average cost that ranges from $1.6/hour to $2.1/hour of operation. The cooling season cost calculations are presented next. This

evaluation is similar to that of the heating season and includes the engine cost, boiler cost, and total cost.

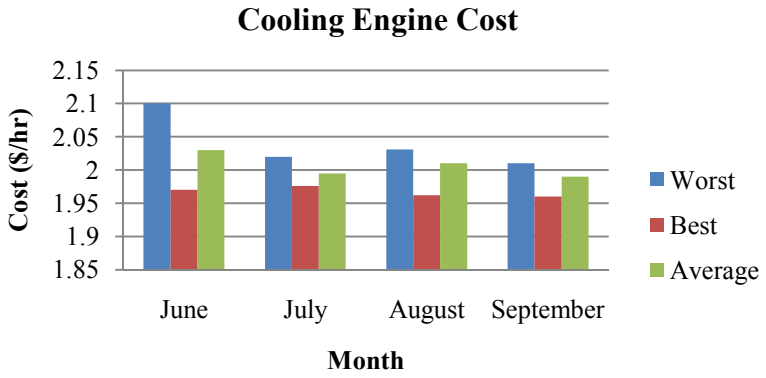

Figure 6.19 Cooling Engine Cost

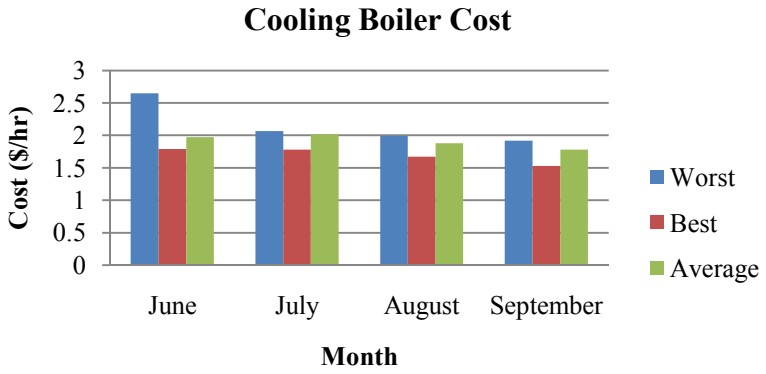

Figure 6.20 Cooling Boiler Cost

Figure 6.19 indicates increased operational cost during cooling season. This is primarily due to the increased electrical load. The boiler cost presented in Figure 6.20 does not fluctuate as much as Figure 6.17 due to constant operation.

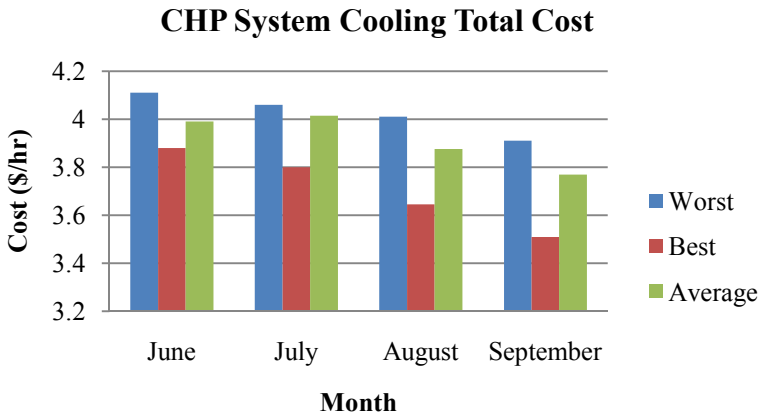

Figure 6.21 CHP System Cooling Total Cost

Figure 6.21 displays the total cooling cost during CHP system operation. This cost ranges from $3.7/hour to $4/hour. This value does not fluctuate much due to the near-constant boiler operation. A comparison of Figure 6.21 and Figure 6.19 indicates the operational cost per hour of the CHP system almost doubles for cooling season as compared to heating season.

The next investigation is the conventional system cost. The conventional system is examined for each component and the total. Figure 6.22 displays the conventional furnace cost from the unit consumption of natural gas. This cost is observed to vary from $0.15/hour to $0.18/hour of operation.

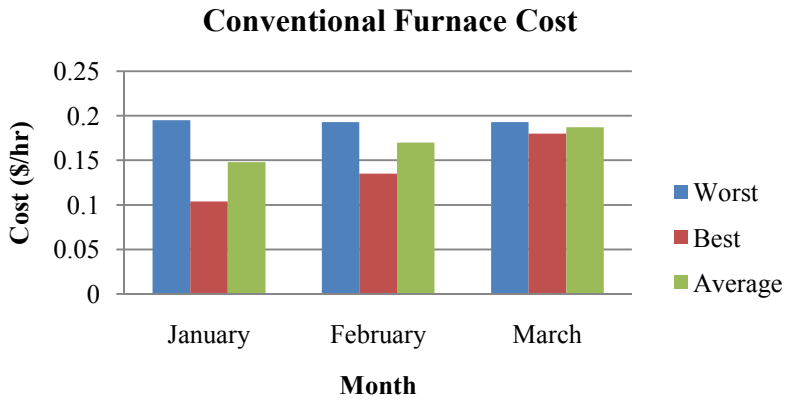

Figure 6.22 Conventional Furnace Cost

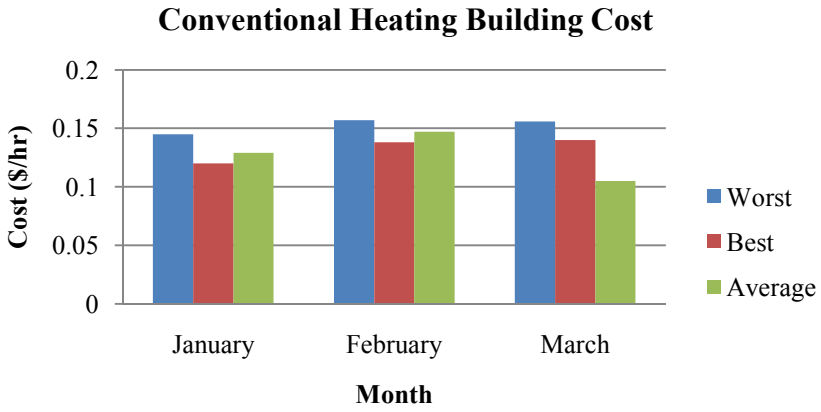

Figure 6.23 Conventional Heating Building Cost

Figure 6.23 describes the conventional heating building cost. This cost is due to the electrical power consumed by the building for lights, HVAC fan, computer, etc.

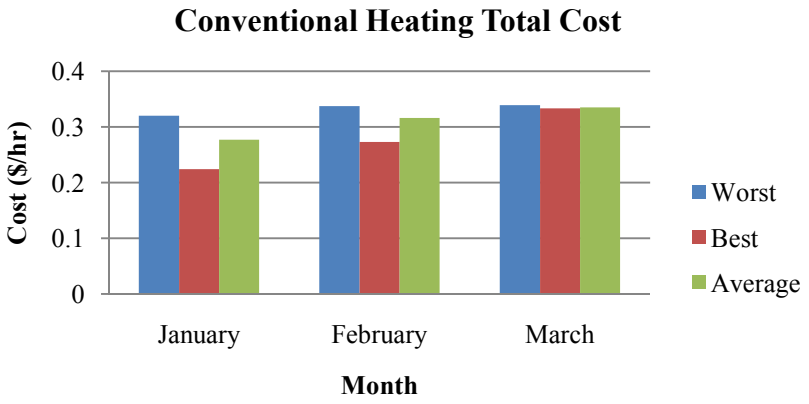

Figure 6.24 Conventional Heating Total Cost

Figure 6.24 presents the conventional heating total cost as the cost for both natural gas and electrical power consumption. This value ranges from $0.28/hour to $0.33/hour of operation. The cooling load is met by a vapor-compression system powered by electricity.

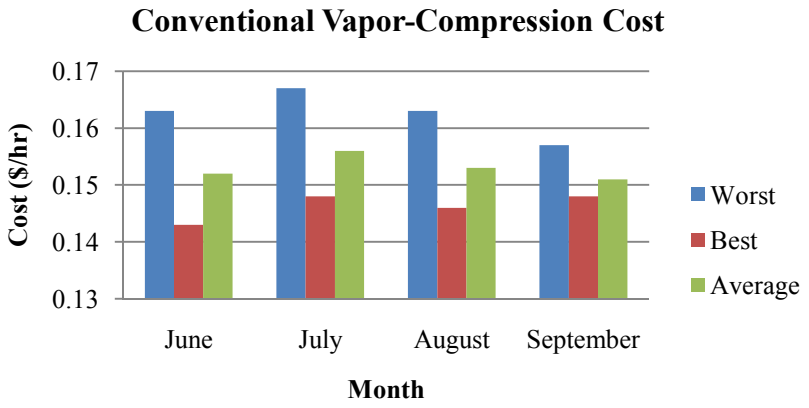

Figure 6.25 Conventional Vapor-Compression Cost

Figure 6.25 depicts the cost of the electrical power consumed by the compressor and fans in the cooling system. The building cost for cooling operation, displayed in Figure 6.26, is the total building electrical cost minus the electrical power utilized by the compressor and fans.

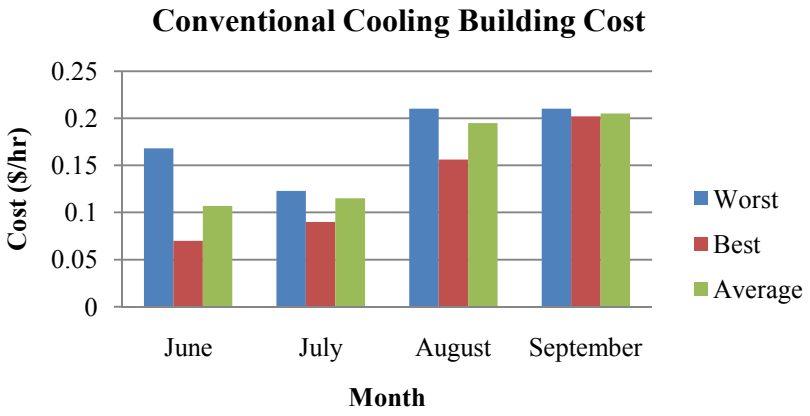

Figure 6.26 Conventional Cooling Building Cost

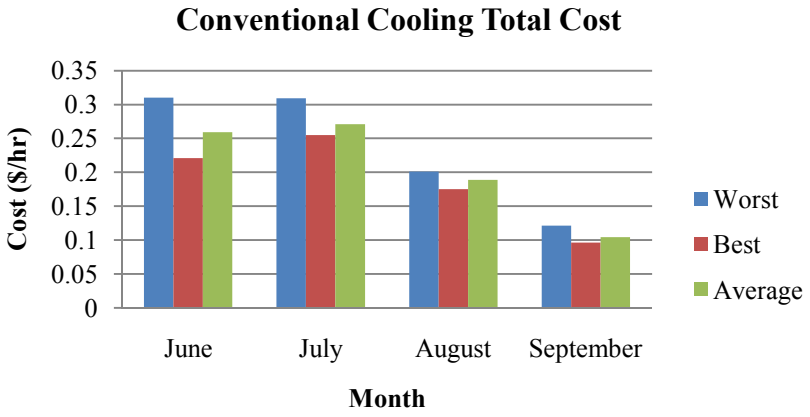

Figure 6.27 Conventional Cooling Total Cost

Figure 6.27 reveals the sum of the two electrical costs yielding the total hourly cooling cost for conventional operation. This cost varies because of the changing cooling loads of different months. The maximum cost is $0.27/hour of operation.

The conventional system is not as costly as the CHP system. For heating operation, CHP system operation costs between $0.27/hour and $1.82/hour more than if

the building was conventionally powered and heated. Cooling season increases this cost difference to $3.42/hour to $3.9/hour of operation. This difference is primarily due to natural gas and electrical power prices. This price difference is called the spark gap. Spark gap represents the cost of electricity per million BTUs minus the cost of natural gas per million BTUs. For the electrical and natural gas cost used in this dissertation the spark gap is $18.82 per million BTUs. The cost per million BTUs for electricity is 18.82$ more than the cost per million BTUs of natural gas.

6.3 SETR Results

SETR represents a performance parameter to evaluate a CHP system as a whole. This ratio is meant to evaluate how well all the components of the CHP system work together to provide power and HVAC for the building. The results for the SETR heating analysis is displayed in Figure 6.28.

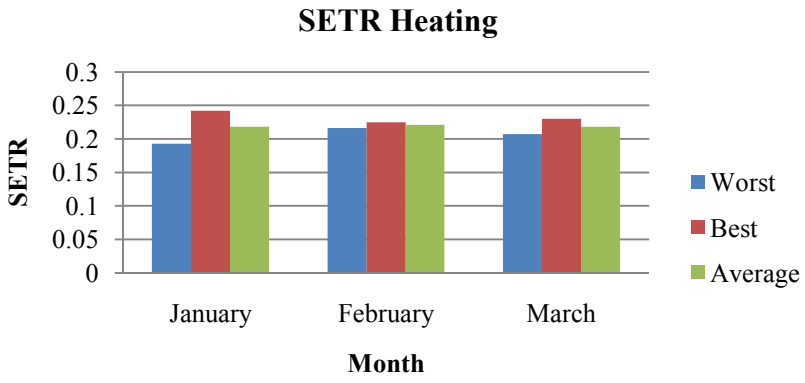

Figure 6.28 SETR Heating Results

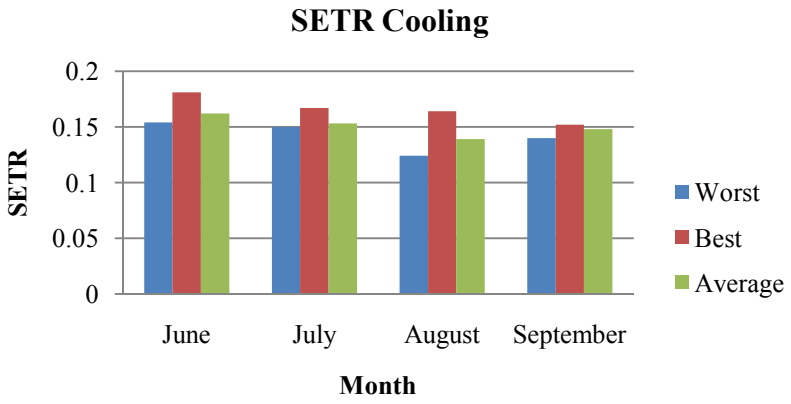

Figure 6.29 SETR Cooling Results

The SETR value stays relatively the same, at approximately 0.22 or 22%. This value indicates that 22% of the fuel energy consumed achieves power production and space heating. Figure 6.29 displays the SETR cooling results. The cooling ratio drops to about 0.15 or 15%. This is a reduction of almost 6% in performance. The primary difference in the SETR results for heating season and cooling season is the addition of the absorption chiller. The drop in SETR is due to the low chiller COP. SETR allows the MSU demonstration facility to be compared with other Micro-CHP system facilities as a whole.

6.4 Particular Considerations

The observation of the CHP system for extended periods of time yielded some interesting results. These results, specific to the demonstration site, are discussed in this

section. To be examined are some phenomena exhibited by the system that could be used to benefit the knowledge base about CHP system operation.

6.4.1 System Start-up Performance

The first item examined describes the transient and steady-state nature of the facility. When the CHP system is starting up it experiences an increase in performance as compared to when the CHP system is operating in steady-state. The notion of 'relative' steady-state acknowledges that the CHP system never reaches full steady-state, but 'relative' steady-state operation is when the hot water tank reaches a certain temperature, allowing for all aspects of the system to function in a predictable manner. CHP system start-up performances for the engine and the boiler are specified before the hot water tank reaches this temperature. Figure 6.30 displays the performance of the system during start-up conditions for heating season.

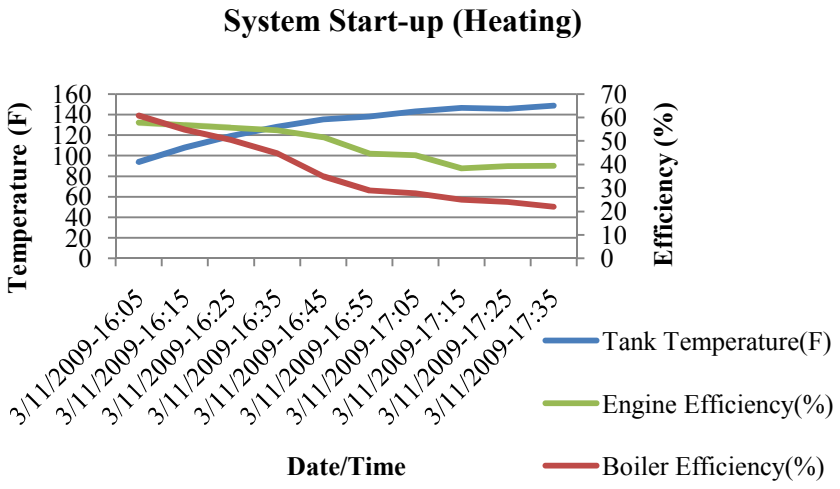

Figure 6.30 Heating System Start-up

In Figure 6.30, the hot water tank temperature begins at approximately 90°F and rises to a steady-state temperature of 150°F. This takes approximately one hour and thirty minutes. During this time, a maximum CHP system efficiency of 57.8% was attained, while a maximum boiler efficiency of 60.8% was reached. Figure 6.31 presents the system start-up performance for cooling mode. The steady-state tank temperature is approximately 165°F. The time required to reach steady-state for the cooling season is one hour and forty-five minutes. The maximum CHP system efficiency during this time is 55.4%, and the maximum boiler efficiency is 43.6%. For both heating and cooling the CHP system displayed better efficiencies for start-up than at steady-state. This increase in performance is due to greater temperature differences during CHP system start-up

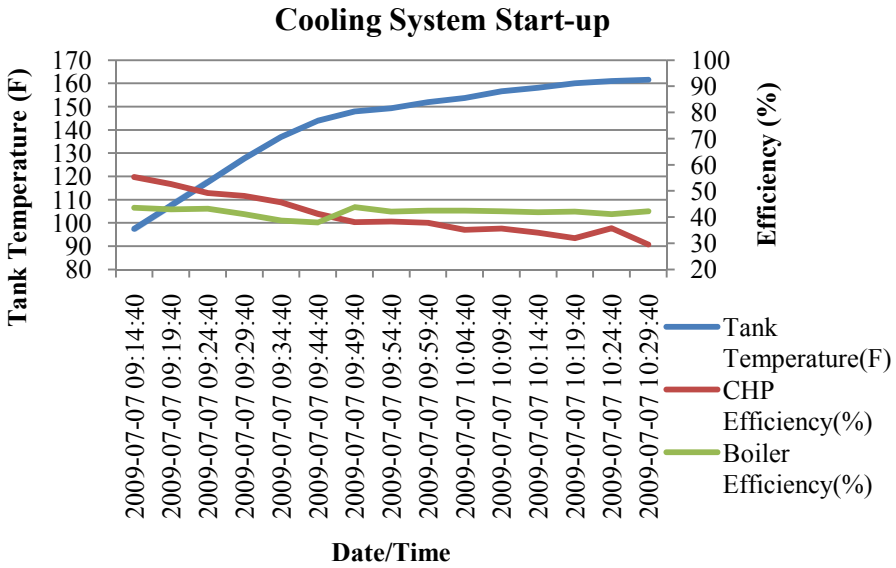

Figure 6.31 Cooling System Start-up

6.4.2 Radiator Bypass Effect on CHP Efficiency

Currently, the radiator operates on a bypass where a sensor detects the leaving coolant temperature from the engine to determine if it exceeds a safe value, approximately 215°F. If the temperature rises more than the safe value, the bypass valve opens to the radiator and dumps the extra heat into the atmosphere. At these times, the CHP system efficiency drops. When the ambient temperature is sufficiently cold, below freezing, the heat recovery system is able to extract enough heat out of the engine coolant so the radiator can be bypassed permanently. Figure 6.32 displays the efficiency and ambient temperature during radiator bypass.

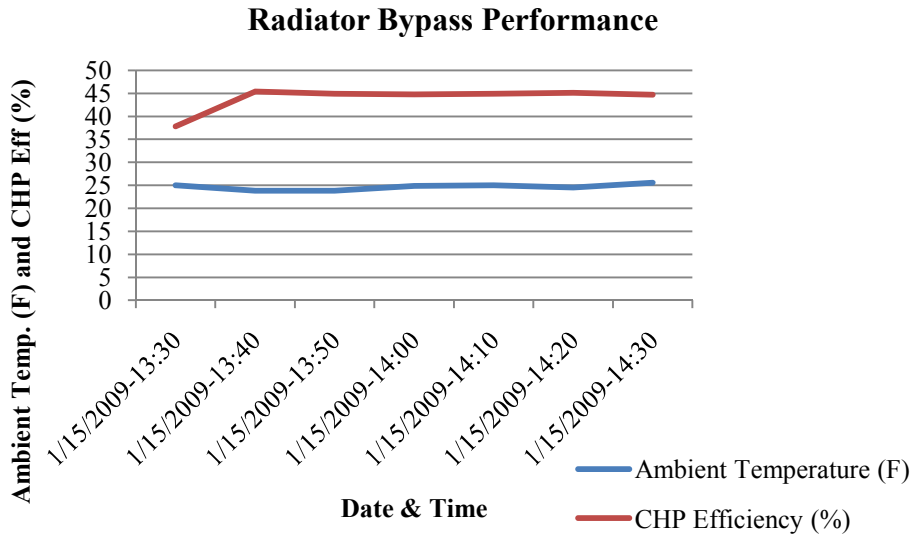

Figure 6.32 Radiator Bypass Performance

CHP system efficiency is improved by approximately 8% when the system is able to bypass the radiator completely. This indicates that this CHP system would be better

suited to a colder climate, so that the CHP system could operate without the need for a radiator.

6.4.3 Incoming Boiler Temperature Effect on Boiler Performance

When computing heat transfer, a major component in the calculations is the temperature difference. Because of this, the incoming temperature can have an effect on the components performance. Figure 6.33 displays the effect of the incoming boiler water temperature on the boiler performance. The performance drops when the incoming boiler water temperature increases. When the same amount of fuel is consumed and the temperature difference of the heat transfer in the boiler water is reduced, the efficiency drops. One way to examine this is to consider the boiler water and the incoming heat as heat reservoirs at two different temperatures. The flame temperature in the boiler remains unchanged, but if the incoming boiler water temperature fluctuates, the driving potential for heat transfer changes. If the incoming boiler water temperature is lower, there is a greater driving potential for heat transfer. This concept is why the boiler efficiency changes based on incoming boiler water temperature.

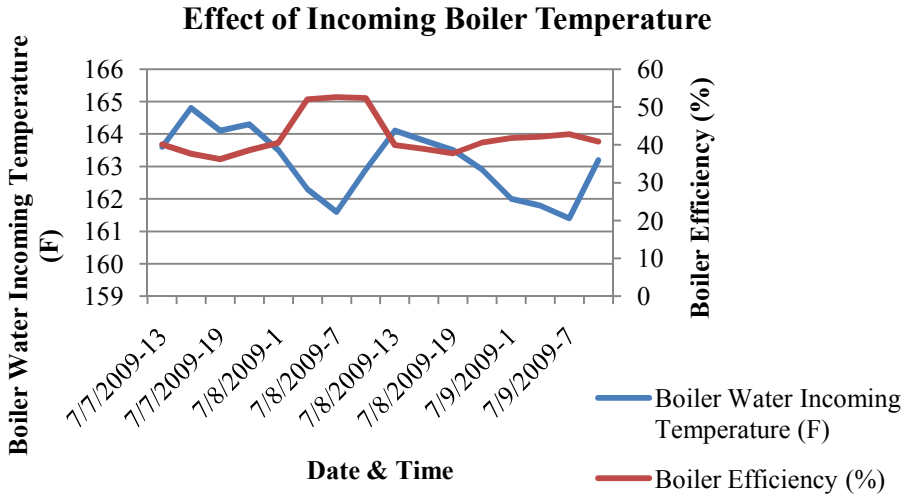

Figure 6.33 Effect of Incoming Boiler Temperature

6.4.4 Incoming Chiller Hot Water Temperature Effect on COP

Incoming temperature also has an effect on the performance of the absorption chiller. Figure 6.34 indicates that the greater the incoming hot water temperature the greater the performance. The chiller is rated at a nominal heat input at a certain temperature. By raising the input temperature, closer to the rated temperature the COP tend towards the rated value.

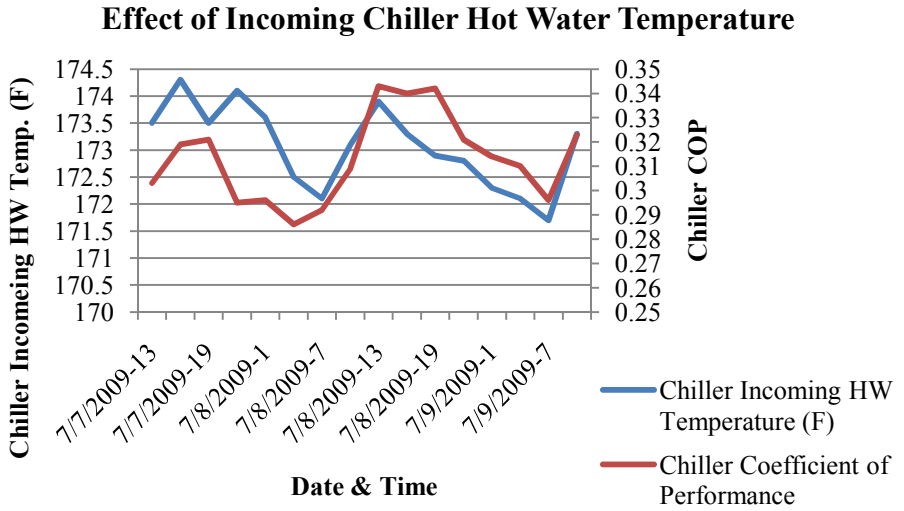

Figure 6.34 Effect of Incoming Chiller Hot Water Temperature

6.4.5 Ambient Temperature Effect on Component Performance

Ambient temperature has the largest effect on the system. The effects of ambient temperature on the engine for heating and cooling season, the boiler, and the absorption chiller are examined in the following figures. Figures 6.35 and 6.36 present the inverse relationship between CHP system efficiency and ambient temperature. Figure 6.36 inverses the y-axis for efficiency to better display the inverse trend for ambient temperature and efficiency.

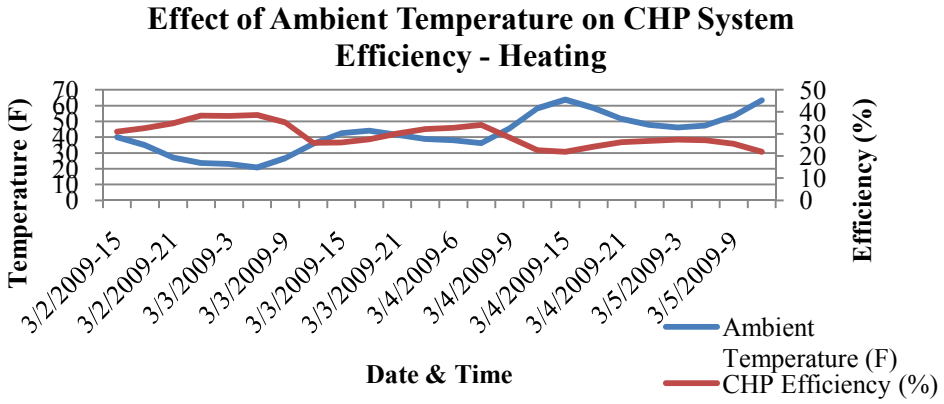

Figure 6.35 Effect of Ambient Temperature on CHP System Efficiency - Heating

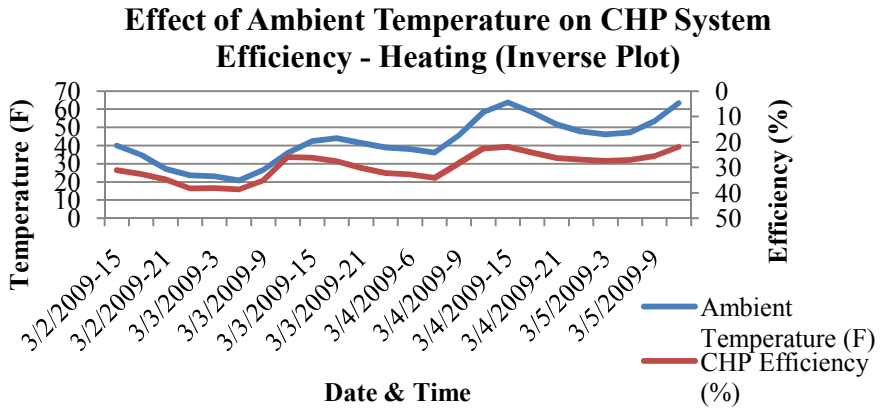

Figure 6.36 Effect of Ambient Temperature on CHP System Efficiency - Heating (Inverse Plot)

Figures 6.37 and 6.38 exhibit similar characteristics as Figures 6.35 and 6.36. This inverse relationship can be explained using the concept of thermodynamic availability or exergy. The concept of exergy examines the enthalpy and entropy of matter relative to the ambient conditions. For example, the thermodynamic availability of the engine coolant is greater when the ambient temperature is lower, rather than higher.

This explains why the CHP system efficiency is greater during times with a lower ambient temperature. The implications of this suggest, as did the radiator bypass situation, that the operation of this CHP system would be better suited for a colder climate.

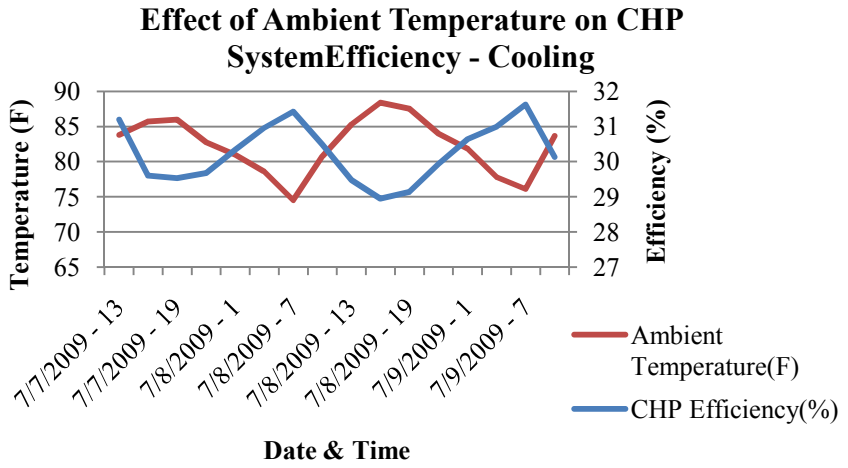

Figure 6.37 Effect of Ambient Temperature on CHP System Efficiency - Cooling

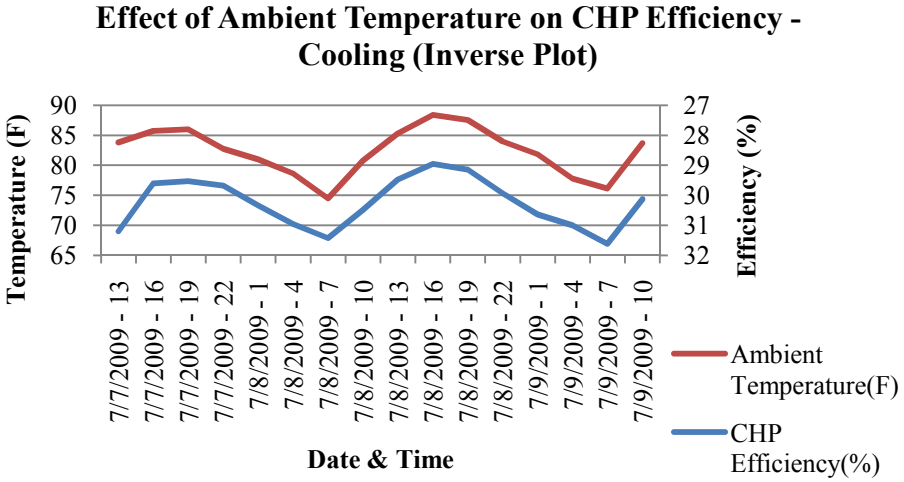

Figure 6.38 Effect of Ambient Temperature on CHP System Efficiency - Cooling (Inverse Plot)

Figure 6.39 examines the ambient temperature effect on boiler performance. This relationship is similar to the CHP system efficiency. This is also explained by thermodynamic availability.

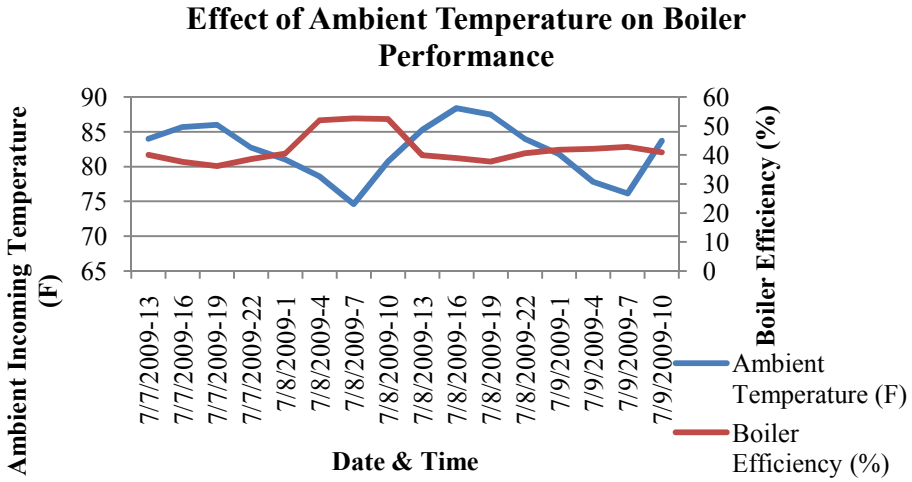

Figure 6.39 Effect of Ambient Temperature on Boiler Performance

Figure 6.40 depicts a different relationship to ambient temperature from that previously seen. The reason for a direct relationship between ambient temperature and chiller performance can be attributed to the cooling load of the building. An increase in ambient temperature results in an increase in the building cooling load. The load required by the building is approximately 2 tons, as the chiller is oversized at 10 tons. The closer the load on the chiller approaches rated load, the closer it will perform to its rated performance.

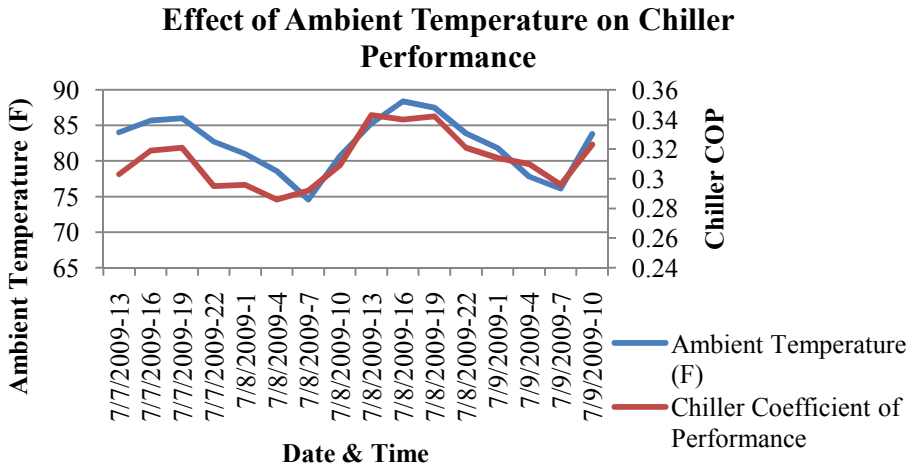

Figure 6.40 Effect of Ambient Temperature on Chiller Performance

6.4.6 Component Interdependence

Interdependency of individual components can be examining by changing one variable common to all, the ambient temperature. Figure 6.41 indicates that for an increase in ambient temperature, the CHP system efficiency drops, the boiler efficiency drops, and the chiller COP increases. For a decrease in ambient temperature, the CHP system efficiency increases, boiler efficiency increases, but the chiller COP decreases. An increase in the performance of the engine and heat recovery system precludes an increase in the boiler efficiency, but a drop in the absorption chiller COP. The inverse can also be seen. From Figure 6.41, multiple relationships between the three primary components of the CHP system may be interpreted.

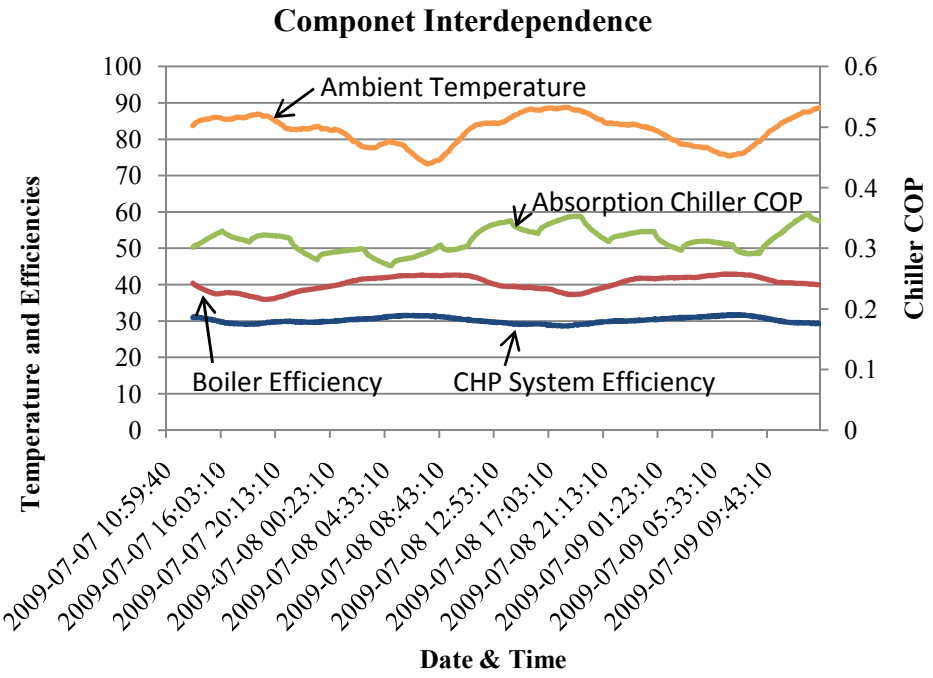

Figure 6.41 Component Interdependence

CHAPTER 7

CONCLUSIONS AND RECOMMENDATIONS

7.1 Conclusions

Conclusions can be made based on the information presented in this investigation. However, the conclusions focus on the impact that they have on CHP systems as an application. From the performance information attained, this system does not perform as well as some systems in the literature. At time, particularly start-up and radiator bypass, the system performs close to the claim in the literature, but it does not appear likely that this system could attain CHP system efficiencies of greater than 60%. The maximum relative steady-state CHP system efficiency is at most 35% suggesting that there are multiple losses unaccounted for in either the heat recovery system or the engine and generator. But, this system is oversized for this particular application.

The results indicate that the conventional system performs much better than the CHP system. For heating, the SETR efficiency was approximately 21% while the conventional furnace operates at an average of 45%. During cooling operation the SETR efficiency was rated at 15%, while the COP for the conventional system is 4.7. While this was already apparent, there are other factors to consider. The comparison presented does not consider the efficiency of the electrical power that is received to the building during

conventional system operation. Central power plant generating efficiency is 36% to 40%, displaying it is superior in performance to CHP system SETR. The final issues to consider are the losses in transmission from the centralized power plant to the demonstration site. These losses are estimated at 7.2% which brings the electrical efficiency to, at worst, approximately 33%. This can be combined with the heating and cooling performance for the conventional system to display that, while the difference in the performance may be somewhat reduced, the conventional system is still superior to the CHP system in terms of performance for this particular application. A comparison of the cost of CHP system and conventional system operation indicate that this is a difficult problem to overcome. The difference in cost is large, but highly dependent on the cost of natural gas. If CHP systems, utilizing natural gas as the fuel, are to become economically feasible, then natural gas prices must drop significantly. Despite this, other factors should be considered when determining the viability of CHP systems operation. These factors, discussed in the literature survey, include primary energy consumption, resource efficiency, and emission reduction.

The values for CHP system efficiency, boiler efficiency, and absorption chiller COP all fell within expected norms. The balance checks assist in this matter. When all balance checks work out, the equations are valid. The only items that at times did not check out were the first heat exchanger, the exhaust heat exchanger, heat transfer ratio and the HVAC heat transfer ratio. These can be attributed to the transient nature of the equipment and the uncertainty associated with the instrumentation. For the times that the

error exceeded the uncertainty, those data sets were discarded to preserve the integrity of the results.

During the literature survey, certain assumptions made in models concerning items such as, boiler efficiency might be exaggerated. Based on the results presented herein, multiple parameters should be tweaked to construct a better model of a real system. To construct an effective model to yield simulation results that can be verified by experimental analysis, the model must use constants, such as CHP system and boiler efficiency, that are similar to a real situation. If proper inputs are provided to the model, the simulation can yield more accurate and useful results; these results can be extrapolated to not only apply to the demonstration site but to other CHP facilities as well.

7.2 Recommendations

Recommendations will be split into two areas, instrumentation recommendations and recommendations for future investigation.

7.2.1 Instrumentation Recommendations

After performing an uncertainty analysis the importance in the accuracy of the instrumentation became evident. If one sensor is more inaccurate than the others, it can raise the uncertainty of a calculation significantly. For this reason, precise calibration and accurate sensors are essential to effective instrumentation. Another recommendation is to

increase the number of temperature sensors. Additional sensors should be placed at intervals along much of the piping system and in the hot water tank to give a better profile of the temperatures in the system. Currently, the only locations with temperature sensors are in proximity to the components such as heat exchangers, the boiler, the absorption chiller, and the four-pipe fan coil unit. Temperature sensors should be added at intervals in the pipes between these components especially at the junctions. Another recommendation is to install temperature sensors in multiple locations in the hot water tank. If temperature sensors were placed in different locations in the tank, then a better idea about the system steady-state temperature and a better profile of the temperature inside the tank could be obtained.

An item that should be added to the instrumentation is a solar radiation detector. This instrument would allow the heating or cooling load for the facility to be accurately computed and be able to detect the possible effects of this on the engine performance.

7.2.2 Investigation Recommendations

The first recommendation pertains to the cooling system. As previously noted, the absorption chiller utilized in the system is greatly oversized and, therefore, exhibits poor performance. The suggestion is to in the operate heating season as usual, while running the vapor-compression to provide for cooling during that season. To do this, the engine would produce more power so that it could provide for the increased electrical load required for the compressor. This would allow the cooling system to operate with a

greatly increased COP. The drawback to this is how to make use of the excess thermal energy during this time. The only recommendation is to use that heat for domestic hot water purposes. While this recommendation does have its drawbacks, it does have potential in yield useful information.

One of the issues with the low performance of the prime mover could be due to it operating at partial load. If an investigation examining the effect of increased loading on performance, one could determine if it would be beneficial to operate the engine at an increased load and sell the excess electrical power back to the grid if allowed by the utility company. If the engine operated at full load, it may be possible to alleviate the need to operate the boiler. The excess natural gas fuel cost to operate the boiler far exceeds the increased natural gas fuel cost to operate the engine at a higher load. An investigation into this could alleviate some of the increased cost for CHP system operation.

The last recommendation is to utilize an electric resistance heater for supplemental heating in place of a boiler. This would require the prime mover to increase its load and provide more electrical power. The previous investigation would yield results that would allow decisions to be made about its effect on the performance of the system. Also investigation of the amount of heat required from this heater, and the heater's efficiency would need to be evaluated to determine its effectiveness as a boiler replacement.

A SETR examination would allow for a proper comparison if the system as a whole were improved or not. A number of the recommendations have the possibility of reducing operational cost by fuel consumption reduction. Performing an analysis similar to the one here on each of the different configurations would allow for a proper evaluation of their worthiness for implementation at other facilities.

REFERENCES

Angel, M., G. Chapa, J. Ramon, and V. Galaz, "Fuel optimization for power, heat and CHP systems constrained by emissions regulations and ambient conditions," IMECE2005-81707.

ASHRAE Handbook – Fundamentals, 2005.

Balli, O., H. Aras, and A. Hepbasli, "Exergoeconomic analysis of a combined heat and power (CHP) system," *International Journal of Energy Research*, 32, 2008, pp.273-289.

Bernotat, K. and T. Sandberg, "Biomass fired small-scale CHP in Sweden and the Baltic States: a case study on the potential of clustered dwellings," *Biomass and Bioenergy*, Vol. 27, 2004, pp.521-530.

Biezma, M.V., and J. R. San Cristobal, "Investment criteria for the selection of cogeneration plants – a state of the art review," *Applied Thermal Engineering*, Vol. 26, 2006, pp.583-588

Bioenergy Feedstock Information Network. Bioenergy.ornl.gov/papers/misc/energy_conv.html

Cardona. E. and A. Piacentino, "Cogeneration: a regulatory framework toward growth," *Energy Policy*. Issue 33, 2005, pp.2100-2111.

Cardona, E., A. Piacentino, and F. Cardona, "Matching economical, energetic and environmental benefits: An analysis for hybrid CHCP-heat pump systems," *Energy Conversion and Management*, Issue 47, 2006, pp.3530-3542.

Cho, Heejin, P. Mago, R. Luck, and L. Chamra, "Evaluation of CCHP systems performance based on operational cost, primary energy consumption, and carbon dioxide emission by utilizing an optimal operation scheme," *Applied Energy*, Issue 86, 2009, pp. 2540-2549.

Critoph, R. E., "Modular regenerative adsorption cycles with fixed beds, applied to trigeneration," *Journal of Process Mechanical Engineering,* Vol. 219, Part E, 2004.

Demirbas, Ayhan. "New Opportunities Resulting from Cogeneration Systems Based on Biomass Gasification," *Energy Sources*, Vol. 27, 2005, pp.941-948.

Fantozzi, F., S. Gerico, and U. Desideri, "Study of a cogeneration plant for agro-food industry," *Applied Thermal Engineering,* Issue 20, 2000, pp.993-1017.

Ferguson, R. Colin and Annan T. Kirkpatrick, *Internal Combustion Engines, Applied Thermo Sciences,* John Wiley & Sons, Inc. 2nd Ed., 2001.

Fumo, N., P. Mago, and L. Chamra, "Cooling, heating, and power energy performance for system feasibility," *Journal of Power and Energy*, Vol. 222, 2008, pp.347-354.

Fumo, N., P. Mago, and L. Chamra, "Analysis of cooling, heating, and power systems based on site energy consumption," *Applied Energy*, Issue 86, 2009, pp.928-932.

Fumo, N., P. Mago, and L. Chamra, "Energy and economic evaluation of cooling, heating, and power systems based on primary energy," *Applied Thermal Engineering*, Issue 29, 2009, 2, pp.2665-2671.

Fumo, N., P. Mago, and L. Chamra, "Hybrid-cooling, combined cooling, heating, and power systems," *Journal of Power and Energy*, Vol 223, 2009, 3, pp.487-495.

Godefroy, J., R. Boukhanouf, and S. Riffat, "Design, testing, and mathematical modeling of small-scale CHP and cooling system (small CHP-ejector trigeneration)," *Applied Thermal Engineering*, Vol. 27, 2007, pp.68-77.

Honton, E. J. and P. L. Lemar, "High Natural Gas Prices and the Updated Market for CHP," *Cogeneration and Distributed Generation Journal*, Vol. 19, No. 4, 2004, pp.54-65.

Incropera, Frank, David DeWitt, Theodore L. Bergman, and Adrienne Lavine, *Fundamentals of Heat Transfer.* John Wiley & Sons, Inc 6th Ed. 2007. Table A.6.

Jiang, Y., H. Li, L. Fu, and K. Geng, "Energy utilization evaluation of CCHP systems," *Energy and Buildings*, Issue 28, 2006, pp.253-257.

Keenan and Keyes, "Psychrometric Data," *ASAE Standards*, D271.2, 1989, pp.4-5.

Kong, X. Q., R.Z. Wang, J.Y. Wu, X.H. Huang, Y.Huangfu, D.W. Wu, and Y.X. Xu, "Experimental investigation of a micro-combined cooling, heating, and power system driven by a gas engine," *International Journal of Refrigeration*, Issue 28, 2005, pp.977-987.

Lemar Jr, Paul L., "The potential impact of policies to promote combined heat and power in US industry," *Energy Policy*, Vol 29, 2001, pp.1243-1254.

Jiang, Y., H. Li, L. Fu, and K. Geng, "Energy utilization evaluation of CCHP systems," *Energy and Buildings*, Issue 28, 2006, pp.253-257.

Lin, L., Y. Wang, R. Al-Shemmeri, T. Ruxton, S. Turner, S. Zeng, J. Huang, Y. He, and X. Huang, "An experimental investigation of a household size trigeneration," *Applied Thermal Engineering,* Vol. 27, 2007, pp.576-585.

Mago, P, N. Fumo, and L. Chamra, "Methodology to perform a non-conventional evaluation of cooling, heating, and power systems," *Journal of Power and Energy*, Vol. 221, 2007, pp.1075-1087.

Mago, P, N. Fumo, and L. Chamra, "Performance analysis of CCHP and CHP systems operating following the thermal and electric load," *International Journal of Energy Research*, Issue 33, 2009, pp.852-864.

Mago, P and L. Chamra, "Analysis and optimization of CCHP systems based on energy, economical, and environmental considerations," *Energy and Buildings*, Issue 41, 2009, 2, pp.1099-1106.

Maidment, G. and G. Prosser, "The use of CHP and absorption cooling in cold storage," *Applied Thermal Engineering*. Issue 20, 2000, pp.1059-1073.

Marechal, F. and B. Kaliventzeff, "Energy integration of industrial sites: tools, methodology, and application," *Applied Thermal Engineering.* Issue 18, 1998, pp.921-922.

micro- Cooling, Heating, and Power (m-CHP) Instructional Module, Mechanical Engineering Department, Mississippi State University, 2005.

Moran, A., P. Mago, and L. Chamra, "Thermoeconomic modeling of micro-CHP (micro-cooling, heating and power) for small commercial applications," *International Journal of Energy Research*, Issue 32, 2009, pp.808-823.

Onoywiona, H. I., V. I. Ugursal, and A. S. Fung, "Modeling of internal combustion engine based cogeneration systems for residential applications," *Applied Thermal Engineering*, 2007, Vol. 27, pp.848-861.

Oztop, H. F. and A. Hepbasli, "Cogeneration and Trigeneration Applications," *Energy Sources*, Part A, 28, 2006, pp.743-750.

Paepe, M., P. Herdt, and D. Mertens, "Micro-CHP systems for residential applications," *Energy Conversion and Management*, Issue 47, 2006, pp.3435-3446.

Popiel, C.O and Wojtkowiak J, "Simple Formulas for Thermophysical Properties of Liquid Water for Heat transfer Calculations," *Heat Transfer Engineering*, 19:3, pp.87-101.

Russell, Lynn and George Adebiyi, *Classical Thermodynamics,* Oxford University Press. 1993. pp.633-637.

Savola, T. and C.J. Fogelholm, "Increased power to heat ratio of small scale CHP plants using biomass fuels and natural gas," *Energy Conversion and Management*. Issue 47, 2006, pp.3105-3118.

Soares, J. B., A. S. Szklo, and M.T. Tolmasquim, "Incentive policies for natural gas-fired cogeneration in Brazil's industrial sector- case studies: chemical plant and pulp mill," *Energy Policy*, Issue 29, 2001, pp.205-215.

Sonntag, Richard, Claus Borgnakke, and Gordon Van Wylen, *Fundamentals of Thermodynamics,* John Wiley & Sons, Inc. 6th Ed. 2003.

Thomas, Bernd, "Benchmark testing of Micro-CHP units," *Applied Thermal Engineering*, 28, 2008, pp.2049-2054.

Tozer, R. and R. W. James, "Heat Powered Refrigeration Cycles," *Applied Thermal Engineering*, Vol. 12, 1998, pp.731-743.

Wu, D. W., and R. Z. Wang, "Combined cooling, heating, and power: A review," *Progress in Energy and Combustion Science*, Vol. 21, Issue 5, 2006, pp. 459-495.

Yoon, J., K. Choi, C. Moon, Y. Kim, and O. Kwon, "A study on the advanced performance of an absorption heater/chiller with a solution preheater using waste gas," *Applied Thermal Engineering.* Issue 23, 2003, pp.757-767.

Ziher, D. and A. Poredos, "Cooling power costs from a trigeneration system in a hospital," *Forsch Ingenieurwes*, 2006, I70, pp.105-113.

APPENDIX A

LABVIEW ENGINE ANALYSIS PROGRAM

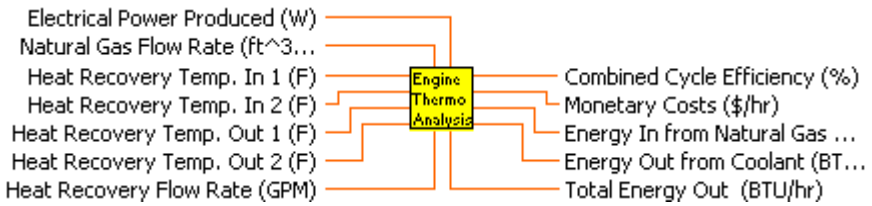

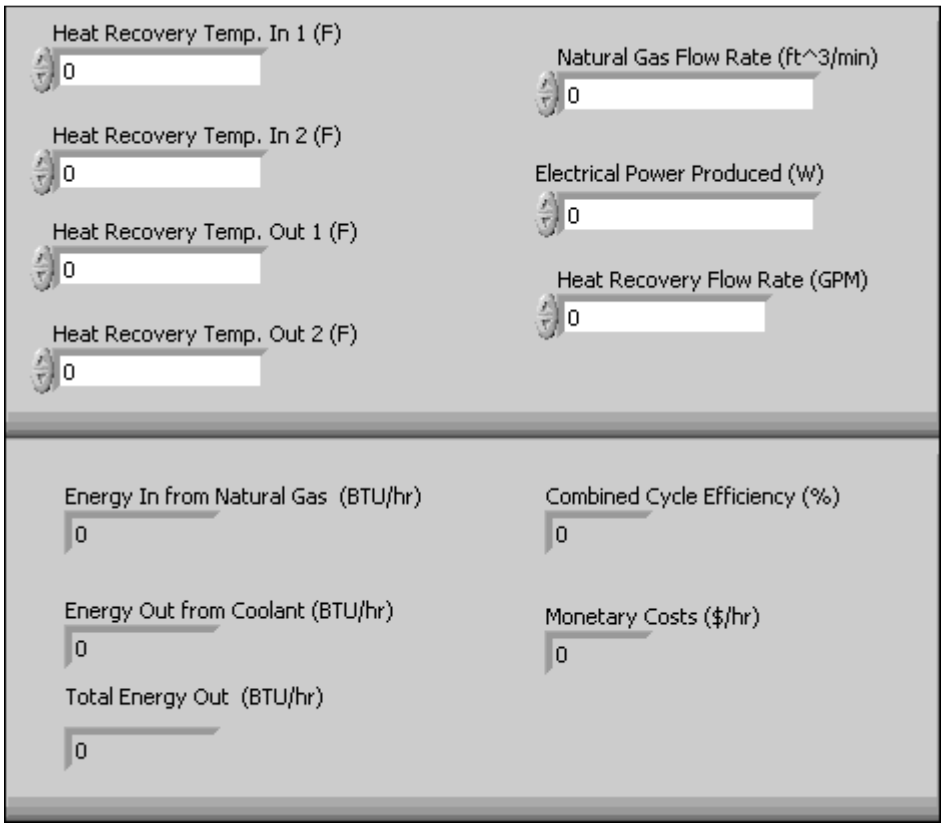

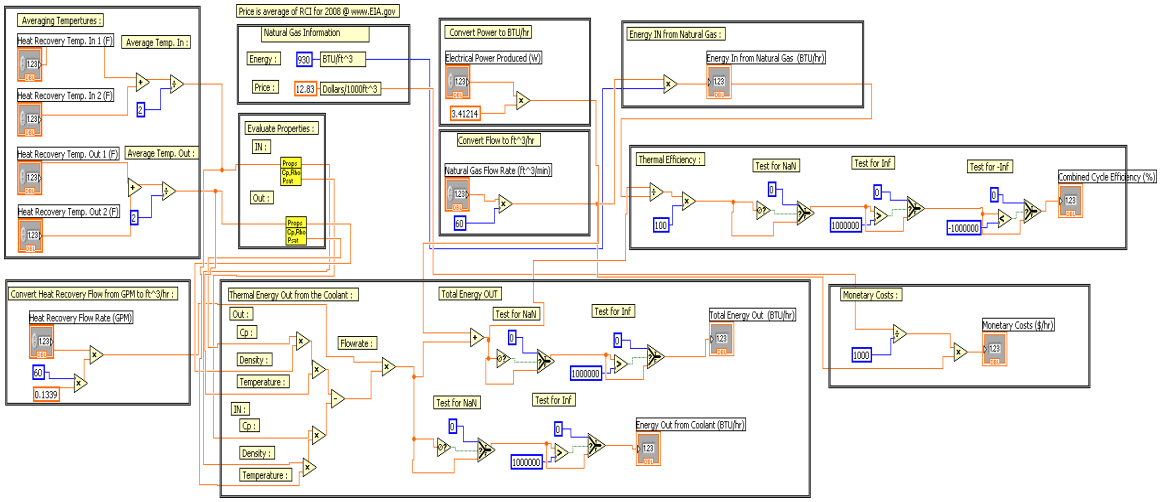

APPENDIX B

LABVIEW HEAT EXCHANGER ANALYSIS PROGRAM

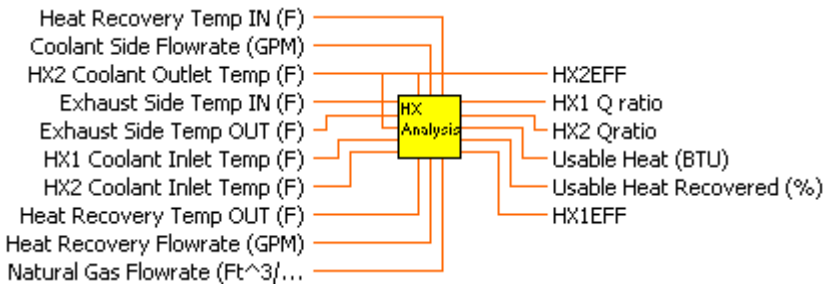

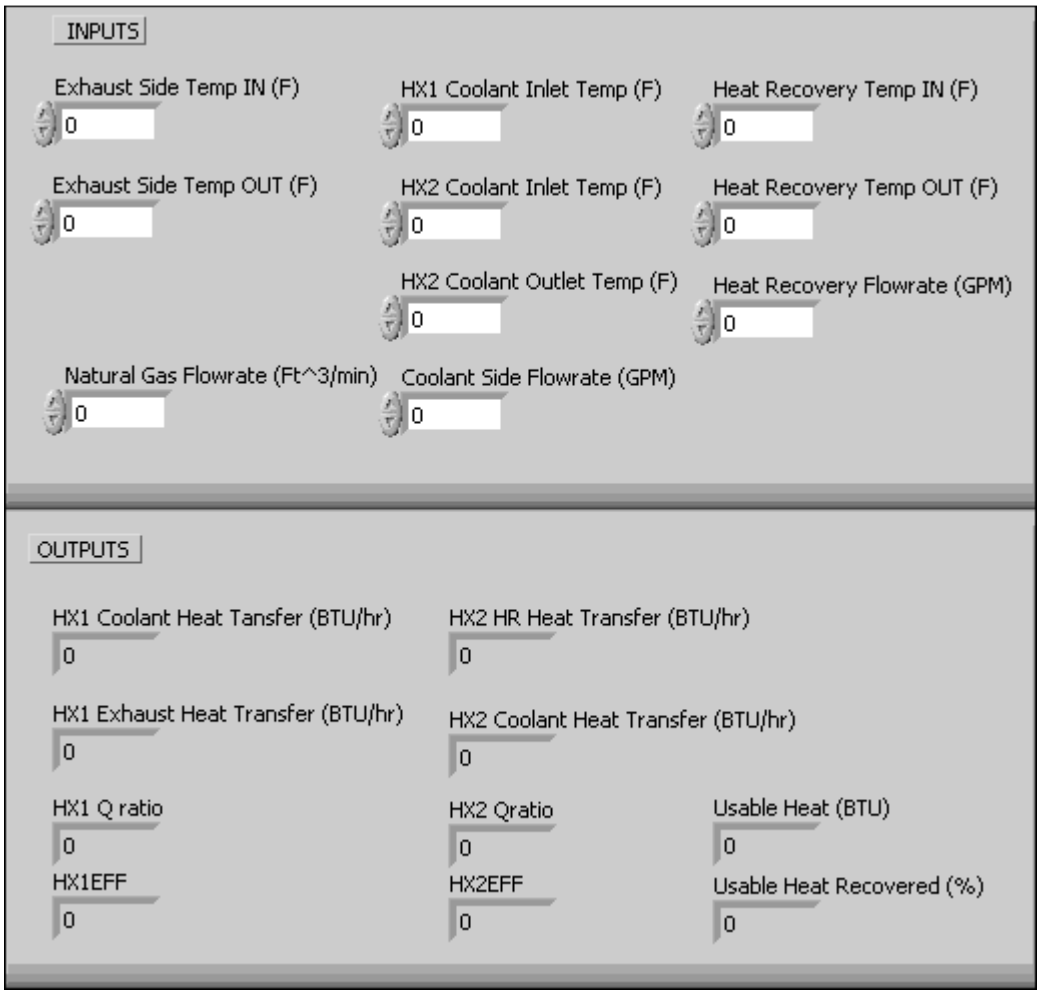

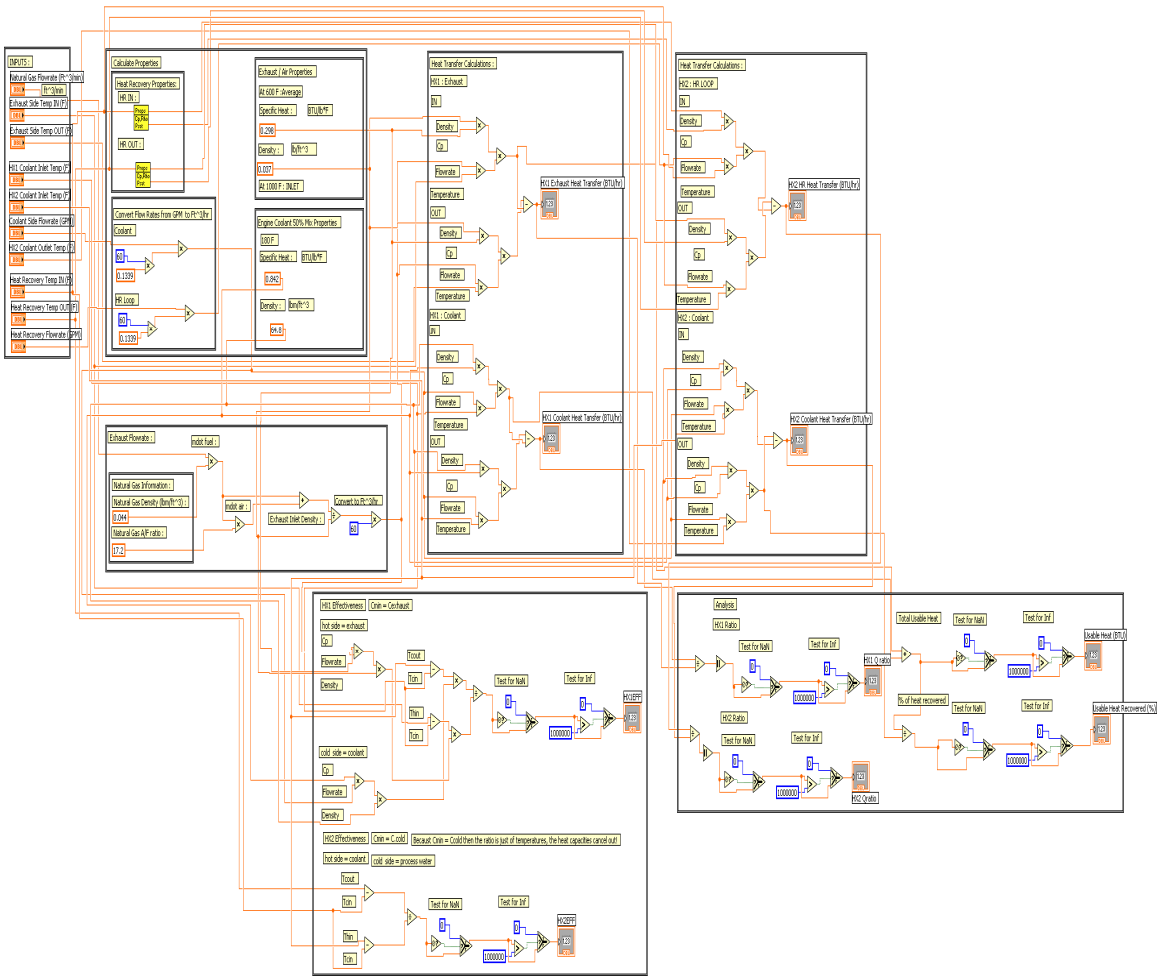

APPENDIX C

LABVIEW BOILER ANALYSIS PROGRAM

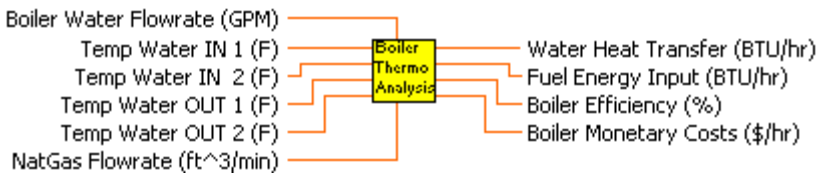

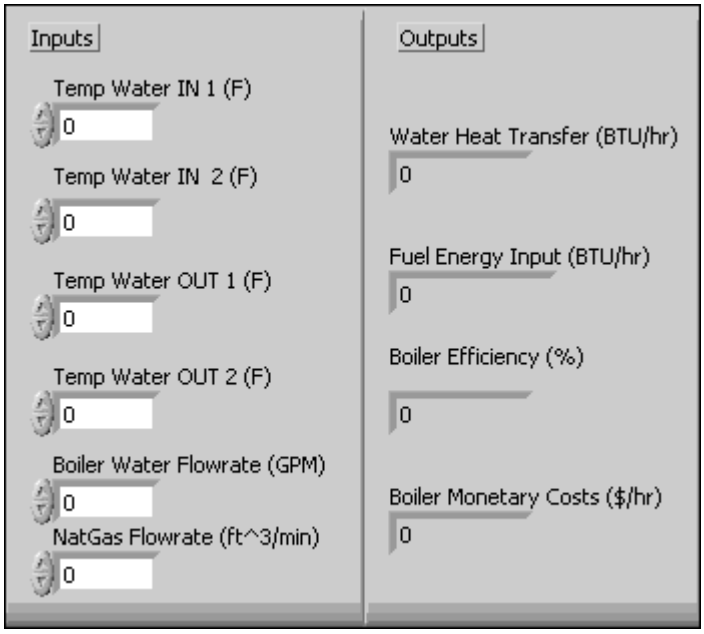

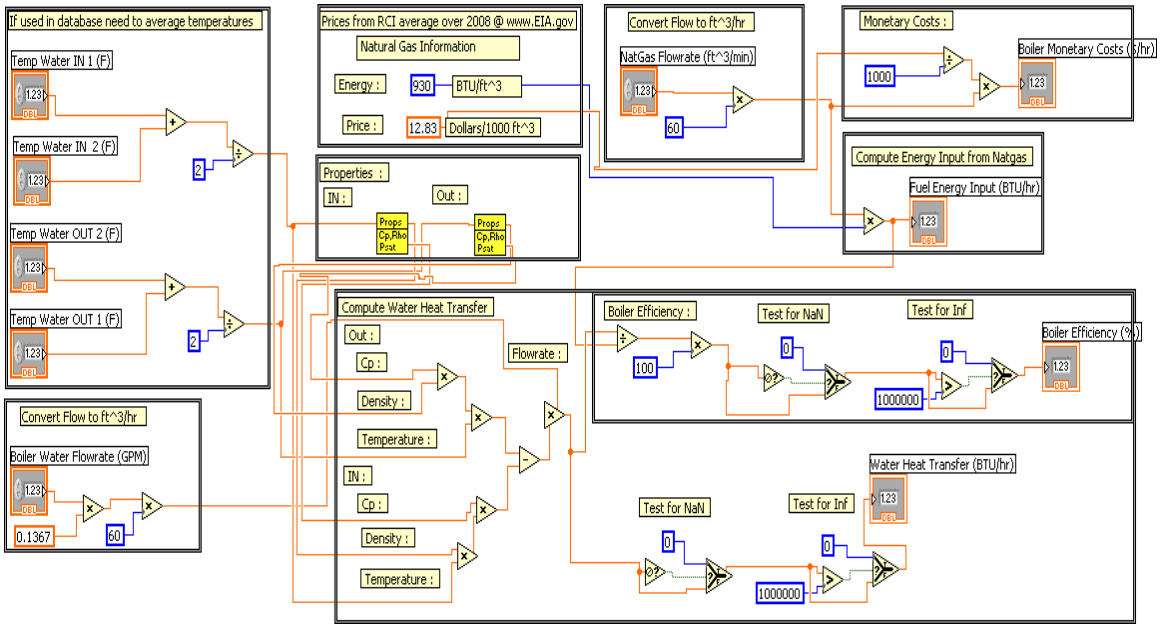

APPENDIX D

LABVIEW ABSORPTION CHILLER ANALYSIS PROGRAM

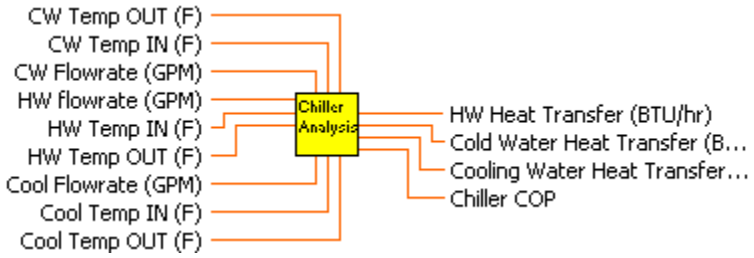

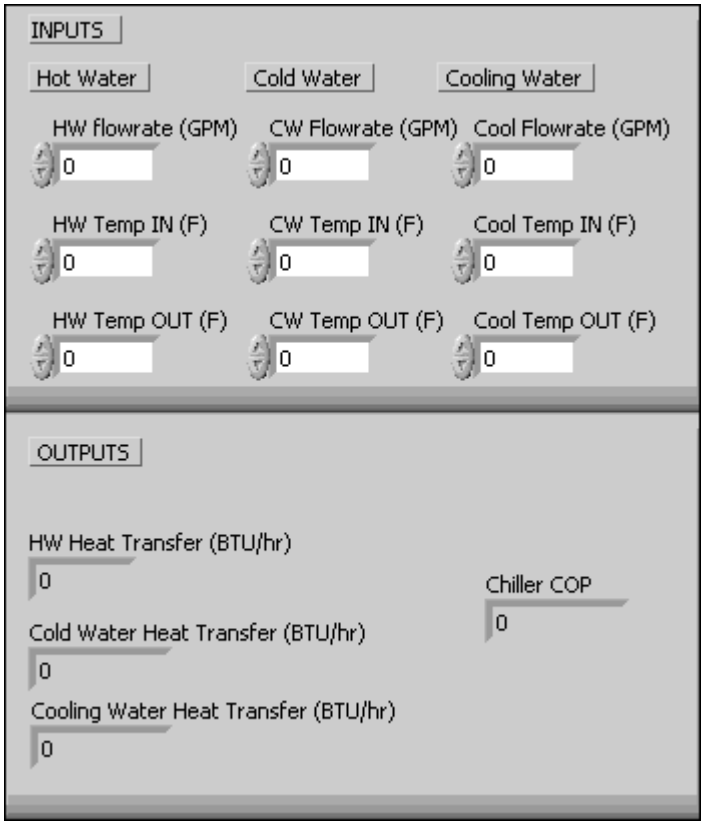

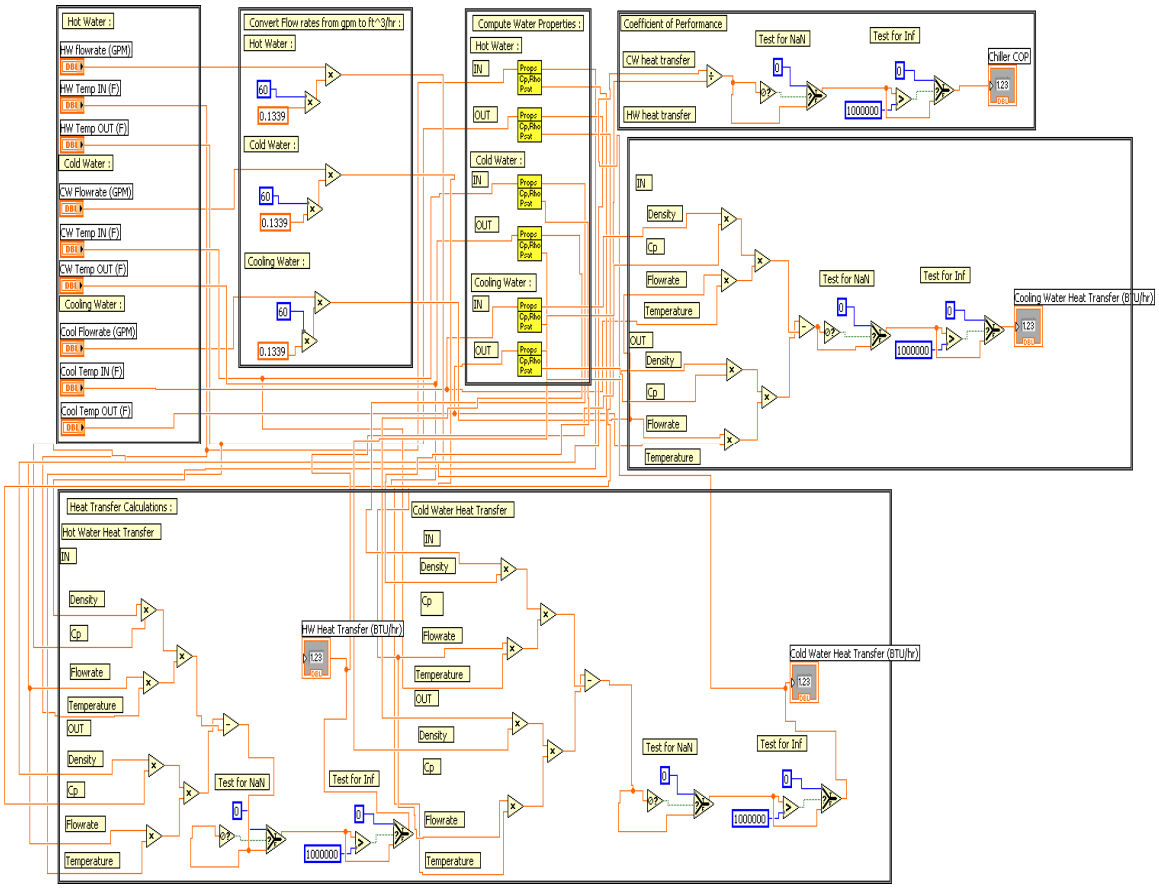

APPENDIX E

LABVIEW CHP SYSTEM HVAC ANALYSIS PROGRAM

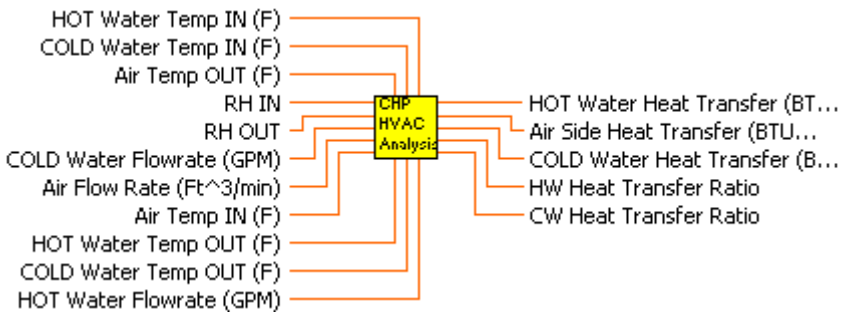

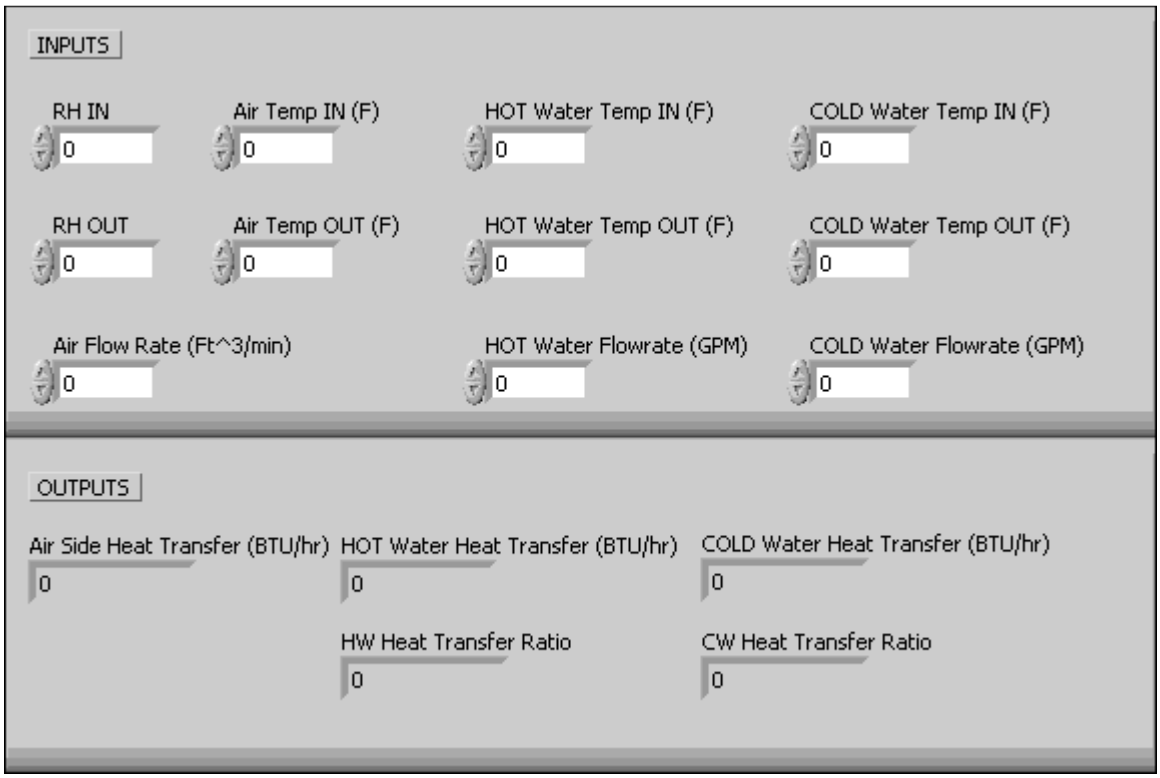

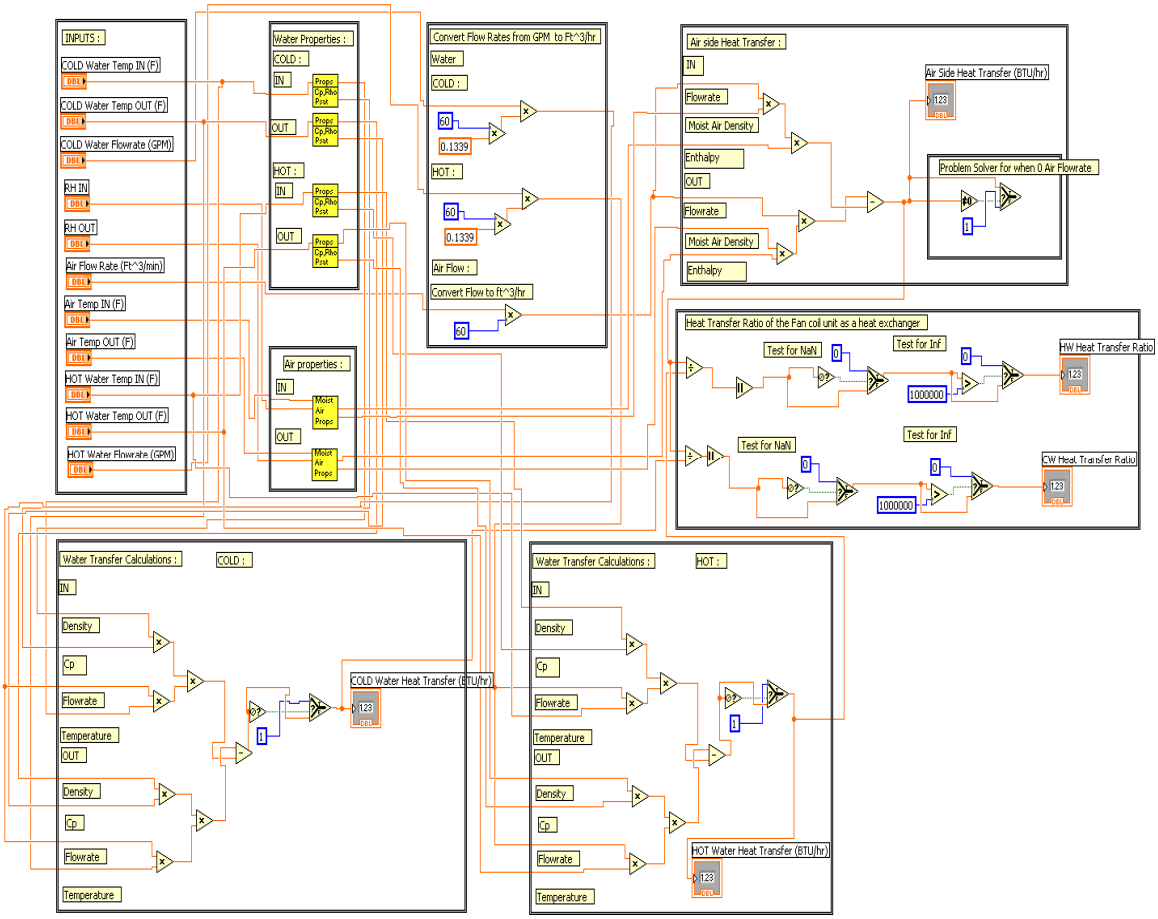

APPENDIX F

LABVIEW CONVENTIONAL HVAC COOLING ANALYSIS PROGRAM

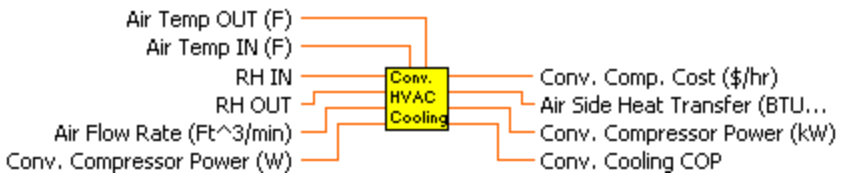

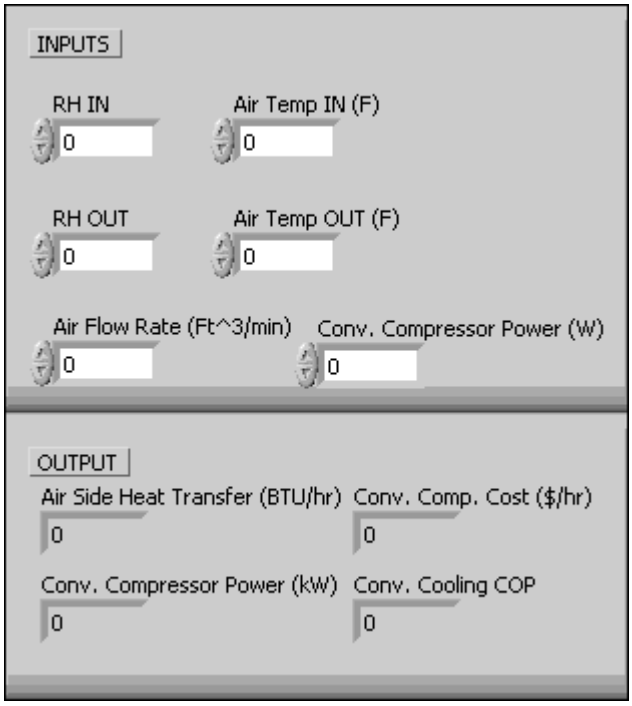

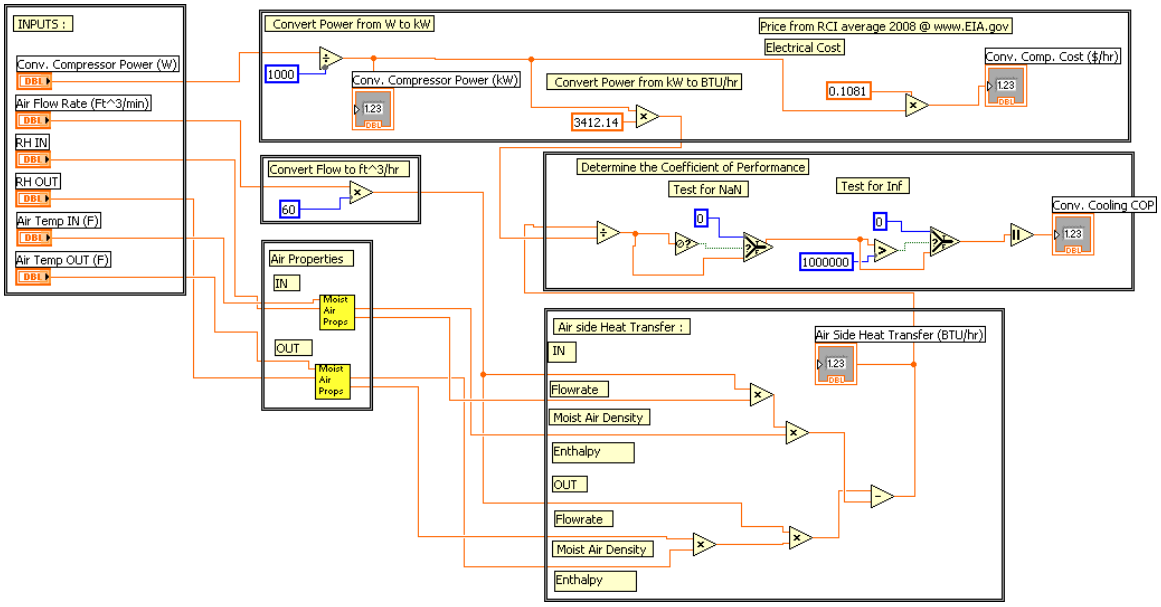

APPENDIX G

LABVIEW CONVENTIONAL HVAC HEATING ANALYSIS PROGRAM

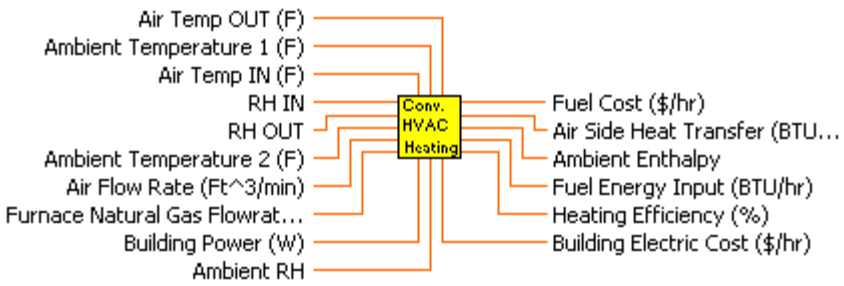

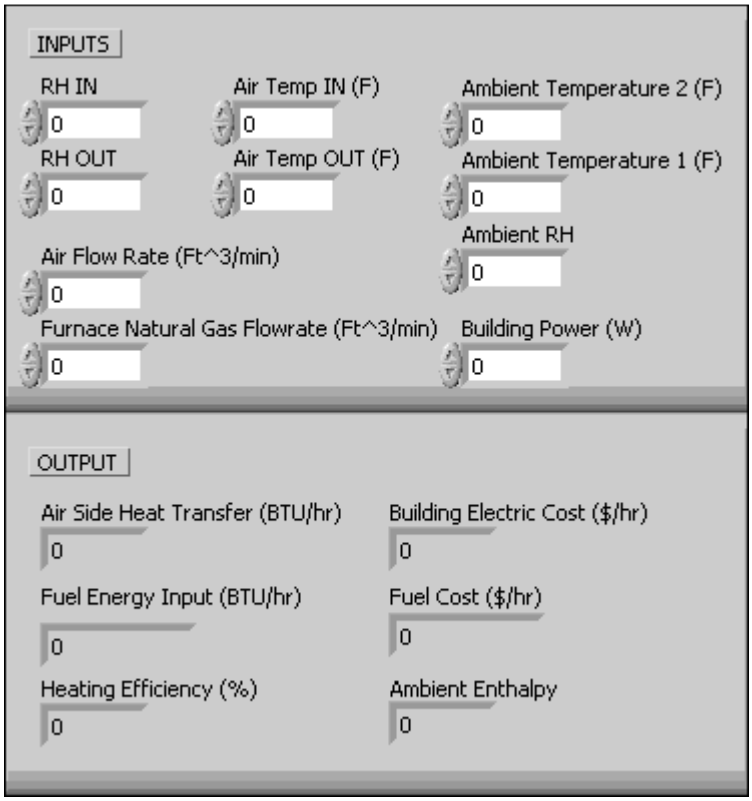

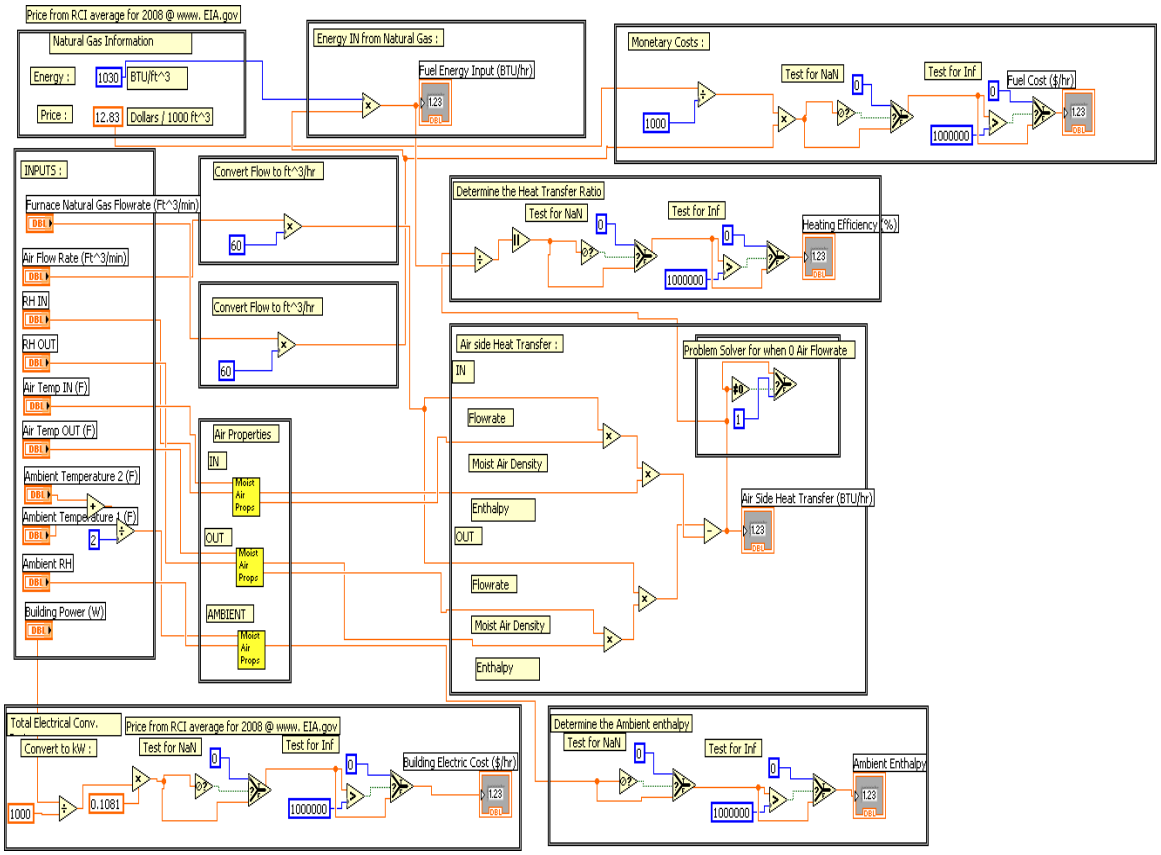

APPENDIX H

LABVIEW CLASS A RTD SUBVI

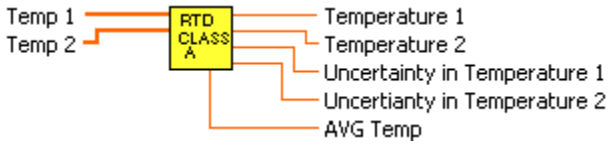

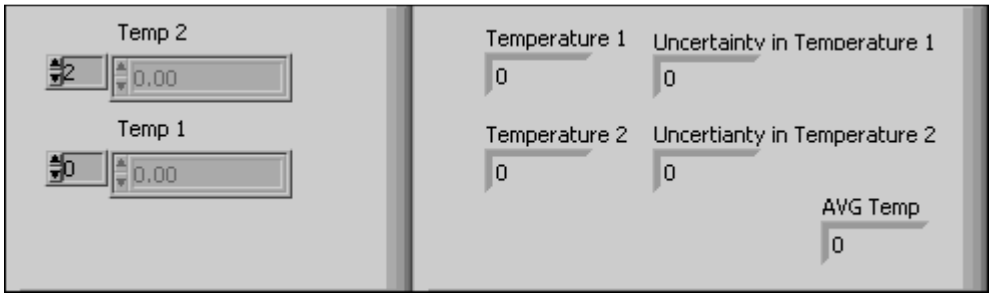

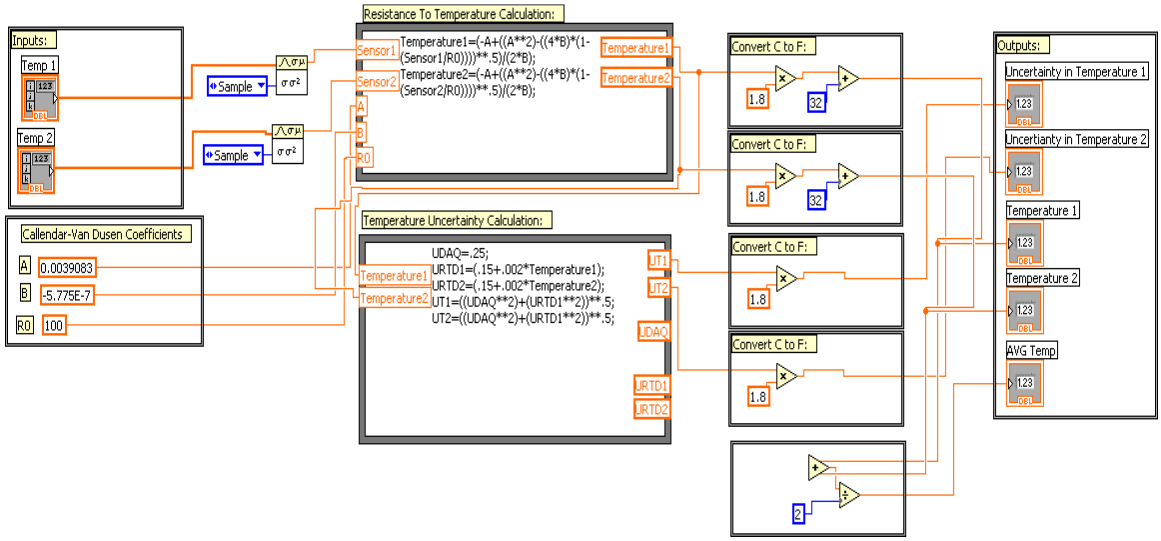

APPENDIX I

LABVIEW WATER PROPERTIES SUBVI

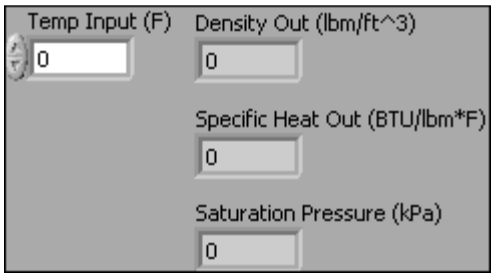

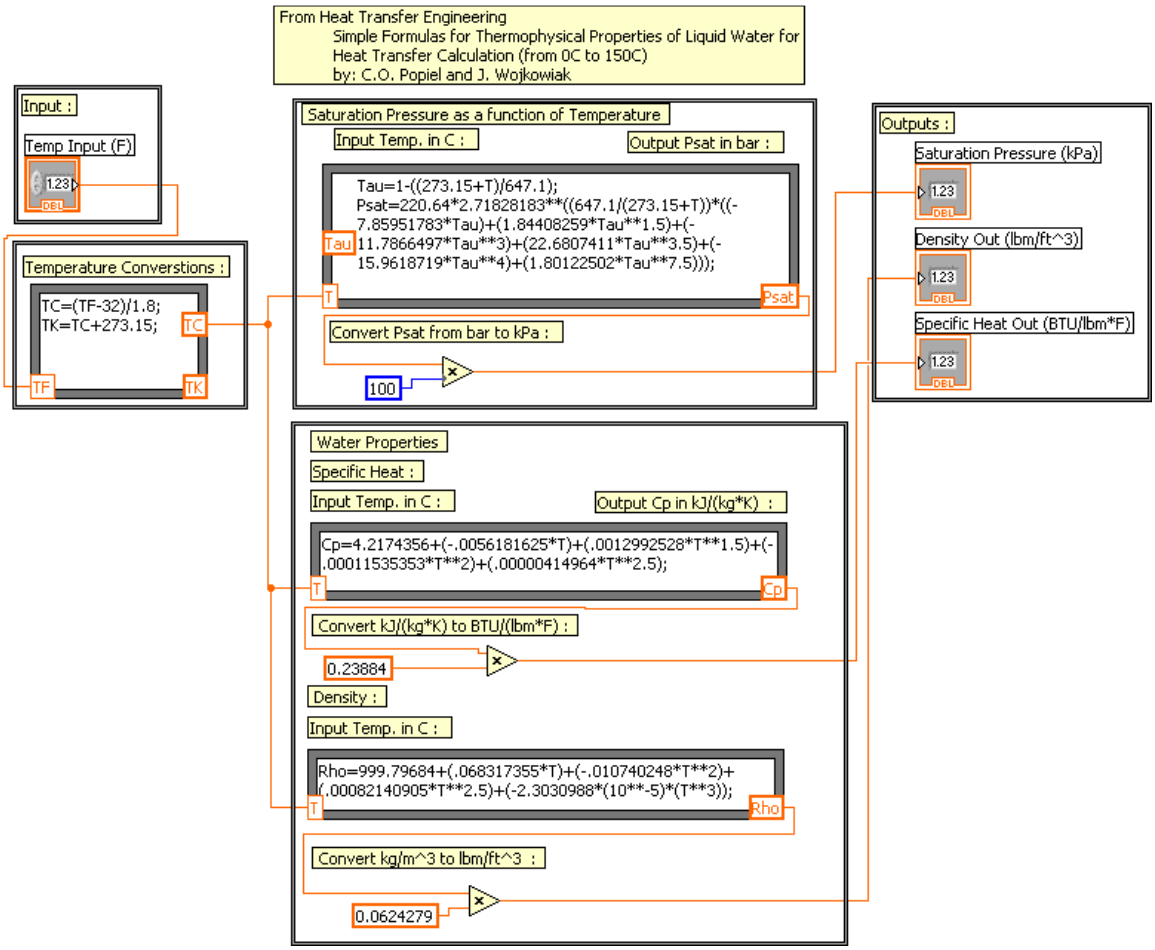

APPENDIX J

LABVIEW MOIST AIR PROPERTIES SUBVI

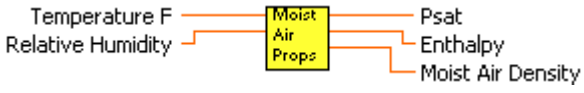

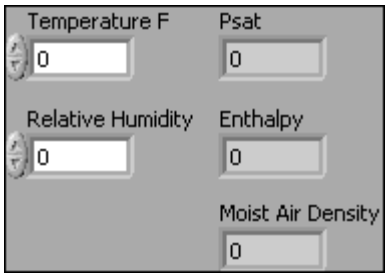

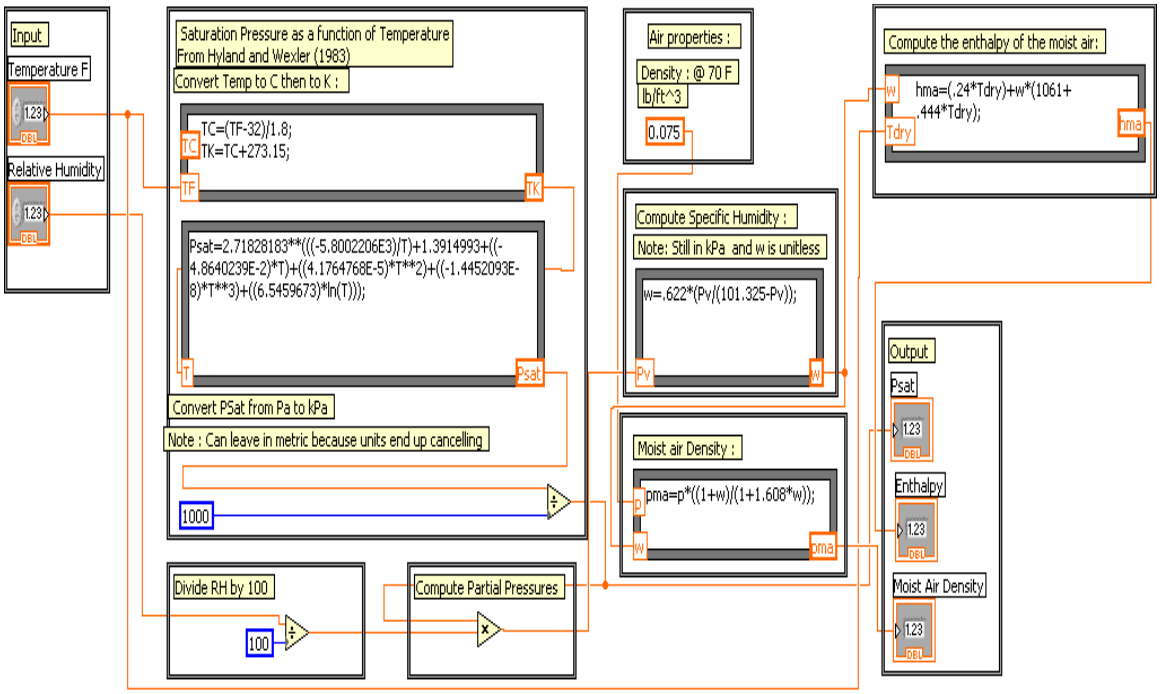

APPENDIX K

LABVIEW BALANCE CHECK SUBVI

.

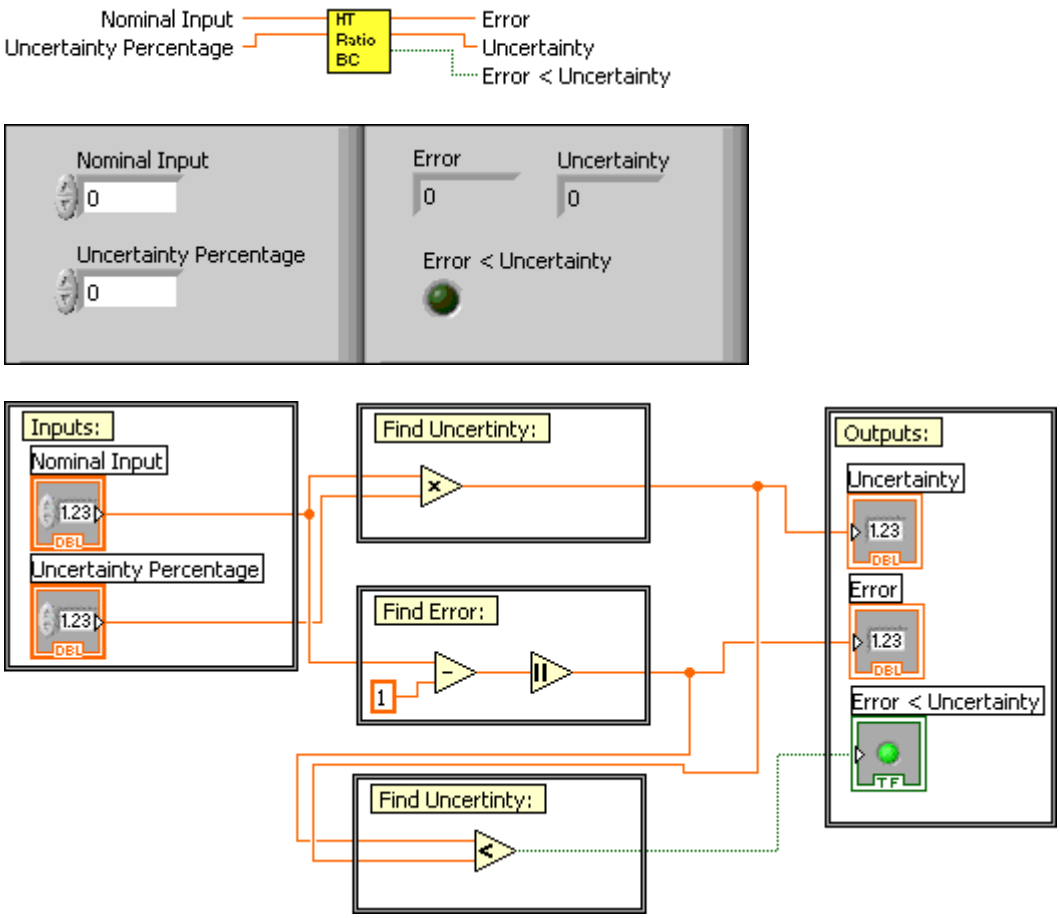

APPENDIX L

MATHCAD ENGINE AND HEAT EXCHANGER UNCERTAINTY ANALYSIS

Inputs (Data Collected 5/11/2009):

Heat Recovery Inlet Temperature Sensor 1:

$HR_{in\_T1} := 145.7721\Delta°F$

Heat Recovery Inlet Temperature Sensor 2:

$HR_{in\_T2} := 143.6228\Delta°F$

Heat Recovery Outlet Temperature Sensor 1:

$HR_{out\_T1} := 155.1624\Delta°F$

Heat Recovery Outlet Temperature Sensor 2:

$HR_{out\_T2} := 154.5353\Delta°F$

Exhaust Inlet Temperature:

$Ex_{in} := 1069.268\Delta°F$

Exhaust Outlet Temperature:

$Ex_{out} := 240.798\Delta°F$

Coolant Inlet Heat Exchanger 1 Temperature Sensor 1:

$Coolant_{inHX1\_T1} := 178.726\Delta°F$

Coolant Inlet Heat Exchanger 1 Temperature Sensor 2:

$Coolant_{inHX1\_T2} := 177.9237\Delta°F$

Coolant Outlet Heat Exchanger 1 / Inlet Heat Exchanger 2 Temperature Sensor 1:

$Coolant_{inHX2\_T1} := 185.2743\Delta°F$

Coolant Outlet Heat Exchanger 1 / Inlet Heat Exchanger 2 Temperature Sensor 2:

$Coolant_{inHX2\_T2} := 184.346\,\Delta°F$

Coolant Outlet Heat Exchanger 2 Temperature Sensor 1:

$Coolant_{outHX2\_T1} := 177.7529\,\Delta°F$

Coolant Outlet Heat Exchanger 2 Temperature Sensor 2:

$Coolant_{outHX2\_T2} := 178.3051\,\Delta°F$

Coolant Flowrate:

$Flow_{Coolant} := 10.1018\,gpm$

Heat Recovery Flowrate:

$Flow_{HR} := 5.7965\,gpm$

Engine Natural Gas Flowrate:

$Flow_{NG} := 2.4429\,\frac{ft^3}{min}$

Power Generated:

$Power_{gen} := 7288.48\,W$

Instrumentation Uncertainties:

Fluid Temperature Sensors:

$U_{Te} := 0.558\,\Delta°F$

Please note that this uncertainty analysis is for the new sensor and the procedure does not change for the old temperature sensor. The only difference is the value above is .9 Degrees F

Exhaust Temperature Sensors:

$U_{T\_Exhaust} := 1.89\,\Delta°F$

Turbine Flowmeter (Heat Recovery and Engine Coolant):

$U_{Flow\_Turbine} := .5\%$

Natural Gas Flowmeter:

$U_{Flow\_NG} := .088 \cdot \frac{ft^3}{min}$

Generator Power Uncertainty:

$U_{Power\_gen} := 75 \cdot W$

DAQ Uncertainties:

Analog Input DAQ Uncertainty:

$U_{DAQ\_AI} := .04 \cdot \%$

RTD Input DAQ Uncertainty:

$U_{DAQ\_RTD} := 0.45\,\Delta°F$

Properties:

HR water Flow:

Density Inlet Flow:

$\rho_{HR\_in} := 61.29 \frac{lbm}{ft^3}$

Specific Heat Inlet Flow:

$Cp_{HR\_in} := .99975 \frac{BTU}{lbm \cdot \Delta°F}$

Density Outlet Flow:

$$\rho_{HR\_out} := 61.0994 \frac{lbm}{ft^3}$$

Specific Heat Outlet Flow:

$$Cp_{HR\_out} := 1.00048 \frac{BTU}{lbm \cdot \Delta°F}$$

Uncertainty:

$$U_{\rho\_Water} := .002\%$$

$$U_{cp\_Water} := .025\%$$

Exhaust (Estimated at the mean temperature):

Density:

$$\rho_{EX\_avg} := .037 \cdot \frac{lbm}{ft^3}$$

Specific Heat:

$$Cp_{EX\_avg} := .295 \frac{BTU}{lbm \cdot \Delta°F}$$

Coolant Properties (Estimated at 180F):

Density:

$$\rho_{Coolant} := 64.8 \frac{lbm}{ft^3}$$

Specific Heat:

$$Cp_{Coolant} := .842 \cdot \frac{BTU}{lbm \cdot \Delta°F}$$

Component Uncertainties (Combined with the DAQ uncertainties):

$$U_T := \left[\left(U_{Te}\right)^2 + \left(U_{DAQ\_RTD}\right)^2 \right]^{\frac{1}{2}}$$

$$U_T = 0.717 \cdot \Delta°F$$

$$U_{T\_Exhaust} := \left[\left(U_{T\_Exhaust}\right)^2 + \left(U_{DAQ\_RTD}\right)^2 \right]^{\frac{1}{2}}$$

$$U_{T\_Exhaust} = 1.943 \cdot \Delta°F$$

$$U_{\rho\_Water\_HROUT} := \left[\left(U_{\rho\_Water} \cdot \rho_{HR\_out}\right)^2 + \left(U_{DAQ\_AI} \cdot \rho_{HR\_out}\right)^2 \right]^{\frac{1}{2}}$$

$$U_{\rho\_Water\_HROUT} = 0.024 \frac{lbm}{ft^3}$$

$$U_{\rho\_Water\_HRIN} := \left[\left(U_{\rho\_Water} \cdot \rho_{HR\_in}\right)^2 + \left(U_{DAQ\_AI} \cdot \rho_{HR\_in}\right)^2 \right]^{\frac{1}{2}}$$

$$U_{\rho\_Water\_HRIN} = 0.025 \frac{lbm}{ft^3}$$

$$U_{cp\_Water\_HROUT} := \left[\left(U_{cp\_Water} \cdot Cp_{HR\_out}\right)^2 + \left(U_{DAQ\_AI} \cdot Cp_{HR\_out}\right)^2 \right]^{\frac{1}{2}}$$

$$U_{cp\_Water\_HROUT} = 4.719 \times 10^{-4} \cdot \frac{BTU}{lbm \cdot \Delta°F}$$

$$U_{cp\_Water\_HRIN} := \left[\left(U_{cp\_Water} \cdot Cp_{HR\_in}\right)^2 + \left(U_{DAQ\_AI} \cdot Cp_{HR\_in}\right)^2 \right]^{\frac{1}{2}}$$

$$U_{cp\_Water\_HRIN} = 4.716 \times 10^{-4} \cdot \frac{BTU}{lbm \cdot \Delta °F}$$

$$U_{Flow\_Turbine\_Coolant} := \left[\left(U_{Flow\_Turbine} \cdot Flow_{Coolant} \right)^2 + \left(U_{DAQ\_AI} \cdot Flow_{Coolant} \right)^2 \right]^{\frac{1}{2}}$$

$$U_{Flow\_Turbine\_Coolant} = 0.051 \cdot gpm$$

$$U_{Flow\_Turbine\_HR} := \left[\left(U_{Flow\_Turbine} \cdot Flow_{HR} \right)^2 + \left(U_{DAQ\_AI} \cdot Flow_{HR} \right)^2 \right]^{\frac{1}{2}}$$

$$U_{Flow\_Turbine\_HR} = 0.029 \, gpm$$

$$U_{Flow\_NG} := \left[\left(U_{Flow\_NG} \right)^2 + \left(U_{DAQ\_AI} \cdot Flow_{NG} \right)^2 \right]^{\frac{1}{2}}$$

$$U_{Flow\_NG} = 0.088 \frac{ft^3}{min}$$

$$U_{Power\_gen} = 75 \, W$$

$$U_{Power\_gen} := \left[\left(U_{Power\_gen} \right)^2 + \left(U_{DAQ\_AI} \cdot Power_{gen} \right)^2 \right]^{\frac{1}{2}}$$

Combined Cycle Efficiency Uncertainty Calculation:

Primary Efficiency Equation:

$$\eta = \frac{Power_{gen} + Q_{HR}}{Energy_{NG}}$$

Where;

$$Q_{HR} = Flow_{HR} \cdot \left[\rho_{HR\_out} \cdot Cp_{HR\_out} \cdot \frac{HR_{out\_1} + HR_{out\_T2}}{2} \ldots \right.$$
$$\left. + \rho_{HR\_in} \cdot Cp_{HR\_in} \cdot \left(\frac{HR_{in\_1} + HR_{in\_T2}}{2} \right) \right]$$

$$Energy_{NG} = Flow_{NG} \cdot 930 \cdot \frac{BTU}{ft^3}$$

Resulting In:

$$\eta := \frac{Power_{gen} + Flow_{HR} \cdot \left[\rho_{HR\_out} \cdot Cp_{HR\_out} \cdot \frac{HR_{out\_T1} + HR_{out\_T2}}{2} \ldots \right.}{Flow_{NG} \cdot 930 \cdot \frac{BTU}{ft^3}}$$
$$\left. + -\rho_{HR\_in} \cdot Cp_{HR\_in} \cdot \left(\frac{HR_{in\_T1} + HR_{in\_T2}}{2} \right) \right]$$

$$\eta = 0.387$$

Compute Partial Derivatives for propagation analysis:

$$\theta HR_{in\_T1} := \frac{d}{dHR_{in\_T1}} \frac{Power_{gen} + Flow_{HR} \cdot \left[\rho_{HR\_out} \cdot Cp_{HR\_out} \cdot \left(\frac{HR_{out\_T1} + HR_{out\_T2}}{2} \right) \ldots \right.}{Flow_{NG} \cdot 930 \cdot \frac{BTU}{ft^3}}$$
$$\left. + -\rho_{HR\_in} \cdot Cp_{HR\_in} \cdot \frac{HR_{in\_T1} + HR_{in\_T2}}{2} \right]$$

$$\theta HR_{in\_T2} := \frac{d}{dHR_{in\_T2}} \frac{Power_{gen} + Flow_{HR} \cdot \left[\rho_{HR\_out} \cdot Cp_{HR\_out} \cdot \left(\frac{HR_{out\_T1} + HR_{out\_T2}}{2} \right) \ldots \right.}{Flow_{NG} \cdot 930 \cdot \frac{BTU}{ft^3}}$$
$$\left. + -\rho_{HR\_in} \cdot Cp_{HR\_in} \cdot \frac{HR_{in\_T1} + HR_{in\_T2}}{2} \right]$$

$$\theta HR_{out\_T1} := \frac{d}{dHR_{out\_T1}} \frac{Power_{gen} + Flow_{HR} \cdot \left[\rho_{HR\_out} \cdot Cp_{HR\_out} \cdot \left(\frac{HR_{out\_T1} + HR_{out\_T2}}{2} \right) \dots \right.}{\left. + -\rho_{HR\_in} \cdot Cp_{HR\_in} \cdot \left(\frac{HR_{in\_T1} + HR_{in\_T2}}{2} \right) \right]}{Flow_{NG} \cdot 930 \cdot \frac{BTU}{ft^3}}$$

$$\theta HR_{out\_T2} := \frac{d}{dHR_{out\_T2}} \frac{Power_{gen} + Flow_{HR} \cdot \left[\rho_{HR\_out} \cdot Cp_{HR\_out} \cdot \frac{HR_{out\_T1} + HR_{out\_T2}}{2} \dots \right.}{\left. + -\rho_{HR\_in} \cdot Cp_{HR\_in} \cdot \left(\frac{HR_{in\_T1} + HR_{in\_T2}}{2} \right) \right]}{Flow_{NG} \cdot 930 \cdot \frac{BTU}{ft^3}}$$

$$\theta Power_{gen} := \frac{d}{dPower_{gen}} \frac{Power_{gen} + Flow_{HR} \cdot \left[\rho_{HR\_out} \cdot Cp_{HR\_out} \cdot \frac{HR_{out\_T1} + HR_{out\_T2}}{2} \dots \right.}{\left. + -\rho_{HR\_in} \cdot Cp_{HR\_in} \cdot \left(\frac{HR_{in\_T1} + HR_{in\_T2}}{2} \right) \right]}{Flow_{NG} \cdot 930 \cdot \frac{BTU}{ft^3}}$$

$$\theta Flow_{HR} := \frac{d}{dFlow_{HR}} \frac{Power_{gen} + Flow_{HR} \cdot \left[\rho_{HR\_out} \cdot Cp_{HR\_out} \cdot \frac{HR_{out\_T1} + HR_{out\_T2}}{2} \dots \right.}{\left. + -\rho_{HR\_in} \cdot Cp_{HR\_in} \cdot \left(\frac{HR_{in\_T1} + HR_{in\_T2}}{2} \right) \right]}{Flow_{NG} \cdot 930 \cdot \frac{BTU}{ft^3}}$$

$$\theta Flow_{NG} := \frac{d}{dFlow_{NG}} \frac{Power_{gen} + Flow_{HR} \cdot \left[\rho_{HR\_out} \cdot Cp_{HR\_out} \cdot \frac{HR_{out\_T1} + HR_{out\_T2}}{2} \dots \right.}{\left. + -\rho_{HR\_in} \cdot Cp_{HR\_in} \cdot \left(\frac{HR_{in\_T1} + HR_{in\_T2}}{2} \right) \right]}{Flow_{NG} \cdot 930 \cdot \frac{BTU}{ft^3}}$$

$$\theta\rho_{HR\_out} := \frac{d}{d\rho_{HR\_out}} \frac{Power_{gen} + Flow_{HR}\cdot\left[\rho_{HR\_out}\cdot Cp_{HR\_out}\cdot\left(\frac{HR_{out\_T1} + HR_{out\_T2}}{2}\right)\ldots\right.}{\left.+-\rho_{HR\_in}\cdot Cp_{HR\_in}\cdot\left(\frac{HR_{in\_T1} + HR_{in\_T2}}{2}\right)\right]}$$
$$Flow_{NG}\cdot 930\cdot\frac{BTU}{ft^3}$$

$$\theta\rho_{HR\_in} := \frac{d}{d\rho_{HR\_in}} \frac{Power_{gen} + Flow_{HR}\cdot\left[\rho_{HR\_out}\cdot Cp_{HR\_out}\cdot\left(\frac{HR_{out\_T1} + HR_{out\_T2}}{2}\right)\ldots\right.}{\left.+-\rho_{HR\_in}\cdot Cp_{HR\_in}\cdot\left(\frac{HR_{in\_T1} + HR_{in\_T2}}{2}\right)\right]}$$
$$Flow_{NG}\cdot 930\cdot\frac{BTU}{ft^3}$$

$$\theta Cp_{HR\_out} := \frac{d}{dCp_{HR\_out}} \frac{Power_{gen} + Flow_{HR}\cdot\left[\rho_{HR\_out}\cdot Cp_{HR\_out}\cdot\frac{HR_{out\_T1} + HR_{out\_T2}}{2}\ldots\right.}{\left.+-\rho_{HR\_in}\cdot Cp_{HR\_in}\cdot\left(\frac{HR_{in\_T1} + HR_{in\_T2}}{2}\right)\right]}$$
$$Flow_{NG}\cdot 930\cdot\frac{BTU}{ft^3}$$

$$\theta Cp_{HR\_in} := \frac{d}{dCp_{HR\_in}} \frac{Power_{gen} + Flow_{HR}\cdot\left[\rho_{HR\_out}\cdot Cp_{HR\_out}\cdot\frac{HR_{out\_T1} + HR_{out\_T2}}{2}\ldots\right.}{\left.+-\rho_{HR\_in}\cdot Cp_{HR\_in}\cdot\left(\frac{HR_{in\_T1} + HR_{in\_T2}}{2}\right)\right]}$$
$$Flow_{NG}\cdot 930\cdot\frac{BTU}{ft^3}$$

Now to compute the uncertainty of the Combined Cycle Efficiency (note: the following is broken up to save space):

$$U\eta\_1 := \theta HR_{in\_T1}^{2}\cdot\left(U_T\right)^2 + \theta HR_{in\_T2}^{2}\cdot\left(U_T\right)^2 + \theta HR_{out\_T1}^{2}\cdot\left(U_T\right)^2$$

$$U\eta\_2 := \left[\theta Power_{gen}^{2}\cdot\left(U_{Power\_gen}\right)^2 + \theta Flow_{HR}^{2}\cdot\left(U_{Flow\_Turbine\_HR}\right)^2 + \theta Flow_{NG}^{2}\cdot\left(U_{Flow\_NG}\right)^2\right]$$

$$U\eta\_3 := \begin{bmatrix} \theta\rho_{HR\_out}{}^{2}\cdot\left(U_{\rho\_Water\_HROUT}\right)^{2} + \theta\rho_{HR\_in}{}^{2}\cdot\left(U_{\rho\_Water\_HRIN}\right)^{2} \cdots \\ + \theta Cp_{HR\_out}{}^{2}\cdot\left(U_{cp\_Water\_HROUT}\right)^{2} \end{bmatrix}$$

$$U\eta\_4 := \theta Cp_{HR\_in}{}^{2}\cdot\left(U_{cp\_Water\_HRIN}\right)^{2} + \theta HR_{out\_T2}{}^{2}\cdot\left(U_{T}\right)^{2}$$

$$U\eta := (U\eta\_1 + U\eta\_2 + U\eta\_3 + U\eta\_4)^{.5}$$

$$U\eta = 2.074\%$$

$$\eta = 38.689\%$$

Percentage Uncertainty in Combined Cycle Efficiency:

$$\frac{U\eta}{\eta} = 5.361\cdot\%$$

Uncertainty Percentage Contribution:

$$UPC_{T} := \frac{\theta HR_{in\_T1}{}^{2}\cdot\left(U_{T}\right)^{2} + \theta HR_{in\_T2}{}^{2}\cdot\left(U_{T}\right)^{2} + \theta HR_{out\_T1}{}^{2}\cdot\left(U_{T}\right)^{2} + \theta HR_{out\_T2}{}^{2}\cdot\left(U_{T}\right)^{2}}{U\eta^{2}}$$

$$UPC_{T} = 52.042\%$$

$$UPC_{Power} := \frac{\theta Power_{gen}{}^{2}\cdot U_{Power\_gen}{}^{2}}{U\eta^{2}}$$

$$UPC_{Power} = 0.82\cdot\%$$

$$UPC_{Flow\_HR} := \frac{\theta Flow_{HR}{}^{2}\cdot\left(U_{Flow\_Turbine\_HR}\right)^{2}}{U\eta^{2}}$$

$$UPC_{Flow\_HR} = 0.244\%$$

$$UPC_{Flow\_NG} := \frac{\theta Flow_{NG}{}^{2}\cdot\left(U_{Flow\_NG}\right)^{2}}{U\eta^{2}}$$

$$UPC_{Flow\_NG} = 45.151\cdot\%$$

$$UPC_{\rho\_Water\_HR} := \frac{\theta\rho_{HR\_out}{}^{2}\cdot\left(U_{\rho\_Water\_HROUT}\right)^{2} + \theta\rho_{HR\_in}{}^{2}\cdot\left(U_{\rho\_Water\_HRIN}\right)^{2}}{U\eta^{2}}$$

$$UPC_{\rho\_Water\_HR} = 0.73\cdot\%$$

$$UPC_{Cp\_HR} := \frac{\theta Cp_{HR\_out}{}^{2}\cdot\left(U_{cp\_Water\_HROUT}\right)^{2} + \theta Cp_{HR\_in}{}^{2}\cdot\left(U_{cp\_Water\_HRIN}\right)^{2}}{U\eta^{2}}$$

$$UPC_{Cp\_HR} = 1.012\cdot\%$$

UPC Check:

$$UPC_{tot} := UPC_{T} + UPC_{Power} + UPC_{Flow\_HR} + UPC_{Flow\_NG} + UPC_{\rho\_Water\_HR} + UPC_{Cp\_HR}$$

$$UPC_{tot} = 1$$

Engine Cost Uncertainty:

Set Dollars as a variable equal to 1:

$$Dollars := 1$$

Specify the natural gas cost as the national 2009 average for Residential and Commercial:

$$Cost_{NG} := 12.83\frac{Dollars}{1000ft^{3}}$$

Cost Equation:

$$Cost_{Engine} := Cost_{NG}\cdot Flow_{NC}$$

$$Cost_{Engine} = 1.881\cdot\frac{Dollars}{hr}$$

Partial Derivatives:

$$\theta Flow_{NG} := \frac{d}{dFlow_{NG}}\left(Cost_{NG} \cdot Flow_{NG}\right)$$

Uncertainty:

$$U_{Cost\_Engine\_95} := \left[\theta Flow_{NG}^{2} \cdot \left(U_{Flow\_NG}\right)^{2}\right]^{.5}$$

$$U_{Cost\_Engine\_95} = 0.068 \frac{Dollars}{hr}$$

Percentage Uncertainty in Engine Cost:

$$\frac{U_{Cost\_Engine\_95}}{Cost_{Engine}} = 3.602\%$$

Note: There is no UPC performed here because there is only one contributor to this uncertainty, the Natural Gas flowrate.

Heat Transfer Ratios and Effectiveness Uncertainty:

Heat Exchanger 1:

Exhaust Flowrate Calculation:

Stoichiometric Air to Fuel Ratio for Natural Gas:

$$A_{F\_ratio} := 17.2$$

Density of natural gas at standard temperature and pressure:

$$\rho_{natgas} := .044 \frac{lbm}{ft^3}$$

$$\rho_{EX\_avg} = 0.037 \frac{lbm}{ft^3}$$

Density of the Exhaust gas at the mean temperature:

Exhaust Flow Equation:

$$Flow_{Exhaust} := \frac{Flow_{NG} \cdot \rho_{natgas} \cdot A_{F\_ratio} + Flow_{NG} \cdot \rho_{natgas}}{\rho_{EX\_avg}}$$

$$Flow_{Exhaust} = 52.872 \frac{ft^3}{min}$$

Partial Derivatives:

$$\theta Flow_{NG} := \frac{d}{dFlow_{NG}} \left(\frac{Flow_{NG} \cdot \rho_{natgas} \cdot A_{F\_ratio} + Flow_{NG} \cdot \rho_{natgas}}{\rho_{EX\_avg}} \right)$$

Uncertainty in Exhaust Flow:

$$U_{Flow\_Exhaust} := \left[\theta Flow_{NG}^{2} \cdot \left(U_{Flow\_NG} \right)^2 \right]^{.5}$$

$$U_{Flow\_Exhaust} = 1.905 \frac{ft^3}{min}$$

Heat Transfer Ratio:

Primary Equation:

$$QHX1ratio = \frac{Q_{coolant}}{Q_{exhaust}}$$

Where;

$$Q_{coolant} := Cp_{Coolant} \cdot \left(Flow_{Coolant} \cdot \rho_{Coolant} \right) \cdot \left(\frac{Coolant_{inHX2\_T1} + Coolant_{inHX2\_T2}}{2} \ldots + - \frac{Coolant_{inHX1\_T1} + Coolant_{inHX1\_T2}}{2} \right)$$

$$Q_{exhaust} := Cp_{EX\_avg} \cdot \left(Flow_{Exhaust} \cdot \rho_{EX\_avg} \right) \cdot \left(Ex_{out} - Ex_{in} \right)$$

Thus:

$$HX1Qratio := \frac{Cp_{Coolant} \cdot Flow_{Coolant} \cdot \rho_{Coolant} \cdot \left(\frac{Coolant_{inHX2\_T1} + Coolant_{inHX2\_T2}}{2} \ldots \right.}{\left. + - \frac{Coolant_{inHX1\_T1} + Coolant_{inHX1\_T2}}{2} \right)}$$
$$-Cp_{EX\_avg} \cdot Flow_{Exhaust} \cdot \rho_{EX\_avg} \cdot \left(Ex_{out} - Ex_{in} \right)$$

$$HX1Qratio = 0.999$$

Compute Partial Derivatives (Computed in the same way as above but hidden to save space):

Uncertainty in Heat Exchanger 1 Heat Transfer Ratio:

$$U_{HX1Qratio\_1} := \theta Coolant_{inHX2\_T1}^{2} \cdot \left(U_T \right)^2 + \theta Coolant_{inHX2\_T2}^{2} \cdot \left(U_T \right)^2$$

$$U_{HX1Qratio\_2} := \theta Coolant_{inHX1\_T1}^{2} \cdot \left(U_T \right)^2 + \theta Coolant_{inHX1\_T2}^{2} \cdot \left(U_T \right)^2$$

$$U_{HX1Qratio\_3} := \theta Ex_{out}^{2} \cdot \left(U_{T\_Exhaust} \right)^2 + \theta Ex_{in}^{2} \cdot \left(U_{T\_Exhaust} \right)^2 + \theta Flow_{Exhaust}^{2} \cdot \left(U_{Flow\_Exhaust} \right)^2$$

$$U_{HX1Qratio\_4} := \theta Flow_{Coolant}^{2} \cdot \left(U_{Flow\_Turbine\_Coolant} \right)^2$$

$$U_{HX1Qratio} := \left(\left| U_{HX1Qratio\_1} + U_{HX1Qratio\_2} + U_{HX1Qratio\_3} + U_{HX1Qratio\_4} \right| \right)^{.5}$$

$$U_{HX1Qratio} = 0.116$$

$$HX1Qratio = 0.999$$

Percentage Uncertainty in HX1QRatio:

$$\frac{U_{HX1Qratio}}{HX1Qratio} = 11.641 \cdot \%$$

Uncertainty Percentage Contribution:

$$UPC_T := \frac{U_{HX1Qratio\_1} + U_{HX1Qratio\_2}}{U_{HX1Qratio}^2}$$

$$UPC_T = 90.156\%$$

$$UPC_{T\_Exhaust} := \frac{\left[\theta Ex_{out}^2 \cdot \left(U_{T\_Exhaust}\right)^2 + \theta Ex_{in}^2 \cdot \left(U_{T\_Exhaust}\right)^2\right]}{U_{HX1Qratio}^2}$$

$$UPC_{T\_Exhaust} = 0.081\%$$

$$UPC_{Flow\_Exhaust} := \frac{\theta Flow_{Exhaust}^2 \cdot \left(U_{Flow\_Exhaust}\right)^2}{U_{HX1Qratio}^2}$$

$$UPC_{Flow\_Exhaust} = 9.577\%$$

$$UPC_{Flow\_Coolant} := \frac{\left[\theta Flow_{Coolant}^2 \cdot \left(U_{Flow\_Turbine\_Coolant}\right)^2\right]}{U_{HX1Qratio}^2}$$

$$UPC_{Flow\_Coolant} = 0.186\%$$

UPC Check:

$$UPC_{tot} := UPC_T + UPC_{T\_Exhaust} + UPC_{Flow\_Exhaust} + UPC_{Flow\_Coolant}$$

$$UPC_{tot} = 1$$

Heat Exchanger 1 Effectiveness:

For this heat exchanger the hot side is the engine exhaust side and the cold side is the engine coolant, thus Cmin = Chot resulting in the following equation:

$$HX1EFF := \frac{Cp_{Coolant} \cdot Flow_{Coolant} \cdot \rho_{Coolant} \cdot \left(\frac{Coolant_{inHX2\_T1} + Coolant_{inHX2\_T2}}{2} \ldots \right.}{Cp_{EX\_avg} \cdot Flow_{Exhaust} \cdot \rho_{EX\_avg} \cdot \left(Ex_{in} - \frac{Coolant_{inHX1\_T1} + Coolant_{inHX1\_T2}}{2} \right)} \left. + - \frac{Coolant_{inHX1\_T1} + Coolant_{inHX1\_T2}}{2} \right)$$

$HX1EFF = 0.9294$

Compute Partial Derivatives (Again collapsed to save space):

Uncertainty:

$$U_{HX1EFF\_1} := \theta Coolant_{inHX2\_T1}^{2} \cdot (U_T)^2 + \theta Coolant_{inHX2\_T2}^{2} \cdot (U_T)^2$$

$$U_{HX1EFF\_2} := \theta Coolant_{inHX1\_T1}^{2} \cdot (U_T)^2 + \theta Coolant_{inHX1\_T2}^{2} \cdot (U_T)^2$$

$$U_{HX1EFF\_3} := \theta Ex_{in}^{2} \cdot (U_{T\_Exhaust})^2 + \theta Flow_{Exhaust}^{2} \cdot (U_{Flow\_Exhaust})^2 \ldots + \theta Flow_{Coolant}^{2} \cdot (U_{Flow\_Turbine\_Coolant})^2$$

$$U_{HX1EFF} := (U_{HX1EFF\_1} + U_{HX1EFF\_2} + U_{HX1EFF\_3})^{.5}$$

$U_{HX1EFF} = 0.10781$

$HX1EFF = 0.929$

Percentage Uncertainty in HX1EFF:

$$\frac{U_{HX1EFF}}{HX1EFF} = 11.6\%$$

Uncertainty Percentage Contribution:

$$UPC_T := \frac{U_{HX1EFF\_2} + U_{HX1EFF\_1}}{U_{HX1EFF}^{2}}$$

$UPC_T = 90.133\%$

$$UPC_{T\_Exhaust} := \frac{\theta Ex_{in}^{2} \cdot \left(U_{T\_Exhaust}\right)^{2}}{U_{HX1EFF}^{2}}$$

$$UPC_{T\_Exhaust} = 0.035\%$$

$$UPC_{Flow\_Exhaust} := \frac{\theta Flow_{Exhaust}^{2} \cdot \left(U_{Flow\_Exhaust}\right)^{2}}{U_{HX1EFF}^{2}}$$

$$UPC_{Flow\_Exhaust} = 9.644\%$$

$$UPC_{Flow\_Coolant} = 0.186\%$$

$$UPC_{Flow\_Coolant} := \frac{\left[\theta Flow_{Coolant}^{2} \cdot \left(U_{Flow\_Turbine\_Coolant}\right)^{2}\right]}{U_{HX1EFF}^{2}}$$

UPC Check:

$$UPC_{tot} := UPC_{T} + UPC_{T\_Exhaust} + UPC_{Flow\_Exhaust} + UPC_{Flow\_Coolant}$$

$$UPC_{tot} = 1$$

Heat Exchanger 2:

Heat Exchanger 2 Heat Transfer Ratio:

Primary Equation:

$$QHX2ratio = \frac{Q_{HR}}{Q_{coolant}}$$

Where;

$$Q_{HR} = Flow_{HR} \cdot \left[\begin{array}{l} \rho_{HR\_out} \cdot Cp_{HR\_out} \cdot \dfrac{HR_{out\_1} + HR_{out\_T2}}{2} \ldots \\ + -\rho_{HR\_in} \cdot Cp_{HR\_in} \cdot \left(\dfrac{HR_{in\_1} + HR_{in\_T2}}{2} \right) \end{array} \right]$$

$$Q_{coolant} = Cp_{Coolant} \cdot Flow_{Coolant} \cdot \rho_{Coolant} \cdot \left(\frac{Coolant_{inHX2\_T1} + Coolant_{inHX2\_T2}}{2} \ldots \right.$$
$$\left. + - \frac{Coolant_{inHX1\_T1} + Coolant_{inHX1\_T2}}{2} \right)$$

Thus:

$$HX2Qratio := \frac{Flow_{HR} \cdot \left[\rho_{HR\_out} \cdot Cp_{HR\_out} \cdot \left(\frac{HR_{out\_T1} + HR_{out\_T2}}{2} \right) \ldots \right.}{\left. + - \rho_{HR\_in} \cdot Cp_{HR\_in} \cdot \left(\frac{HR_{in\_T1} + HR_{in\_T2}}{2} \right) \right]}$$
$$Cp_{Coolant} \cdot Flow_{Coolant} \cdot \rho_{Coolant} \cdot \left(\frac{Coolant_{inHX2\_T1} + Coolant_{inHX2\_T2}}{2} \ldots \right.$$
$$\left. + - \frac{Coolant_{outHX2\_T1} + Coolant_{outHX2\_T2}}{2} \right)$$

$$HX2Qratio = 0.93$$

Compute Partial Derivatives (Again Collapsed):

Uncertainties:

$$U_{HX2Qratio\_1} := \theta Coolant_{inHX2\_T1}^{2} \cdot (U_T)^2 + \theta Coolant_{inHX2\_T2}^{2} \cdot (U_T)^2$$

$$U_{HX2Qratio\_2} := \theta Coolant_{outHX2\_T1}^{2} \cdot (U_T)^2 + \theta Coolant_{outHX2\_T2}^{2} \cdot (U_T)^2$$

$$U_{HX2Qratio\_3} := \theta HR_{in\_T1}^{2} \cdot (U_T)^2 + \theta HR_{in\_T2}^{2} \cdot (U_T)^2 + \theta HR_{out\_T1}^{2} \cdot (U_T)^2$$

$$U_{HX2Qratio\_4} := \theta Flow_{Coolant}^{2} \cdot \left(U_{Flow\_Turbine\_Coolant}\right)^2 + \theta Flow_{HR}^{2} \cdot \left(U_{Flow\_Turbine\_HR}\right)^2$$

$$U_{HX2Qratio\_5} := \theta\rho_{HR\_out}^{2} \cdot \left(U_{\rho\_Water\_HROUT}\right)^2 \cdots + \theta\rho_{HR\_in}^{2} \cdot \left(U_{\rho\_Water\_HRIN}\right)^2 + \theta Cp_{HR\_out}^{2} \cdot \left(U_{cp\_Water\_HROUT}\right)^2$$

$$U_{HX2Qratio\_6} := \theta Cp_{HR\_in}^{2} \cdot \left(U_{cp\_Water\_HRIN}\right)^2 + \theta HR_{out\_T2}^{2} \cdot \left(U_T\right)^2$$

$$U_{HX2Qratio} := \left(U_{HX2Qratio\_1} + U_{HX2Qratio\_2} + U_{HX2Qratio\_3} + U_{HX2Qratio\_4} \cdots + U_{HX2Qratio\_5} + U_{HX2Qratio\_6}\right)^{.5}$$

$$U_{HX2Qratio} = 0.12$$

$$HX2Qratio = 0.93$$

Percentage Uncertainty in HX2QRatio:

$$\frac{U_{HX2Qratio}}{HX2Qratio} = 12.947\%$$

Uncertainty Percentage Contribution:

$$UPC_T := \frac{U_{HX2Qratio\_1} + U_{HX2Qratio\_2} + U_{HX2Qratio\_3} + \theta HR_{out\_T2}^{2} \cdot \left(U_T\right)^2}{U_{HX2Qratio}^{2}}$$

$$UPC_T = 98.63\%$$

$$UPC_{Flow\_Turbine} := \frac{U_{HX2Qratio\_4}}{U_{HX2Qratio}^{2}}$$

$$UPC_{Flow\_Turbine} = 0.3\%$$

$$UPC_{\rho\_Water\_HR} := \frac{\theta\rho_{HR\_out}{}^{2}\cdot\left(U_{\rho\_Water\_HROUT}\right)^{2} + \theta\rho_{HR\_in}{}^{2}\cdot\left(U_{\rho\_Water\_HRIN}\right)^{2}}{U_{HX2Qratio}{}^{2}}$$

$$UPC_{\rho\_Water\_HR} = 0.448\,\%$$

$$UPC_{Cp\_HR} := \frac{\theta Cp_{HR\_out}{}^{2}\cdot\left(U_{cp\_Water\_HROUT}\right)^{2} + \theta Cp_{HR\_in}{}^{2}\cdot\left(U_{cp\_Water\_HRIN}\right)^{2}}{U_{HX2Qratio}{}^{2}}$$

$$UPC_{Cp\_HR} = 0.621\cdot\%$$

UPC Check:

$$UPC_{tot} := UPC_{T} + UPC_{Flow\_Turbine} + UPC_{\rho\_Water\_HR} + UPC_{Cp\_HR}$$

$$UPC_{tot} = 1$$

Heat Exchanger 2 Effectiveness:

For this heat exchanger the Hot Side is the engine coolant and the cold side the heat recovery side, thus the Cmin is Cc. Because of this now the equation is effectively just a temperature ratio.

Primary Equation:

$$HX2EFF = \frac{Tcout - Tcin}{(Thin - Tcin)}$$

$$UPC_{Cp\_HR} = 0.621\cdot\%$$

$$HX2EFF := \frac{\left(\frac{HR_{out\_T1} + HR_{out\_T2}}{2}\right) - \left(\frac{HR_{in\_T1} + HR_{in\_T2}}{2}\right)}{\frac{Coolant_{inHX2\_T1} + Coolant_{inHX2\_T2}}{2} - \left(\frac{HR_{in\_T1} + HR_{in\_T2}}{2}\right)}$$

$$HX2EFF = 0.253$$

Compute Partial Derivatives (Not collapsed, equations fit on page as is):

$$\theta HR_{out\_T1} := \frac{d}{dHR_{out\_T1}} \frac{\left(\frac{HR_{out\_T1} + HR_{out\_T2}}{2}\right) - \left(\frac{HR_{in\_T1} + HR_{in\_T2}}{2}\right)}{\frac{Coolant_{inHX2\_T1} + Coolant_{inHX2\_T2}}{2} - \left(\frac{HR_{in\_T1} + HR_{in\_T2}}{2}\right)}$$

$$\theta HR_{out\_T2} := \frac{d}{dHR_{out\_T2}} \frac{\left(\frac{HR_{out\_T1} + HR_{out\_T2}}{2}\right) - \left(\frac{HR_{in\_T1} + HR_{in\_T2}}{2}\right)}{\frac{Coolant_{inHX2\_T1} + Coolant_{inHX2\_T2}}{2} - \left(\frac{HR_{in\_T1} + HR_{in\_T2}}{2}\right)}$$

$$\theta HR_{in\_T1} := \frac{d}{dHR_{in\_T1}} \frac{\left(\frac{HR_{out\_T1} + HR_{out\_T2}}{2}\right) - \left(\frac{HR_{in\_T1} + HR_{in\_T2}}{2}\right)}{\frac{Coolant_{inHX2\_T1} + Coolant_{inHX2\_T2}}{2} - \left(\frac{HR_{in\_T1} + HR_{in\_T2}}{2}\right)}$$

$$\theta HR_{in\_T2} := \frac{d}{dHR_{in\_T2}} \frac{\left(\frac{HR_{out\_T1} + HR_{out\_T2}}{2}\right) - \left(\frac{HR_{in\_T1} + HR_{in\_T2}}{2}\right)}{\frac{Coolant_{inHX2\_T1} + Coolant_{inHX2\_T2}}{2} - \left(\frac{HR_{in\_T1} + HR_{in\_T2}}{2}\right)}$$

$$\theta Coolant_{inHX2\_T1} := \frac{d}{dHR_{in\_T2}} \frac{\left(\frac{HR_{out\_T1} + HR_{out\_T2}}{2}\right) - \left(\frac{HR_{in\_T1} + HR_{in\_T2}}{2}\right)}{\frac{Coolant_{inHX2\_T1} + Coolant_{inHX2\_T2}}{2} - \left(\frac{HR_{in\_T1} + HR_{in\_T2}}{2}\right)}$$

$$\theta Coolant_{inHX2\_T2} := \frac{d}{dHR_{in\_T2}} \frac{\left(\frac{HR_{out\_T1} + HR_{out\_T2}}{2}\right) - \left(\frac{HR_{in\_T1} + HR_{in\_T2}}{2}\right)}{\frac{Coolant_{inHX2\_T1} + Coolant_{inHX2\_T2}}{2} - \left(\frac{HR_{in\_T1} + HR_{in\_T2}}{2}\right)}$$

Compute the Uncertainties:

$$U_{HX2Qratio\_1} := \theta Coolant_{inHX2\_T1}^{2} \cdot (U_T)^2 + \theta Coolant_{inHX2\_T2}^{2} \cdot (U_T)^2$$

$$U_{HX2Qratio\_2} := \theta HR_{in\_T1}^{2} \cdot (U_T)^2 + \theta HR_{in\_T2}^{2} \cdot (U_T)^2 + \theta HR_{out\_T1}^{2} \cdot (U_T)^2$$

$$U_{HX2Qratio\_3} := \theta HR_{out\_T2}^{2} \cdot (U_T)^2$$

$$U_{HX2EFF} := (U_{HX2Qratio\_1} + U_{HX2Qratio\_2} + U_{HX2Qratio\_3})^{.5}$$

$$U_{HX2EFF} = 0.018$$

$$HX2EFF = 0.253$$

Percentage Uncertainty in HX2EFF:

$$\frac{U_{HX2EFF}}{HX2EFF} = 7.263\%$$

Uncertainty Percentage Contribution:

$$UPC_{T\_Coolant} := \frac{U_{HX2Qratio\_1}}{U_{HX2EFF}^{2}}$$

$$UPC_{T\_Coolant} = 26.368\%$$

$$UPC_{T\_HR} := \frac{U_{HX2Qratio\_2} + U_{HX2Qratio\_3}}{U_{HX2EFF}^{2}}$$

$$UPC_{T\_HR} = 73.632\%$$

UPC Check:

$$UPC_{tot} := UPC_{T\_Coolant} + UPC_{T\_HR} \qquad UPC_{tot} = 1$$

APPENDIX M

MATHCAD BOILER UNCERTAINTY ANALYSIS

Inputs (Data collected 7/11/2009):

Boiler Input Water Temperature Sensor 1:

$Water_{in\_T1} := 164.5 \cdot \Delta°F$

Boiler Input Water Temperature Sensor 2:

$Water_{in\_T2} := 165 \cdot \Delta°F$

Boiler Output Water Temperature Sensor 1:

$Water_{out\_T1} := 172.2 \cdot \Delta°F$

Boiler Output Water Temperature Sensor 2:

$Water_{out\_T2} := 167.6 \cdot \Delta°F$

Boiler Water Flowrate:

$Flow_{Water} := 19.39 gpm$

Boiler Natural Gas Flowrate:

$Flow_{NG} := 2.31 \frac{ft^3}{min}$

Uncertainties:

Fluid Temperature Sensor Uncertainty:

$U_{Te} := .9 \, \Delta°F$

Boiler Water Flowrate Uncertainty:

$U_{Flow\_Turbine} := .5\%$

Boiler Natural Gas Flowmeter Uncertainty:

$$U_{Flow\_NG} := .088 \cdot \frac{ft^3}{min}$$

DAQ Uncertainties:

DAQ Analog Input Uncertainty:

$$U_{DAQ\_AI} := .04 \cdot \%$$

DAQ RTD Input Uncertainty:

$$U_{DAQ\_RTD} := 0.45\,\Delta°F$$

Properties:

Boiler Water Flow:

Density Inlet Flow:

$$\rho_{in} := 61.29 \frac{lbm}{ft^3}$$

Specific Heat Inlet Flow:

$$Cp_{in} := .99975 \frac{BTU}{lbm \cdot \Delta°F}$$

Density Outlet Flow:

$$\rho_{out} := 61.0994 \frac{lbm}{ft^3}$$

Specific Heat Outlet Flow:

$$Cp_{out} := 1.00048 \frac{BTU}{lbm \cdot \Delta°F}$$

Uncertainty:

$$U_{\rho\_Water} := .002\%$$

$$U_{cp\_Water} := .025\%$$

Component Uncertainties:

$$U_T := \left[\left(U_{Te}\right)^2 + \left(U_{DAQ\_RTD}\right)^2 \right]^{\frac{1}{2}}$$

$$U_T = 1.006 \Delta°F$$

$$U_{\rho\_Water\_OUT} := \left[\left(U_{\rho\_Water} \cdot \rho_{out}\right)^2 + \left(U_{DAQ\_AI} \cdot \rho_{out}\right)^2 \right]^{\frac{1}{2}}$$

$$U_{\rho\_Water\_OUT} = 0.024 \frac{lbm}{ft^3}$$

$$U_{\rho\_Water\_IN} := \left[\left(U_{\rho\_Water} \cdot \rho_{in}\right)^2 + \left(U_{DAQ\_AI} \cdot \rho_{in}\right)^2 \right]^{\frac{1}{2}}$$

$$U_{\rho\_Water\_IN} = 0.025 \frac{lbm}{ft^3}$$

$$U_{cp\_Water\_OUT} := \left[\left(U_{cp\_Water} \cdot Cp_{out}\right)^2 + \left(U_{DAQ\_AI} \cdot Cp_{out}\right)^2 \right]^{\frac{1}{2}}$$

$$U_{cp\_Water\_OUT} = 4.719 \times 10^{-4} \cdot \frac{BTU}{lbm \cdot \Delta°F}$$

$$U_{cp\_Water\_IN} := \left[\left(U_{cp\_Water} \cdot Cp_{in}\right)^2 + \left(U_{DAQ\_AI} \cdot Cp_{in}\right)^2 \right]^{\frac{1}{2}}$$

$$U_{cp\_Water\_IN} = 4.716 \times 10^{-4} \cdot \frac{BTU}{lbm \cdot \Delta°F}$$

$$U_{Flow\_Turbine\_Water} := \left[\left(U_{Flow\_Turbine} \cdot Flow_{Water} \right)^2 + \left(U_{DAQ\_AI} \cdot Flow_{Water} \right)^2 \right]^{\frac{1}{2}}$$

$$U_{Flow\_Turbine\_Water} = 0.097 \cdot gpm$$

$$U_{Flow\_NG} := \left[\left(U_{Flow\_NG} \right)^2 + \left(U_{DAQ\_AI} \cdot Flow_{NG} \right)^2 \right]^{\frac{1}{2}}$$

$$U_{Flow\_NG} = 0.088 \cdot \frac{ft^3}{min}$$

Primary Efficiency Equation:

$$\eta := \frac{Flow_{Water} \cdot \left[\rho_{out} \cdot Cp_{out} \cdot \frac{Water_{out\_T1} + Water_{out\_T2}}{2} \ldots \right.}{Flow_{NG} \cdot 930 \cdot \frac{BTU}{ft^3}} \left. \begin{array}{l} \\ + -\rho_{in} \cdot Cp_{in} \cdot \left(\frac{Water_{in\_T1} + Water_{in\_T2}}{2} \right) \end{array} \right]$$

$$\eta = 0.351$$

Compute Partial Derivatives (Computed as in Engine and Heat Exchanger Analysis):

Uncertainties:

$$U\eta\_1 := \theta Water_{in\_T1}^{\ 2} \cdot \left(U_T \right)^2 + \theta Water_{in\_T2}^{\ 2} \cdot \left(U_T \right)^2 + \theta Water_{out\_T1}^{\ 2} \cdot \left(U_T \right)^2$$

$$U\eta\_2 := \left[\theta Flow_{Water}^{\ 2} \cdot \left(U_{Flow\_Turbine\_Water} \right)^2 + \theta Flow_{NG}^{\ 2} \cdot \left(U_{Flow\_NG} \right)^2 \right]$$

$$U\eta\_3 := \left[\theta \rho_{out}^{\ 2} \cdot \left(U_{\rho\_Water\_OUT} \right)^2 + \theta \rho_{in}^{\ 2} \cdot \left(U_{\rho\_Water\_IN} \right)^2 + \theta Cp_{out}^{\ 2} \cdot \left(U_{cp\_Water\_OUT} \right)^2 \right]$$

$$U\eta\_4 := \theta Cp_{in}^{\ 2} \cdot \left(U_{cp\_Water\_IN} \right)^2 + \theta Water_{out\_T2}^{\ 2} \cdot \left(U_T \right)^2$$

$$U\eta := (U\eta\_1 + U\eta\_2 + U\eta\_3 + U\eta\_4)^{.5}$$

$$U\eta = 7.629\%$$

$$\eta = 35.083\%$$

Percentage Uncertainty in Boiler Efficiency:

$$\frac{U\eta}{\eta} = 21.745\%$$

Uncertainty Percentage Contribution:

$$UPC_T := \frac{\theta Water_{in\_T1}{}^2 \cdot (U_T)^2 + \theta Water_{in\_T2}{}^2 \cdot (U_T)^2 \ldots + \left[\theta Water_{out\_T1}{}^2 \cdot (U_T)^2 + \theta Water_{out\_T2}{}^2 \cdot (U_T)^2\right]}{U\eta^2}$$

$$UPC_T = 94.868\%$$

$$UPC_{Flow\_Water} := \frac{\theta Flow_{Water}{}^2 \cdot (U_{Flow\_Turbine\_Water})^2}{U\eta^2}$$

$$UPC_{Flow\_Water} = 0.053\%$$

$$UPC_{Flow\_NG} := \frac{\theta Flow_{NG}{}^2 \cdot (U_{Flow\_NG})^2}{U\eta^2}$$

$$UPC_{Flow\_NG} = 3.07\%$$

$$UPC_{\rho\_Water} := \frac{\theta\rho_{out}{}^2 \cdot (U_{\rho\_Water\_OUT})^2 + \theta\rho_{in}{}^2 \cdot (U_{\rho\_Water\_IN})^2}{U\eta^2}$$

$$UPC_{\rho\_Water} = 0.842\%$$

$$UPC_{Cp} := \frac{\theta Cp_{out}^{2} \cdot \left(U_{cp\_Water\_OUT}\right)^{2} + \theta Cp_{in}^{2} \cdot \left(U_{cp\_Water\_IN}\right)^{2}}{U\eta^{2}}$$

$$UPC_{Cp} = 1.168\%$$

UPC Check:

$$UPC_{tot} := UPC_{T} + UPC_{Flow\_NG} + UPC_{Flow\_Water} + UPC_{\rho\_Water} + UPC_{Cp}$$

$$UPC_{tot} = 1$$

Boiler Cost Uncertainty:

Create variable for Dollars and set equal to 1:

$$Dollars := 1$$

$$Cost_{NG} := 12.83 \frac{Dollars}{1000 ft^{3}}$$

Designate Natural Gas Cost:

Boiler Cost Equation:

$$Cost_{Boiler} := Cost_{NG} \cdot Flow_{NG}$$

$$Cost_{Boiler} = 1.778 \frac{Dollars}{hr}$$

Partial Derivatives:

$$\theta Flow_{NG} := \frac{d}{dFlow_{NG}} \left(Cost_{NG} \cdot Flow_{NG}\right)$$

Boiler Cost Uncertainty:

$$U_{Cost\_Boiler} := \left[\theta Flow_{NG}^{2} \cdot \left(U_{Flow\_NG}\right)^{2}\right]^{.5}$$

$$U_{Cost\_Boiler} = 0.068 \frac{Dollars}{hr}$$

Percentage Uncertainty in Boiler Cost:

$$\frac{U_{Cost\_Boiler}}{Cost_{Boiler}} = 3.81 \cdot \%$$

APPENDIX N

MATHCAD ABSORPTION CHILLER UNCERTAINTY ANALYSIS

Inputs (Data Collected 7/11/09):

Cold Water Inlet Temperature Sensor 1:

$CW_{in\_T1} := 58.7 \cdot \Delta°F$

Cold Water Inlet Temperature Sensor 2:

$CW_{in\_T2} := 58.7 \cdot \Delta°F$

Cold Water Outlet Temperature Sensor 1:

$CW_{out\_T1} := 55.6 \cdot \Delta°F$

Cold Water Outlet Temperature Sensor 2:

$CW_{out\_T2} := 55.6 \cdot \Delta°F$

Hot Water Inlet Temperature Sensor 1:

$HW_{in\_T1} := 174 \cdot \Delta°F$

Hot Water Inlet Temperature Sensor 2:

$HW_{in\_T2} := 173.9 \cdot \Delta°F$

Hot Water Outlet Temperature Sensor 1:

$HW_{out\_T1} := 168.2 \cdot \Delta°F$

Hot Water Outlet Temperature Sensor 2:

$HW_{out\_T2} := 167.1 \cdot \Delta°F$

Cold Water Flowrate:

$Flow_{CW} := 28gpm$

Hot Water Flowrate:

$Flow_{HW} := 37.7 gpm$

Uncertainties:

Hot Water Temperature Sensor Uncertainty:

$U_{Tcw} := .317 \Delta°F$

Cold Water Temperature Sensor Uncertainty:

$U_{Thw} := .558 \cdot \Delta°F$

Flowrate Uncertainty:

$U_{Flow\_Turbine} := .5\%$

DAQ Uncertainties:

DAQ Analog Input Uncertainty:

$U_{DAQ\_AI} := .04 \cdot \%$

DAQ RTD Input Uncertainty:

$U_{DAQ\_RTD} := 0.45 \Delta°F$

Properties:

Hot Water Flow:

Density Inlet Flow:

$\rho_{HWin} := 61.29 \cdot \frac{lbm}{ft^3}$

Specific Heat Inlet Flow:

$Cp_{HWin} := .99975 \frac{BTU}{lbm \cdot \Delta°F}$

Density Outlet Flow:

$$\rho_{HWout} := 61.0994 \frac{lbm}{ft^3}$$

Specific Heat Outlet Flow:

$$Cp_{HWout} := 1.00048 \frac{BTU}{lbm \cdot \Delta°F}$$

Cold Water Flow:

Density Inlet Flow:

$$\rho_{CWin} := 61.29 \frac{lbm}{ft^3}$$

Specific Heat Inlet Flow:

$$Cp_{CWin} := .99975 \frac{BTU}{lbm \cdot \Delta°F}$$

Density Outlet Flow:

$$\rho_{CWout} := 61.0994 \frac{lbm}{ft^3}$$

Specific Heat Outlet Flow:

$$Cp_{CWout} := 1.00048 \frac{BTU}{lbm \cdot \Delta°F}$$

Uncertainty:

$U_{\rho\_Water} := .002\%$

$U_{cp\_Water} := .025\%$

Component Uncertainties:

$$U_{T\_CW} := \left[\left(U_{Tcw}\right)^2 + \left(U_{DAQ\_RTD}\right)^2 \right]^{\frac{1}{2}}$$

$U_{T\_CW} = 0.55 \cdot \Delta°F$

$$U_{T\_HW} := \left[\left(U_{Thw}\right)^2 + \left(U_{DAQ\_RTD}\right)^2 \right]^{\frac{1}{2}}$$

$U_{T\_HW} = 0.717 \cdot \Delta°F$

$$U_{\rho\_Water\_HWOUT} := \left[\left(U_{\rho\_Water} \cdot \rho_{HWout}\right)^2 + \left(U_{DAQ\_AI} \cdot \rho_{HWout}\right)^2 \right]^{\frac{1}{2}}$$

$$U_{\rho\_Water\_HWOUT} = 0.024 \frac{lbm}{ft^3}$$

$$U_{\rho\_Water\_HWIN} := \left[\left(U_{\rho\_Water} \cdot \rho_{HWin}\right)^2 + \left(U_{DAQ\_AI} \cdot \rho_{HWin}\right)^2 \right]^{\frac{1}{2}}$$

$$U_{\rho\_Water\_HWIN} = 0.025 \cdot \frac{lbm}{ft^3}$$

$$U_{\rho\_Water\_CWOUT} := \left[\left(U_{\rho\_Water} \cdot \rho_{CWout}\right)^2 + \left(U_{DAQ\_AI} \cdot \rho_{CWout}\right)^2 \right]^{\frac{1}{2}}$$

$$U_{\rho\_Water\_CWOUT} = 0.024 \frac{lbm}{ft^3}$$

$$U_{\rho\_Water\_CWIN} := \left[\left(U_{\rho\_Water} \cdot \rho_{CWin} \right)^2 + \left(U_{DAQ\_AI} \cdot \rho_{CWin} \right)^2 \right]^{\frac{1}{2}}$$

$$U_{\rho\_Water\_CWIN} = 0.025 \cdot \frac{lbm}{ft^3}$$

$$U_{cp\_Water\_HWOUT} := \left[\left(U_{cp\_Water} \cdot Cp_{HWout} \right)^2 + \left(U_{DAQ\_AI} \cdot Cp_{HWout} \right)^2 \right]^{\frac{1}{2}}$$

$$U_{cp\_Water\_HWOUT} = 4.719 \times 10^{-4} \cdot \frac{BTU}{lbm \cdot \Delta°F}$$

$$U_{cp\_Water\_HWIN} := \left[\left(U_{cp\_Water} \cdot Cp_{HWin} \right)^2 + \left(U_{DAQ\_AI} \cdot Cp_{HWin} \right)^2 \right]^{\frac{1}{2}}$$

$$U_{cp\_Water\_HWIN} = 4.716 \times 10^{-4} \cdot \frac{BTU}{lbm \cdot \Delta°F}$$

$$U_{cp\_Water\_CWIN} := \left[\left(U_{cp\_Water} \cdot Cp_{CWin} \right)^2 + \left(U_{DAQ\_AI} \cdot Cp_{CWin} \right)^2 \right]^{\frac{1}{2}}$$

$$U_{cp\_Water\_CWIN} = 4.716 \times 10^{-4} \cdot \frac{BTU}{lbm \cdot \Delta°F}$$

$$U_{cp\_Water\_CWOUT} := \left[\left(U_{cp\_Water} \cdot Cp_{CWout} \right)^2 + \left(U_{DAQ\_AI} \cdot Cp_{CWout} \right)^2 \right]^{\frac{1}{2}}$$

$$U_{cp\_Water\_CWOUT} = 4.719 \times 10^{-4} \cdot \frac{BTU}{lbm \cdot \Delta°F}$$

$$U_{Flow\_Turbine\_HW} := \left[\left(U_{Flow\_Turbine} \cdot Flow_{HW} \right)^2 + \left(U_{DAQ\_AI} \cdot Flow_{HW} \right)^2 \right]^{\frac{1}{2}}$$

$$U_{Flow\_Turbine\_HW} = 0.189 \cdot gpm$$

$$U_{Flow\_Turbine\_CW} := \left[\left(U_{Flow\_Turbine} \cdot Flow_{CW} \right)^2 + \left(U_{DAQ\_AI} \cdot Flow_{CW} \right)^2 \right]^{\frac{1}{2}}$$

$$U_{Flow\_Turbine\_CW} = 0.14 \cdot gpm$$

Primary COP Equation:

$$COP := \frac{Flow_{CW} \cdot \left[\rho_{CWout} \cdot Cp_{CWout} \cdot \left(\frac{CW_{out\_T1} + CW_{out\_T2}}{2} \right) \ldots \right.}{\left. + -\rho_{CWin} \cdot Cp_{CWin} \cdot \left(\frac{CW_{in\_T1} + CW_{in\_T2}}{2} \right) \right]}$$
$$Flow_{HW} \cdot \left[\rho_{HWout} \cdot Cp_{HWout} \cdot \left(\frac{HW_{out\_T1} + HW_{out\_T2}}{2} \right) \ldots \right.$$
$$\left. + -\rho_{HWin} \cdot Cp_{HWin} \cdot \left(HW_{in\_T1} \right) \right]$$

$$COP = 0.356$$

Compute Partial Derivatives (Again Hidden):

Uncertainties:

$$UCOP\_1 := \theta HW_{in\_T1}^{\ 2} \cdot \left(U_{T\_HW} \right)^2 + \theta HW_{out\_T2}^{\ 2} \cdot \left(U_{T\_HW} \right)^2 + \theta HW_{out\_T1}^{\ 2} \cdot \left(U_{T\_HW} \right)^2$$

$$UCOP\_2 := \theta Flow_{CW}^{\ 2} \cdot \left(U_{Flow\_Turbine\_CW} \right)^2 + \theta Flow_{HW}^{\ 2} \cdot \left(U_{Flow\_Turbine\_HW} \right)^2$$

$$UCOP\_3 := \theta \rho_{CWout}^{\ 2} \cdot \left(U_{\rho\_Water\_CWOUT} \right)^2 + \theta \rho_{CWin}^{\ 2} \cdot \left(U_{\rho\_Water\_CWIN} \right)^2 \ldots + \theta \rho_{HWout}^{\ 2} \cdot \left(U_{\rho\_Water\_HWOUT} \right)^2$$

$$UCOP\_4 := \theta Cp_{CWin}^{\ 2} \cdot \left(U_{cp\_Water\_CWIN} \right)^2 + \theta Cp_{CWout}^{\ 2} \cdot \left(U_{cp\_Water\_CWOUT} \right)^2 \ldots + \theta \rho_{HWin}^{\ 2} \cdot \left(U_{\rho\_Water\_HWIN} \right)^2$$

$$UCOP\_5 := \theta CW_{in\_T1}^{\ 2} \cdot \left(U_{T\_CW} \right)^2 + \theta CW_{out\_T2}^{\ 2} \cdot \left(U_{T\_CW} \right)^2$$

$$UCOP\_6 := \theta Cp_{HWin}^{\ 2} \cdot \left(U_{cp\_Water\_HWIN} \right)^2 + \theta Cp_{HWout}^{\ 2} \cdot \left(U_{cp\_Water\_HWOUT} \right)^2$$

$$UCOP := (UCOP\_1 + UCOP\_2 + UCOP\_3 + UCOP\_4 + UCOP\_5 + UCOP\_6)^{.5}$$

$$UCOP = 0.064$$

$$COP = 0.356$$

$$\frac{UCOP}{COP} = 17.927\%$$

Percentage Uncertainty in Chiller COP:

Uncertainty Percentage Contribution:

$$UPC_T := \frac{UCOP\_1 + UCOP\_5}{UCOP^2}$$

$$UPC_T = 97.576\%$$

$$UPC_{Flow} := \frac{UCOP\_2}{UCOP^2}$$

$$UPC_{Flow} = 0.157\%$$

$$UPC_\rho := \frac{\begin{array}{l}\theta\rho_{CWout}{}^2 \cdot \left(U_{\rho\_Water\_CWOUT}\right)^2 + \theta\rho_{CWin}{}^2 \cdot \left(U_{\rho\_Water\_CWIN}\right)^2 \cdots \\ + \theta\rho_{HWout}{}^2 \cdot \left(U_{\rho\_Water\_HWOUT}\right)^2 + \theta\rho_{HWin}{}^2 \cdot \left(U_{\rho\_Water\_HWIN}\right)^2\end{array}}{UCOP^2}$$

$$UPC_\rho = 0.95\%$$

$$UPC_{Cp} := \frac{\begin{array}{l}\theta Cp_{CWin}{}^2 \cdot \left(U_{cp\_Water\_CWIN}\right)^2 + \theta Cp_{CWout}{}^2 \cdot \left(U_{cp\_Water\_CWOUT}\right)^2 \cdots \\ + \theta Cp_{HWin}{}^2 \cdot \left(U_{cp\_Water\_HWIN}\right)^2 + \theta Cp_{HWout}{}^2 \cdot \left(U_{cp\_Water\_HWOUT}\right)^2\end{array}}{UCOP^2}$$

$$UPC_{Cp} = 1.317\%$$

UPC Check:

$$UPC_{tot} := UPC_T + UPC_{Flow} + UPC_\rho + UPC_{Cp}$$

$$UPC_{tot} = 1$$

APPENDIX O

MATHCAD CHP SYSTEM HVAC UNCERTAINTY ANALYSIS

Inputs (Data Collected 7/11/09 Cooling and 12/22/2008 Heating):

Water Inlet Temperature Sensor 1:

$CW_{in\_T1} := 57.1 \cdot \Delta°F$

Water Inlet Temperature Sensor 2:

$CW_{in\_T2} := 57.1 \cdot \Delta°F$

Water Outlet Temperature Sensor 1:

$CW_{out\_T1} := 64.5 \cdot \Delta°F$

Water Outlet Temperature Sensor 2:

$CW_{out\_T2} := 62.7 \cdot \Delta°F$

Water Flowrate:

$Flow_{CW} := 3.57gpm$

Air Conditioning Inlet Relative Humidity:

$RH_{in} := .76$

Air Conditioning Outlet Relative Humidity:

$RH_{out} := 1$

Air Conditioning Inlet Temperature:

$AC_{in} := 71.8 \cdot \Delta°F$

Air Conditioning Outlet Temperature:

$AC_{out} := 63.4 \cdot \Delta°F$

Air Flowrate:

$$Flow_{AIR} := 1145.6 \frac{ft^3}{min}$$

Generator Natural Gas Flowrate:

$$GNGFR := 2.63 \cdot \frac{ft^3}{min}$$

Boiler Natural Gas Flowrate:

$$BNGFR := 2.31 \cdot \frac{ft^3}{min}$$

Generator Power Produced:

$$GTP := 7132 \cdot W$$

Uncertainties:

Fluid Temperature Uncertainty:

$$U_{Te} := .317 \cdot \Delta°F$$

Fluid Flowmeter Uncertainty:

$$U_{Flow\_Turbine} := .5\%$$

Relative Humidity Uncertainty:

$$U_{RH} := 2 \cdot \%$$

Air Flowrate Sensor Uncertainty:

$$U_{Flow\_AIR\_Sensors} := 2 \cdot \%$$

Air Differential Pressure:

$$U_{Flow\_DP} := .25 \cdot \%$$

Air Temperature Sensor:

Air sensor full scale:

$ACFS := 225\,\Delta°F$

$U_{TAC1} := .06\%$

$U_{TAC2} := .1\% \cdot ACFS$

$U_{TAC2} = 0.225 \cdot \Delta°F$

Natural Gas Flowmeter:

$U_{Flow\_NG} := .088 \cdot \frac{ft^3}{min}$

Generator Power Uncertainty:

$U_{Power\_gen} := 75 \cdot W$

DAQ Uncertainties:

DAQ Analog Input Uncertainty:

$U_{DAQ\_AI} := .04 \cdot \%$

DAQ RTD Input Uncertainty:

$U_{DAQ\_RTD} := 0.45\,\Delta°F$

Properties:

Water Flow:

Inlet Density:

$\rho_{CWin} := 61.29 \cdot \frac{lbm}{ft^3}$

Inlet Specific Heat:

$$Cp_{CWin} := .99975 \frac{BTU}{lbm \cdot \Delta°F}$$

Outlet Density:

$$\rho_{CWout} := 61.0994 \frac{lbm}{ft^3}$$

Outlet Specific Heat:

$$Cp_{CWout} := 1.00048 \frac{BTU}{lbm \cdot \Delta°F}$$

Density Uncertainty:

$$U_{\rho\_Water} := .002\%$$

Specific Heat Uncertainty:

$$U_{cp\_Water} := .025\%$$

Component Uncertainties:

$$U_T := \left[\left(U_{Te}\right)^2 + \left(U_{DAQ\_RTD}\right)^2 \right]^{\frac{1}{2}}$$

$$U_T = 0.55 \cdot \Delta°F$$

$$U_{\rho\_Water\_CWOUT} := \left[\left(U_{\rho\_Water} \cdot \rho_{CWout}\right)^2 + \left(U_{DAQ\_AI} \cdot \rho_{CWout}\right)^2 \right]^{\frac{1}{2}}$$

$$U_{\rho\_Water\_CWOUT} = 0.024 \frac{lbm}{ft^3}$$

$$U_{\rho\_Water\_CWIN} := \left[\left(U_{\rho\_Water} \cdot \rho_{CWin}\right)^2 + \left(U_{DAQ\_AI} \cdot \rho_{CWin}\right)^2 \right]^{\frac{1}{2}}$$

$$U_{\rho\_Water\_CWIN} = 0.025 \cdot \frac{lbm}{ft^3}$$

$$U_{cp\_Water\_CWIN} := \left[\left(U_{cp\_Water} \cdot Cp_{CWin} \right)^2 + \left(U_{DAQ\_AI} \cdot Cp_{CWin} \right)^2 \right]^{\frac{1}{2}}$$

$$U_{cp\_Water\_CWIN} = 4.716 \times 10^{-4} \cdot \frac{BTU}{lbm \cdot \Delta°F}$$

$$U_{cp\_Water\_CWOUT} := \left[\left(U_{cp\_Water} \cdot Cp_{CWout} \right)^2 + \left(U_{DAQ\_AI} \cdot Cp_{CWout} \right)^2 \right]^{\frac{1}{2}}$$

$$U_{cp\_Water\_CWOUT} = 4.719 \times 10^{-4} \cdot \frac{BTU}{lbm \cdot \Delta°F}$$

$$U_{Flow\_Turbine\_CW} := \left[\left(U_{Flow\_Turbine} \cdot Flow_{CW} \right)^2 + \left(U_{DAQ\_AI} \cdot Flow_{CW} \right)^2 \right]^{\frac{1}{2}}$$

$$U_{Flow\_Turbine\_CW} = 0.018 \cdot gpm$$

$$U_{Flow\_AIR} := \left[\begin{array}{l} \left(U_{Flow\_DP} \cdot Flow_{AIR} \right)^2 + \left(U_{Flow\_AIR\_Sensors} \cdot Flow_{AIR} \right)^2 \ldots \\ + \left(U_{DAQ\_AI} \cdot Flow_{AIR} \right)^2 \end{array} \right]^{\frac{1}{2}}$$

$$U_{Flow\_AIR} = 23.095 \frac{ft^3}{min}$$

$$U_{RH\_IN} := \left[\left(U_{RH} \cdot RH_{in} \right)^2 + \left(U_{DAQ\_AI} \cdot RH_{in} \right)^2 \right]^{\frac{1}{2}}$$

$$U_{RH\_IN} = 0.015$$

$$U_{RH\_OUT} := \left[\left(U_{RH} \cdot RH_{out} \right)^2 + \left(U_{DAQ\_AI} \cdot RH_{out} \right)^2 \right]^{\frac{1}{2}}$$

$$U_{RH\_OUT} = 0.02$$

$$U_{AC\_IN} := \left[\left(U_{TAC1} \cdot AC_{in} \right)^2 + \left(U_{TAC2} \right)^2 + \left(U_{DAQ\_RTD} \right)^2 \right]^{\frac{1}{2}}$$

$$U_{AC\_IN} = 0.505 \cdot \Delta°F$$

$$U_{AC\_OUT} := \left[\left(U_{TAC1} \cdot AC_{out} \right)^2 + \left(U_{TAC2} \right)^2 + \left(U_{DAQ\_RTD} \right)^2 \right]^{\frac{1}{2}}$$

$$U_{AC\_OUT} = 0.505 \cdot \Delta°F$$

$$U_{Flow\_NG\_GNGFR} := \left[\left(U_{Flow\_NG} \right)^2 + \left(U_{DAQ\_AI} \cdot GNGFR \right)^2 \right]^{\frac{1}{2}}$$

$$U_{Flow\_NG\_GNGFR} = 0.088 \cdot \frac{ft^3}{min}$$

$$U_{Flow\_NG\_BNGFR} := \left[\left(U_{Flow\_NG} \right)^2 + \left(U_{DAQ\_AI} \cdot BNGFR \right)^2 \right]^{\frac{1}{2}}$$

$$U_{Flow\_NG\_BNGFR} = 0.088 \cdot \frac{ft^3}{min}$$

$$Flow_{NG} \cdot 930 \cdot \frac{BTU}{ft^3}$$

$$U_{Power\_gen} := \left[\left(U_{Power\_gen} \right)^2 + \left(U_{DAQ\_AI} \cdot GTP \right)^2 \right]^{\frac{1}{2}}$$

$$U_{Power\_gen} = 75.054W$$

Air Enthalpy Uncertainty:

To find saturation pressure the Keenan And Keyes Relation was used. Hidden to save space.

Saturation Pressure at Inlet:

$$Psat_{entrance} = 2.66 \cdot kPa$$

Saturation Pressure at Exit:

$$Psat_{exit} = 1.991 \cdot kPa$$

Uncertainty in Inlet Saturation Pressure:

$$U_{Psat\_entrance} = 0.053 Pa$$

Uncertainty in Outlet Saturation Pressure:

$$U_{Psat\_exit} = 0.04 Pa$$

Primary Enthalpy Equation:

Entrance:

$$h_{maentrance} := \left[1.004 \frac{kJ}{kg \cdot K} \cdot \left[1 + \frac{1.86 \cdot \frac{kJ}{kg \cdot K}}{1.004 \frac{kJ}{kg \cdot K}} \cdot \left(.622 \cdot \frac{RH_{in} \cdot Psat_{entrance}}{101.325 kPa \ldots + -RH_{in} \cdot Psat_{entrance}} \right) \right] \cdot \left(\begin{matrix} AC_{in} \ldots \\ + -273.15 \cdot K \end{matrix} \right) \right] \ldots + .622 \cdot \frac{RH_{in} \cdot Psat_{entrance}}{101.325 kPa - RH_{in} \cdot Psat_{entrance}} \cdot \left(1075 \cdot \frac{BTU}{lb} \right)$$

$$h_{maentrance} = 23.49 \cdot \frac{BTU}{lb}$$

Partial Derivatives (hidden to save space):

Uncertainty in Entrance Enthalpy:

$$U_{h\_IN} := \sqrt{\theta RH_{in}^{2} \cdot \left(U_{RH\_IN} \right)^2 + \theta AC_{in}^{2} \cdot \left(U_{AC\_IN} \right)^2 + \theta PSAT_{in}^{2} \cdot \left(U_{Psat\_entrance} \right)^2}$$

$$U_{h\_IN} = 0.311 \cdot \frac{BTU}{lb}$$

Exit Air Enthalpy:

$$h_{maexit} := \left[1.004 \frac{kJ}{kg \cdot K} \cdot \left[1 + \frac{1.86 \cdot \frac{kJ}{kg \cdot K}}{1.004 \frac{kJ}{kg \cdot K}} \cdot \left(.622 \cdot \frac{RH_{out} \cdot Psat_{exit}}{101.325kPa \ldots + -RH_{out} \cdot Psat_{exit}} \right) \right] \cdot \left(AC_{out} - 273.16K \right) \right] \ldots + .622 \cdot \frac{RH_{out} \cdot Psat_{exit}}{101.325kPa - RH_{out} \cdot Psat_{exit}} \cdot \left(1075 \cdot \frac{BTU}{lb} \right)$$

$$h_{maexit} = 21.104 \frac{BTU}{lbm}$$

Partial Derivatives (Hidden):

Uncertainty in Entrance Enthalpy:

$$U_{h\_OUT} := \sqrt{\theta RH_{out}^{2} \cdot \left(U_{RH\_OUT} \right)^{2} + \theta AC_{out}^{2} \cdot \left(U_{AC\_OUT} \right)^{2} + \theta PSAT_{out}^{2} \cdot U_{Psat\_exit}^{2}}$$

$$U_{h\_OUT} = 0.303 \cdot \frac{BTU}{lbm}$$

Primary Moist Air Density Equation:

Entrance:

$$\rho ma_{entrance} := .075 \cdot \frac{lb}{ft^3} \cdot \left[\frac{1 + .622 \cdot \frac{RH_{in} \cdot Psat_{entrance}}{101.325kPa - RH_{in} \cdot Psat_{entrance}}}{1 + 1.608 \left(.622 \cdot \frac{RH_{in} \cdot Psat_{entrance}}{101.325kPa - RH_{in} \cdot Psat_{entrance}} \right)} \right]$$

$$\rho ma_{entrance} = 0.074 \cdot \frac{lbm}{ft^3}$$

Partial Derivatives (Shown):

$$\theta RH_{in} := \frac{d}{dRH_{in}}\left[.075\cdot\frac{lb}{ft^3}\cdot\left[\frac{1+.622\cdot\frac{RH_{in}\cdot Psat_{entrance}}{101.325kPa-RH_{in}\cdot Psat_{entrance}}}{1+1.608\left(.622\cdot\frac{RH_{in}\cdot Psat_{entrance}}{101.325kPa-RH_{in}\cdot Psat_{entrance}}\right)}\right]\right]$$

$$\theta PSAT_{in} := \frac{d}{dPsat_{entrance}}\left[.075\cdot\frac{lb}{ft^3}\cdot\left[\frac{1+.622\cdot\frac{RH_{in}\cdot Psat_{entrance}}{101.325kPa-RH_{in}\cdot Psat_{entrance}}}{1+1.608\left(.622\cdot\frac{RH_{in}\cdot Psat_{entrance}}{101.325kPa-RH_{in}\cdot Psat_{entrance}}\right)}\right]\right]$$

Uncertainty in Entrance Moist Air Density:

$$U_{\rho ma\_IN} := \sqrt{\theta RH_{in}^{\ 2}\cdot\left(U_{RH\_IN}\right)^2+\theta PSAT_{in}^{\ 2}\cdot U_{Psat\_entrance}^{\ 2}}$$

$$U_{\rho ma\_IN} = 0.000011\cdot\frac{lbm}{ft^3}$$

Moist Air Density Exit:

$$\rho ma_{exit} := .075\cdot\frac{lb}{ft^3}\cdot\left[\frac{1+.622\cdot\frac{RH_{out}\cdot Psat_{exit}}{101.325kPa-RH_{out}\cdot Psat_{exit}}}{1+1.608\left(.622\cdot\frac{RH_{out}\cdot Psat_{exit}}{101.325kPa-RH_{out}\cdot Psat_{exit}}\right)}\right]$$

$$\rho ma_{exit} = 1.192\frac{kg}{m^3}$$

Partial Derivatives:

$$\theta RH_{out} := \frac{d}{dRH_{out}}\left[.075\cdot\frac{lb}{ft^3}\cdot\left[\frac{1+.622\cdot\frac{RH_{out}\cdot Psat_{exit}}{101.325kPa-RH_{out}\cdot Psat_{exit}}}{1+1.608\left(.622\cdot\frac{RH_{out}\cdot Psat_{exit}}{101.325kPa-RH_{out}\cdot Psat_{exit}}\right)}\right]\right]$$

$$\theta PSAT_{out} := \frac{d}{dPsat_{exit}}\left[.075 \cdot \frac{lb}{ft^3} \cdot \left[\frac{1 + .622 \cdot \frac{RH_{out} \cdot Psat_{exit}}{101.325kPa - RH_{out} \cdot Psat_{exit}}}{1 + 1.608 \cdot \left(.622 \cdot \frac{RH_{out} \cdot Psat_{exit}}{101.325kPa - RH_{out} \cdot Psat_{exit}} \right)} \right] \right]$$

Uncertainty in Exit Moist air density:

$$U_{\rho ma\_OUT} := \sqrt{\theta RH_{out}^{\ 2} \cdot \left(U_{RH\_OUT}\right)^2 + \theta PSAT_{out}^{\ 2} \cdot U_{Psat\_exit}^{\ 2}}$$

$$U_{\rho ma\_OUT} = 0.000011 \frac{lbm}{ft^3}$$

Primary Heat Transfer Ratio Equation:

$$Qratio := \frac{\left| Flow_{AIR} \cdot \left(\rho ma_{exit} h_{maexit} - \rho ma_{entrance} \cdot h_{maentrance} \right) \right|}{\left| Flow_{CW} \cdot \left[\begin{array}{l} \rho_{CWout} \cdot Cp_{CWout} \cdot \left(\frac{CW_{out\_T1} + CW_{out\_T2}}{2} \right) \ldots \\ + -\rho_{CWin} \cdot Cp_{CWin} \cdot \left(\frac{CW_{in\_T1} + CW_{in\_T2}}{2} \right) \end{array} \right] \right|}$$

$$Qratio = 1.094$$

Uncertainty in Heat Transfer Ratio:

Compute Partial Derivatives (Hidden):

Uncertainties:

$$UQR\_1 := \theta CW_{in\_T1}^{\ 2} \cdot \left(U_T\right)^2 + \theta CW_{out\_T2}^{\ 2} \cdot \left(U_T\right)^2 + \theta CW_{out\_T1}^{\ 2} \cdot \left(U_T\right)^2 + \theta CW_{in\_T2}^{\ 2} \cdot \left(U_T\right)^2$$

$$UQR\_2 := \theta Flow_{CW}^{\ 2} \cdot \left(U_{Flow\_Turbine\_CW}\right)^2 + \theta Flow_{AIR}^{\ 2} \cdot \left(U_{Flow\_AIR}\right)^2$$

$$UQR\_3 := \theta \rho_{CWout}^{\ 2} \cdot \left(U_{\rho\_Water\_CWOUT}\right)^2 + \theta \rho_{CWin}^{\ 2} \cdot \left(U_{\rho\_Water\_CWIN}\right)^2$$

$$UQR\_4 := \theta Cp_{CWin}^{\ 2} \cdot \left(U_{cp\_Water\_CWIN}\right)^2 + \theta Cp_{CWout}^{\ 2} \cdot \left(U_{cp\_Water\_CWOUT}\right)^2$$

$$UQR\_5 := \theta h_{maentrance}{}^{2}\cdot\left(U_{h\_IN}\right)^{2} + \theta h_{maexit}{}^{2}\cdot\left(U_{h\_OUT}\right)^{2} \ldots + \left(\theta\rho ma_{exit}\right)^{2}\cdot\left(U_{\rho ma\_OUT}\right)^{2} + \theta\rho ma_{entrance}{}^{2}\cdot\left(U_{\rho ma\_IN}\right)^{2}$$

$$UQR := (UQR\_1 + UQR\_2 + UQR\_3 + UQR\_4 + UQR\_5)^{.5}$$

$$UQR = 0.222$$

$$Qratio = 1.094$$

Percentage Uncertainty in Heat Transfer Ratio:

$$\frac{UQR}{Qratio} = 20.305\%$$

Uncertainty Percentage Contribution:

$$UPC_{T} := \frac{UQR\_1}{UQR^{2}}$$

$$UPC_{T} = 18.19\%$$

$$UPC_{Flow} := \frac{UQR\_2}{UQR^{2}}$$

$$UPC_{Flow} = 1.047\%$$

$$UPC_{\rho} := \frac{\theta\rho_{CWout}{}^{2}\cdot\left(U_{\rho\_Water\_CWOUT}\right)^{2} + \theta\rho_{CWin}{}^{2}\cdot\left(U_{\rho\_Water\_CWIN}\right)^{2}}{UQR^{2}}$$

$$UPC_{\rho} = 0.07\%$$

$$UPC_{Cp} := \frac{\theta Cp_{CWin}{}^{2}\cdot\left(U_{cp\_Water\_CWIN}\right)^{2} + \theta Cp_{CWout}{}^{2}\cdot\left(U_{cp\_Water\_CWOUT}\right)^{2}}{UQR^{2}}$$

$$UPC_{Cp} = 0.098\%$$

$$UPC_{\rho ma} := \frac{\theta\rho ma_{exit}^{2} \cdot \left(U_{\rho ma\_OUT}\right)^2 + \theta\rho ma_{entrance}^{2} \cdot \left(U_{\rho ma\_IN}\right)^2}{UQR^2}$$

$$UPC_{\rho ma} = 0.01\cdot\%$$

$$UPC_{ha} := \frac{\theta h_{maentrance}^{2} \cdot \left(U_{h\_IN}\right)^2 + \theta h_{maexit}^{2} \cdot \left(U_{h\_OUT}\right)^2}{UQR^2}$$

$$UPC_{ha} = 80.585\cdot\%$$

UPC Check:

$$UPC_{tot} := UPC_T + UPC_{Flow} + UPC_{\rho} + UPC_{Cp} + UPC_{ha} + UPC_{\rho ma}$$

$$UPC_{tot} = 1$$

Now to Compute the System Energy Transfer Ratio:

$$SETR := \frac{GTP + \left|Flow_{AIR} \cdot \left(\rho ma_{exit} \cdot h_{maexit} - \rho ma_{entrance} \cdot h_{maentrance}\right)\right|}{930 \cdot \frac{BTU}{ft^3} \cdot (BNGFR + GNGFR)}$$

$$SETR = 0.132$$

Uncertainty for SETR:

Compute Partial Derivatives (Hidden):

Uncertainty:

$$USETR\_1 := \theta GTP^2 \cdot U_{Power\_gen}^{2} + \theta GNGFR^2 \cdot U_{Flow\_NG\_GNGFR}^{2}$$

$$USETR\_2 := \theta BNGFR^2 \cdot U_{Flow\_NG\_BNGFR}^{2} + \theta Flow_{AIR}^{2} \cdot \left(U_{Flow\_AIR}\right)^2$$

$$USETR\_3 := \theta h_{maentrance}^{2} \cdot \left(U_{h\_IN}\right)^2 + \theta h_{maexit}^{2} \cdot \left(U_{h\_OUT}\right)^2 \ldots + \left(\theta\rho ma_{exit}\right)^2 \cdot \left(U_{\rho ma\_OUT}\right)^2 + \theta\rho ma_{entrance}^{2} \cdot \left(U_{\rho ma\_IN}\right)^2$$

$$USETR := (USETR\_1 + USETR\_2 + USETR\_3)^{.5}$$

$$USETR = 0.009$$

Percentage Uncertainty in SETR:

$$\frac{USETR}{SETR} = 6.655\cdot\%$$

Uncertainty Percentage Contribution:

$$UPC_{Flow\_NG} := \frac{\theta GNGFR^2 \cdot U_{Flow\_NG\_GNGFR}^2 + \theta BNGFR^2 \cdot U_{Flow\_NG\_BNGFR}^2}{USETR^2}$$

$$UPC_{Flow\_NG} = 14.331\cdot\%$$

$$UPC_{GTP} := \frac{\theta GTP^2 \cdot U_{Power\_gen}^2}{USETR^2}$$

$$UPC_{GTP} = 1.11\cdot\%$$

$$UPC_{\rho ma} := \frac{\theta \rho ma_{exit}^2 \cdot \left(U_{\rho ma\_OUT}\right)^2 + \theta \rho ma_{entrance}^2 \cdot \left(U_{\rho ma\_IN}\right)^2}{USETR^2}$$

$$UPC_{\rho ma} = 0.01\cdot\%$$

$$UPC_{ha} := \frac{\theta h_{maentrance}^2 \cdot \left(U_{h\_IN}\right)^2 + \theta h_{maexit}^2 \cdot \left(U_{h\_OUT}\right)^2}{USETR^2}$$

$$UPC_{ha} = 83.527\cdot\%$$

$$UPC_{Flow\_AIR} := \frac{\theta Flow_{AIR}^2 \cdot \left(U_{Flow\_AIR}\right)^2}{USETR^2}$$

$$UPC_{Flow\_AIR} = 1.022\cdot\%$$

UPC Check:

$$UPC_{tot} := UPC_{GTP} + UPC_{Flow\_NG} + UPC_{Flow\_AIR} + UPC_{ha} + UPC_{\rho ma}$$

$$UPC_{tot} = 1$$

APPENDIX P

MATHCAD CONVENTIONAL HVAC AND MISCELLANEOUS UNCERTAINTY ANALYSIS

Inputs (Data Collected 1/12/09 Heating and 7/6/2009 Cooling):

Cooling:

Compressor Power Used:

$Power_{comp} := 1.24kW$

Heating:

Natural Gas Flowrate:

$Flow_{NG} := .237\frac{ft^3}{min}$

Both:

Air Flow Input Relative Humidity:

$RH_{in} := .63$

Air Flow Output Relative Humidity:

$RH_{out} := .954$

Air Flow Input Temperature:

$AC_{in} := 68.3 \cdot \Delta°F$

Air Flow Output Temperature:

$AC_{out} := 58 \cdot \Delta°F$

Air Flowrate:

$Flow_{AIR} := 1682 \cdot \frac{ft^3}{min}$

Ambient Temperature Sensor 1:

$AMBT1 := 88.4 °F$

Ambient Temperature Sensor 2:

$AMBT2 := 88.9 °F$

Ambient Relative Humidity:

$AMBRH := .34$

Building Power Used:

$GTP := 5kW$

Uncertainties:

Compressor Power Uncertainty:

$U_{comp} := .25\% \cdot 25 \cdot A \cdot 240V$

$U_{comp} = 15\,W$

Natural Gas Flowmeter:

$$U_{Flow\_NG} := 0.035 \frac{ft^3}{min}$$

Relative Humidity Uncertainty:

$U_{RH} := 2 \cdot \%$

Air Flowrate Sensor Uncertainty:

$U_{Flow\_AIR\_Sensors} := 2 \cdot \%$

Air Differential Pressure:

$U_{Flow\_DP} := .25 \cdot \%$

Air Temperature Sensor:

$U_{TAC1} := .06\%$

$U_{TAC2} := 0.225\,\Delta°F$

Ambient Temperature Uncertainty:

$U_T := .45\Delta°F$

Ambient Relative Humidity Uncertainty:

$U_{AMBRH} := 2\%$

Generator Power Uncertainty:

$U_{Power\_gen} := 75 \cdot W$

DAQ Uncertainties:

DAQ Analog Input Uncertainty:

$U_{DAQ\_AI} := .04 \cdot \%$

DAQ RTD Input Uncertainty:

$U_{DAQ\_RTD} := 0.45\,\Delta°F$

Component Uncertainties:

$$U_T := \left[(U_T)^2 + (U_{DAQ\_RTD})^2 \right]^{\frac{1}{2}}$$

$U_T = 0.636 \cdot \Delta°F$

$$U_{Flow\_NG} := \left[(U_{Flow\_NG})^2 + (U_{DAQ\_AI} \cdot Flow_{NG})^2 \right]^{\frac{1}{2}}$$

$U_{Flow\_NG} = 0.035 \cdot \frac{ft^3}{min}$

$$U_{Flow\_AIR} := \left[\begin{array}{l} \left(U_{Flow\_DP} \cdot Flow_{AIR}\right)^2 + \left(U_{Flow\_AIR\_Sensors} \cdot Flow_{AIR}\right)^2 \ldots \\ + \left(U_{DAQ\_AI} \cdot Flow_{AIR}\right)^2 \end{array} \right]^{\frac{1}{2}}$$

$$U_{Flow\_AIR} = 33.908 \frac{ft^3}{min}$$

$$U_{RH\_IN} := \left[\left(U_{RH} \cdot RH_{in}\right)^2 + \left(U_{DAQ\_AI} \cdot RH_{in}\right)^2 \right]^{\frac{1}{2}}$$

$$U_{RH\_IN} = 0.013$$

$$U_{RH\_OUT} := \left[\left(U_{RH} \cdot RH_{out}\right)^2 + \left(U_{DAQ\_AI} \cdot RH_{out}\right)^2 \right]^{\frac{1}{2}}$$

$$U_{RH\_OUT} = 1.908\,\%$$

$$U_{AC\_IN} := \left[\left(U_{TAC1} \cdot AC_{in}\right)^2 + \left(U_{TAC2}\right)^2 + \left(U_{DAQ\_RTD}\right)^2 \right]^{\frac{1}{2}}$$

$$U_{AC\_IN} = 0.505\,\Delta°F$$

$$U_{AC\_OUT} := \left[\left(U_{TAC1} \cdot AC_{out}\right)^2 + \left(U_{TAC2}\right)^2 + \left(U_{DAQ\_RTD}\right)^2 \right]^{\frac{1}{2}}$$

$$U_{AC\_OUT} = 0.504\,\Delta°F$$

$$U_{Power\_gen} = 75\,W$$

$$U_{Power\_gen} := \left[\left(U_{Power\_gen}\right)^2 + \left(U_{DAQ\_AI} \cdot GTP\right)^2 \right]^{\frac{1}{2}}$$

$$U_{AMBRH} := \left[\left(U_{AMBRH} \cdot AMBRH \right)^2 + \left(U_{DAQ\_AI} \cdot AMBRH \right)^2 \right]^{\frac{1}{2}}$$

$$U_{AMBRH} = 0.68 \cdot \%$$

$$U_{comp} := \left[\left(U_{comp} \right)^2 + \left(U_{DAQ\_AI} \cdot Power_{comp} \right)^2 \right]^{\frac{1}{2}}$$

$$U_{comp} = 15.008 W$$

Find the saturation pressure and its uncertainty using the Keenan and Keyes relation for water vapor saturation pressure (Hidden to save space):

Saturation Pressure at the Inlet:

$$Psat_{entrance} = 2.361 \cdot kPa$$

Saturation Pressure at the Outlet:

$$Psat_{exit} = 1.644 \cdot kPa$$

Uncertainty in Saturation Pressure at the Inlet:

$$U_{Psat\_entrance} = 0.047 Pa$$

Uncertainty in Saturation Pressure at the Outlet:

$$U_{Psat\_exit} = 0.033 Pa$$

Primary Enthalpy Equation:

Entrance Enthalpy Calculation:

$$h_{maentrance} := \left[1.004 \frac{kJ}{kg \cdot K} \cdot \left[1 + \frac{1.86 \cdot \frac{kJ}{kg \cdot K}}{1.004 \frac{kJ}{kg \cdot K}} \cdot \left(.622 \cdot \frac{RH_{in} \cdot Psat_{entrance}}{101.325 kPa \ldots + -RH_{in} \cdot Psat_{entrance}} \right) \right] \cdot \left(AC_{in} \ldots + -273.16 K \right) \right] \ldots + .622 \cdot \frac{RH_{in} \cdot Psat_{entrance}}{101.325 kPa - RH_{in} \cdot Psat_{entrance}} \cdot \left(1075 \cdot \frac{BTU}{lb} \right)$$

$$h_{maentrance} = 18.81 \cdot \frac{BTU}{lbm}$$

Partial Derivatives (Hidden):

Uncertainty in Entrance Enthalpy:

$$U_{h\_IN} := \sqrt{\theta RH_{in}^{2} \cdot \left(U_{RH\_IN}\right)^{2} + \theta AC_{in}^{2} \cdot \left(U_{AC\_IN}\right)^{2} + \theta PSAT_{in}^{2} \cdot U_{Psat\_entrance}^{2}}$$

$$U_{h\_IN} = 0.239 \cdot \frac{BTU}{lb}$$

UPC for Enthalpy:

$$UPC_{RH} := \frac{\theta RH_{in}^{2} \cdot \left(U_{RH\_IN}\right)^{2}}{U_{h\_IN}^{2}}$$

$$UPC_{RH} = 73.534\%$$

$$UPC_{AC} := \frac{\theta AC_{in}^{2} \cdot \left(U_{AC\_IN}\right)^{2}}{U_{h\_IN}^{2}}$$

$$UPC_{AC} = 26.466\%$$

$$UPC_{psat} := \frac{\theta PSAT_{in}^{2} \cdot U_{Psat\_entrance}^{2}}{U_{h\_IN}^{2}}$$

$$UPC_{psat} = 7.35 \times 10^{-5} \cdot \%$$

Enthalpy Calculation at the Outlet:

$$h_{maexit} := \left[1.004 \frac{kJ}{kg \cdot K} \cdot \left[1 + \frac{1.86 \frac{kJ}{kg \cdot K}}{1.004 \frac{kJ}{kg \cdot K}} \cdot \left(.622 \cdot \frac{RH_{out} \cdot Psat_{exit}}{101.325 kPa \ldots + -RH_{out} \cdot Psat_{exit}} \right) \right] \cdot \left(\begin{matrix} AC_{out} \ldots \\ + -273.16 K \end{matrix} \right) \right] \ldots + .622 \cdot \frac{RH_{out} \cdot Psat_{exit}}{101.325 kPa - RH_{out} \cdot Psat_{exit}} \cdot \left(1075 \cdot \frac{BTU}{lb} \right)$$

$$h_{maexit} = 16.857 \cdot \frac{BTU}{lbm}$$

Partial Derivatives (Hidden):

Uncertainty in Entrance Enthalpy:

$$U_{h\_OUT} := \sqrt{\theta RH_{out}^{2} \cdot \left(U_{RH\_OUT} \right)^{2} + \theta AC_{out}^{2} \cdot \left(U_{AC\_OUT} \right)^{2} + \theta PSAT_{out}^{2} \cdot U_{Psat\_exit}^{2}}$$

$$U_{h\_OUT} = 0.249 \cdot \frac{BTU}{lbm}$$

Primary Moist Air Density Equation:

Entrance:

$$\rho ma_{entrance} := .075 \cdot \frac{lb}{ft^{3}} \cdot \left[\frac{1 + .622 \cdot \frac{RH_{in} \cdot Psat_{entrance}}{101.325 kPa - RH_{in} \cdot Psat_{entrance}}}{1 + 1.608 \left(.622 \cdot \frac{RH_{in} \cdot Psat_{entrance}}{101.325 kPa - RH_{in} \cdot Psat_{entrance}} \right)} \right]$$

$$\rho ma_{entrance} = 0.075 \cdot \frac{lbm}{ft^{3}}$$

Partial Derivatives (Hidden):

Uncertainty in Entrance Moist air density:

$$U_{\rho ma\_IN} := \sqrt{\theta RH_{in}^{2} \cdot \left(U_{RH\_IN} \right)^{2} + \theta PSAT_{in}^{2} \cdot U_{Psat\_entrance}^{2}}$$

$$U_{\rho ma\_IN} = 0.000008 \frac{lbm}{ft^3}$$

Exit Moist Air Density:

$$\rho ma_{exit} := .075 \cdot \frac{lb}{ft^3} \cdot \left[\frac{1 + .622 \cdot \frac{RH_{out} \cdot Psat_{exit}}{101.325kPa - RH_{out} \cdot Psat_{exit}}}{1 + 1.608 \left(.622 \cdot \frac{RH_{out} \cdot Psat_{exit}}{101.325kPa - RH_{out} \cdot Psat_{exit}} \right)} \right]$$

$$\rho ma_{exit} = 0.075 \frac{lbm}{ft^3}$$

Partial Derivatives (Hidden):

Uncertainty in Exit Moist Air Density:

$$U_{\rho ma\_OUT} := \sqrt{\theta RH_{out}^{\ 2} \cdot \left(U_{RH\_OUT}\right)^2 + \theta PSAT_{out}^{\ 2} \cdot U_{Psat\_exit}^{\ 2}}$$

$$U_{\rho ma\_OUT} = 0.000009 \frac{lbm}{ft^3}$$

$$Flow_{AIR} \cdot \left(\rho ma_{exit} \cdot h_{maexit} - \rho ma_{entrance} \cdot h_{maentrance}\right) = -4.319 \times 10^3 \, W$$

Cooling HVAC Results:

Coefficient of Performance:

$$COP := \frac{-Flow_{AIR} \cdot \left(\rho ma_{exit} \cdot h_{maexit} - \rho ma_{entrance} \cdot h_{maentrance}\right)}{Power_{comp}}$$

$$COP = 3.483$$

Uncertainty in COP:

Compute Partial Derivatives (Hidden):

Uncertainties:

$$UCOP\_1 := \theta h_{maentrance}^{2} \cdot \left(U_{h\_IN}\right)^2 + \theta h_{maexit}^{2} \cdot \left(U_{h\_OUT}\right)^2 \ldots + \theta \rho ma_{exit}^{2} \cdot \left(U_{\rho ma\_OUT}\right)^2 + \theta \rho ma_{entrance}^{2} \cdot \left(U_{\rho ma\_IN}\right)^2$$

$$UCOP\_2 := \theta Power_{comp}^{2} \cdot \left(U_{comp}\right)^2 + \theta Flow_{AIR}^{2} \cdot \left(U_{Flow\_AIR}\right)^2$$

$$UCOP := (UCOP\_1 + UCOP\_2)^{.5}$$

$$UCOP = 0.619$$

$$COP = 3.483$$

Percentage Uncertainty in COP:

$$\frac{UCOP}{COP} = 17.776\%$$

Uncertainty Percentage Contribution:

$$UPC_{Power} := \frac{\theta Power_{comp}^{2} \cdot \left(U_{comp}\right)^2}{UCOP^2}$$

$$UPC_{Power} = 0.464\%$$

$$UPC_{Flow} := \frac{\theta Flow_{AIR}^{2} \cdot \left(U_{Flow\_AIR}\right)^2}{UCOP^2}$$

$$UPC_{Flow} = 1.286\%$$

$$UPC_{\rho ma} := \frac{\theta \rho ma_{exit}^{2} \cdot \left(U_{\rho ma\_OUT}\right)^2 + \theta \rho ma_{entrance}^{2} \cdot \left(U_{\rho ma\_IN}\right)^2}{UCOP^2}$$

$$UPC_{\rho ma} = 0.007\%$$

$$UPC_{ha} := \frac{\theta h_{maentrance}^{2} \cdot \left(U_{h\_IN}\right)^2 + \theta h_{maexit}^{2} \cdot \left(U_{h\_OUT}\right)^2}{UCOP^2}$$

$UPC_{ha} = 98.243\%$

UPC Check:

$UPC_{tot} := UPC_{Power} + UPC_{Flow} + UPC_{ha} + UPC_{\rho ma}$

$UPC_{tot} = 1$

Conventional Compressor Cost:

Designate Value for Dollars:

$Dollars := 1$

Designate Value for kWh:

$kWh := kW \cdot hr$

Electrical Power Cost:

$Cost_{Elec} := .10801 \cdot \frac{Dollars}{kWh}$

Compressor cost Equation:

$Cost_{Comp} := Cost_{Elec} \cdot Power_{comp}$

$Cost_{Comp} = 0.134 \cdot \frac{Dollars}{hr}$

Partial Derivatives (Shown):

$\theta Power_{comp} := \frac{d}{dPower_{comp}} \left(Cost_{Elec} \cdot Power_{comp} \right)$

Uncertainty in Compressor Cost:

$U_{Cost\_Comp} := \left[\theta Power_{comp}^{2} \cdot \left(U_{comp} \right)^{2} \right]^{.5}$

$$U_{Cost\_Comp} = 0.002 \cdot \frac{Dollars}{hr}$$

Percentage Uncertainty in Compressor Cost:

$$\frac{U_{Cost\_Comp}}{Cost_{Comp}} = 1.21 \cdot \%$$

Conventional Heating Efficiency Calculation:

$$\eta := \frac{\left| Flow_{AIR} \cdot \left(\rho ma_{exit} \cdot h_{maexit} - \rho ma_{entrance} \cdot h_{maentrance} \right) \right|}{930 \cdot \frac{BTU}{ft^3} \cdot Flow_{NG}}$$

$$\eta = 1.114$$

Uncertainty in Heating Efficiency:

Compute Partial Derivatives (Hidden):

Uncertainties:

$$UEFF\_1 := \theta h_{maentrance}{}^2 \cdot \left(U_{h\_IN}\right)^2 + \theta h_{maexit}{}^2 \cdot \left(U_{h\_OUT}\right)^2 \ldots + \theta \rho ma_{exit}{}^2 \cdot \left(U_{\rho ma\_OUT}\right)^2 + \theta \rho ma_{entrance}{}^2 \cdot \left(U_{\rho ma\_IN}\right)^2$$

$$UEFF\_2 := \theta Flow_{NG}{}^2 \cdot \left(U_{Flow\_NG}\right)^2 + \theta Flow_{AIR}{}^2 \cdot \left(U_{Flow\_AIR}\right)^2$$

$$UEFF := (UEFF\_1 + UEFF\_2)^{.5}$$

$$UEFF = 0.257$$

$$\eta = 1.114$$

$$\frac{UEFF}{\eta} = 23.079\%$$

Percentage Uncertainty in efficiency ratio:

Uncertainty Percentage Contribution:

$$UPC_{Power} = 0.464\%$$

$$UPC_{NG} := \frac{\theta Flow_{NG}^{2} \cdot \left(U_{Flow\_NG}\right)^{2}}{UEFF^{2}}$$

$$UPC_{Flow} = 1.286\%$$

$$UPC_{Flow} := \frac{\theta Flow_{AIR}^{2} \cdot \left(U_{Flow\_AIR}\right)^{2}}{UEFF^{2}}$$

$$UPC_{\rho ma} = 0.007\%$$

$$UPC_{\rho ma} := \frac{\theta \rho ma_{exit}^{2} \cdot \left(U_{\rho ma\_OUT}\right)^{2} + \theta \rho ma_{entrance}^{2} \cdot \left(U_{\rho ma\_IN}\right)^{2}}{UEFF^{2}}$$

$$UPC_{ha} = 98.243\%$$

$$UPC_{ha} := \frac{\theta h_{maentrance}^{2} \cdot \left(U_{h\_IN}\right)^{2} + \theta h_{maexit}^{2} \cdot \left(U_{h\_OUT}\right)^{2}}{UEFF^{2}}$$

UPC Check:

$$UPC_{tot} := UPC_{NG} + UPC_{Flow} + UPC_{ha} + UPC_{\rho ma}$$

$$UPC_{tot} = 1$$

Conventional Heating Cost:

Electrical Power Cost:

$$Cost_{Elec} := .10801 \cdot \frac{Dollars}{kWh}$$

Natural Gas Fuel Cost:

$$Cost_{NG} := 12.83 \cdot \frac{Dollars}{1000 \cdot ft^3}$$

Natural Gas Cost Equation:

$$Cost_{Conv\_NG} := Cost_{NG} \cdot Flow_{NG}$$

$$Cost_{Conv\_NG} = 0.182 \cdot \frac{Dollars}{hr}$$

Partial Derivatives (Shown):

$$\theta Flow_{NG} := \frac{d}{dFlow_{NG}} \left(Cost_{NG} \cdot Flow_{NG} \right)$$

Uncertainty in Conventional Natural Gas Cost:

$$U_{Cost\_Conv\_NG} := \left[\theta Flow_{NG}^{2} \cdot \left(U_{Flow\_NG} \right)^2 \right]^{.5}$$

$$U_{Cost\_Conv\_NG} = 0.027 \cdot \frac{Dollars}{hr}$$

Percentage Uncertainty in Heating Cost:

$$\frac{U_{Cost\_Conv\_NG}}{Cost_{Conv\_NG}} = 14.768\%$$

Conventional Building Electrical Cost Equation:

$$Cost_{Conv} := Cost_{Elec} \cdot GTP$$

$$Cost_{Conv} = 0.54 \cdot \frac{Dollars}{hr}$$

Partial Derivatives (Shown):

$$\theta GTP := \frac{d}{dGTP} \left(Cost_{Elec} \cdot GTP \right)$$

Uncertainty in Building Electrical Cost:

$$U_{Cost\_Conv} := \left[\theta GTP^2 \cdot \left(U_{Power\_gen}\right)^2\right]^{.5}$$

$$U_{Cost\_Conv} = 8.104 \times 10^{-3} \cdot \frac{Dollars}{hr}$$

Percentage Uncertainty in Compressor Cost:

$$\frac{U_{Cost\_Conv}}{Cost_{Conv}} = 1.501 \cdot \%$$

Ambient Enthalpy Calculation:

Primary Equation:

$$AMBT := \frac{AMBT1 + AMBT2}{2}$$

$$AMBT = 88.65 \Delta°F$$

Now find the saturation pressure and its uncertainty:

$$Psat = 4.611 \cdot kPa$$

$$U_{Psat} = 0.092 Pa$$

Primary Enthalpy Equation:

Ambient:

$$h_{ma} := \left[1.004 \frac{kJ}{kg \cdot K} \cdot \left[1 + \frac{1.86 \frac{kJ}{kg \cdot K}}{1.004 \frac{kJ}{kg \cdot K}} \cdot \left(.622 \cdot \frac{AMBRH \cdot Psat}{101.325 kPa - AMBRH \cdot Psat}\right)\right] \cdot \left(\begin{matrix} AMBT \ldots \\ + -273.16 K \end{matrix}\right)\right] \ldots$$
$$+ .622 \cdot \frac{AMBRH \cdot Psat}{101.325 kPa - AMBRH \cdot Psat} \cdot \left(1075 \frac{BTU}{lb}\right)$$

$$h_{ma} = 24.335 \frac{BTU}{lbm}$$

Partial Derivatives (Hidden):

Uncertainty in Ambient Enthalpy:

$$U_{h\_AMB} := \sqrt{\theta AMBRH^2 \cdot \left(U_{AMBRH}\right)^2 + \theta AMBT^2 \cdot \left(U_T\right)^2 + \theta Psat^2 \cdot U_{Psat}{}^2}$$

$$U_{h\_AMB} = 0.268 \frac{BTU}{lb}$$

Percentage Uncertainty in Ambient Enthalpy:

$$\frac{U_{h\_AMB}}{h_{ma}} = 1.102\%$$

UPC for Enthalpy:

$$UPC_{RH} := \frac{\theta AMBRH^2 \cdot \left(U_{AMBRH}\right)^2}{U_{h\_AMB}{}^2}$$

$$UPC_{RH} = 66.422\%$$

$$UPC_{AMBT} := \frac{\theta AMBT^2 \cdot \left(U_T\right)^2}{U_{h\_AMB}{}^2}$$

$$UPC_{AMBT} = 33.578\%$$

$$UPC_{psat} := \frac{\theta Psat^2 \cdot U_{Psat}{}^2}{U_{h\_AMB}{}^2}$$

$$UPC_{psat} = 6.64 \times 10^{-5} \cdot \%$$

UPC Check:

$$UPC_{check} := UPC_{RH} + UPC_{AMBT} + UPC_{psat}$$

$$UPC_{check} = 1$$